

GELFAND–TSETLIN BASIS FOR PARTIALLY TRANSPOSED PERMUTATIONS, WITH APPLICATIONS TO QUANTUM INFORMATION

DMITRY GRINKO¹, ADAM BURCHARDT¹, AND MARIS OZOLS^{1,2}

ABSTRACT. We study representation theory of the partially transposed permutation matrix algebra, a matrix representation of the diagrammatic walled Brauer algebra. This algebra plays a prominent role in mixed Schur–Weyl duality that appears in various contexts in quantum information. Our main technical result is an explicit formula for the action of the walled Brauer algebra generators in the Gelfand–Tsetlin basis. It generalizes the well-known Gelfand–Tsetlin basis for the symmetric group (also known as Young’s orthogonal form or Young–Yamanouchi basis).

We provide two applications of our result to quantum information. First, we show how to simplify semidefinite optimization problems over unitary-equivariant quantum channels by performing a symmetry reduction. Second, we derive an efficient quantum circuit for implementing the optimal port-based quantum teleportation protocol, exponentially improving the known trivial construction. As a consequence, this also exponentially improves the known lower bound for the amount of entanglement needed to implement unitaries non-locally.

Both applications require a generalization of quantum Schur transform to tensors of mixed unitary symmetry. We develop an efficient quantum circuit for this mixed quantum Schur transform and provide a matrix product state representation of its basis vectors. For constant local dimension, this yields an efficient classical algorithm for computing any entry of the mixed quantum Schur transform unitary.

CONTENTS

1. Introduction	2
1.1. Background	2
1.2. Historical context	3
1.3. Strategy	4
1.4. Summary of our results	4
1.5. Related work	5
2. Preliminaries	6
2.1. Young diagrams and tableaux	6
2.2. Bratteli diagram and Gelfand–Tsetlin basis	7
2.3. Gelfand–Tsetlin patterns	9
2.4. Mixed Young diagrams and tableaux	9
3. Representation theory of partially transposed permutation matrix algebra	11
3.1. Walled Brauer algebra $\mathcal{B}_{p,q}^d$	11
3.2. Matrix algebra $\mathcal{A}_{p,q}^d$ of partially transposed permutations	12
3.3. Representation theory of the algebra $\mathcal{A}_{p,q}^d$	12
4. Mixed quantum Schur transform	15
4.1. Mixed Schur–Weyl duality	15
4.2. Mixed Schur transform	16
4.3. MPS representation of mixed Schur basis vectors	17
4.4. Mixed Schur transform achieves the Gelfand–Tsetlin basis	18
4.5. Quantum circuit for mixed Schur transform	19
4.6. Quantum circuit for Clebsch–Gordan transforms	19
5. Unitary-equivariant SDPs	22
5.1. Unitary-equivariant quantum channels	22
5.2. Full trace	23
5.3. Partial trace	24
5.4. Unitary-equivariant SDPs	25
6. Efficient quantum circuit for optimal port-based teleportation	27
6.1. Naimark’s dilation	28
6.2. Efficient quantum circuit for the pretty good measurement	30

¹INSTITUTE FOR LOGIC, LANGUAGE, AND COMPUTATION, UNIVERSITY OF AMSTERDAM AND QUSOFT, AMSTERDAM, THE NETHERLANDS

²KORTEWEG-DE VRIES INSTITUTE FOR MATHEMATICS AND INSTITUTE FOR THEORETICAL PHYSICS, UNIVERSITY OF AMSTERDAM, THE NETHERLANDS

E-mail addresses: dmitry.grinko@cwi.nl, adam.burchardt@cwi.nl, marozols@gmail.com.

6.3. Exponentially improved lower bound for non-local quantum computation	31
Acknowledgements	32
References	32
Appendix A. Clebsch–Gordan coefficients	37
Appendix B. Proof of Theorem 3.2	38

1. INTRODUCTION

1.1. Background. Symmetry plays a fundamental role in physics and mathematics, and is a common problem-solving technique in both fields. The unitary group of symmetries is particularly important in quantum mechanics and particle physics, since it captures the properties of the basic building blocks of our universe. Unitary symmetry is closely intertwined with permutational symmetry. Indeed, permuting identical particles or simultaneously applying the same unitary rotation on each of them are two commuting actions. This observation is captured by *Schur–Weyl duality*, which has become an important tool in quantum information, quantum algorithms, and quantum many-body physics.

The simplest instance of Schur–Weyl duality is for two qubits. Let $|\psi^-\rangle := (|01\rangle - |10\rangle)/\sqrt{2}$ denote the maximally entangled *singlet state*, which is the unique anti-symmetric state on two qubits. It has the property that $(U \otimes U)|\psi^-\rangle = \det(U)|\psi^-\rangle$ for any $U \in U_2$. In addition, $\text{SWAP}|\psi^-\rangle = -|\psi^-\rangle$ where $\text{SWAP} \in U_4$ exchanges the two qubits. The three-dimensional symmetric subspace orthogonal to $|\psi^-\rangle$ is similarly invariant under the actions of both $U \otimes U$ and SWAP . Hence, we can decompose $(\mathbb{C}^2)^{\otimes 2}$ into mutually orthogonal subspaces invariant under the commuting unitary and permutation actions. Schur–Weyl duality generalizes this observation to $(\mathbb{C}^d)^{\otimes p}$ for any local dimension d and number of systems p .

Schur–Weyl duality is particularly useful in quantum information where one often needs to deal with many identical copies of a quantum state or to apply the same unitary to many systems in parallel. Its algorithmic manifestation, quantum Schur transform, can be efficiently implemented [Har05; BCH06; KS18; Kro19] and has many applications [Wri16; Har05], such as quantum spectrum [KW01a] and entropy estimation [AISW20], quantum state tomography [Key06; HHJWY17; OW16; OW17], and quantum majority vote [BLMMO22].

The main focus of our paper is a variant of Schur–Weyl duality, known as *mixed Schur–Weyl duality*, which is equally important in quantum information but has received less attention due to its more complicated nature [GO22]. The simplest instance of mixed Schur–Weyl duality is also for two qubits. Here, instead of the singlet state $|\psi^-\rangle$, we single out the canonical maximally entangled state $|\phi^+\rangle := (|00\rangle + |11\rangle)/\sqrt{2}$. This state is invariant under a slightly different unitary action, namely $(U \otimes \bar{U})|\phi^+\rangle = |\phi^+\rangle$ for any $U \in U_2$. In addition, $\text{SWAP}^\Gamma|\phi^+\rangle = 2|\phi^+\rangle$ where $\text{SWAP}^\Gamma = 2|\phi^+\rangle\langle\phi^+|$ denotes the partial transpose of SWAP . Similarly, the three-dimensional orthogonal complement of $|\phi^+\rangle$ is also invariant under the action of both $U \otimes \bar{U}$ and SWAP^Γ . Mixed Schur–Weyl duality generalizes this observation by partitioning $(\mathbb{C}^d)^{p+q}$ into subspaces that are invariant under the unitary action $U^{\otimes p} \otimes \bar{U}^{\otimes q}$ and the matrix algebra $\mathcal{A}_{p,q}^d$ of partially transposed permutations that are transposed only on the last q systems [Koi89; Ben+94; Hal96; Nik07]. In particular, $[\mathcal{A}_{p,q}^d, U^{\otimes p} \otimes \bar{U}^{\otimes q}] = 0$ for all $U \in U_d$. The usual Schur–Weyl duality corresponds to the special case when either $p = 0$ or $q = 0$.

Partially transposed permutations can be easily visualized as diagrams. If $\sigma \in S_{p+q}$ is a permutation on $p+q$ objects then its partial transpose σ^Γ is obtained by exchanging the last q inputs and outputs of σ :

$$\left(\begin{array}{c} \text{Diagram with } p=3 \text{ inputs and } q=2 \text{ outputs} \end{array} \right)^\Gamma = \begin{array}{c} \text{Diagram with } p=3 \text{ inputs and } q=2 \text{ outputs, inputs and outputs swapped} \end{array}. \quad (1)$$

While σ^Γ is no longer a permutation, we can still multiply such diagrams by concatenating them in the same way as permutations (in case closed loops appear in this process, we remove them and multiply the diagram by d^l where l is the number of loops). The set of all partially transposed permutation diagrams under this composition forms the *walled Brauer algebra* $\mathcal{B}_{p,q}^d := \text{span}_{\mathbb{C}}\{\sigma^\Gamma : \sigma \in S_{p+q}\}$, a diagrammatic algebra of dimension $\dim(\mathcal{B}_{p,q}^d) = (p+q)!$. In contrast, in quantum information we encounter only its matrix representation

$$\mathcal{A}_{p,q}^d := \psi_{p,q}^d(\mathcal{B}_{p,q}^d), \quad (2)$$

$\pi \in S_3$	e	$\sigma_2\sigma_1$	$\sigma_1\sigma_2$	σ_1	$\sigma_1\sigma_2\sigma_1$	σ_2
Diagram of π						
$R_{\text{nat}}(\pi)$	$\begin{pmatrix} 1 & 0 \\ 0 & 1 \end{pmatrix}$	$\begin{pmatrix} -1 & -1 \\ 1 & 0 \end{pmatrix}$	$\begin{pmatrix} 0 & 1 \\ -1 & -1 \end{pmatrix}$	$\begin{pmatrix} 1 & 0 \\ -1 & -1 \end{pmatrix}$	$\begin{pmatrix} -1 & -1 \\ 0 & 1 \end{pmatrix}$	$\begin{pmatrix} 0 & 1 \\ 1 & 0 \end{pmatrix}$
$R_{\text{semi}}(\pi)$	$\begin{pmatrix} 1 & 0 \\ 0 & 1 \end{pmatrix}$	$\frac{1}{2} \begin{pmatrix} -1 & -3 \\ 1 & -1 \end{pmatrix}$	$\frac{1}{2} \begin{pmatrix} -1 & 3 \\ -1 & -1 \end{pmatrix}$	$\begin{pmatrix} 1 & 0 \\ 0 & -1 \end{pmatrix}$	$\frac{1}{2} \begin{pmatrix} -1 & -3 \\ -1 & 1 \end{pmatrix}$	$\frac{1}{2} \begin{pmatrix} -1 & 3 \\ 1 & 1 \end{pmatrix}$
$R_{\text{orth}}(\pi)$	$\begin{pmatrix} 1 & 0 \\ 0 & 1 \end{pmatrix}$	$\frac{1}{2} \begin{pmatrix} -1 & -\sqrt{3} \\ \sqrt{3} & -1 \end{pmatrix}$	$\frac{1}{2} \begin{pmatrix} -1 & \sqrt{3} \\ -\sqrt{3} & -1 \end{pmatrix}$	$\begin{pmatrix} 1 & 0 \\ 0 & -1 \end{pmatrix}$	$\frac{1}{2} \begin{pmatrix} -1 & -\sqrt{3} \\ -\sqrt{3} & 1 \end{pmatrix}$	$\frac{1}{2} \begin{pmatrix} -1 & \sqrt{3} \\ \sqrt{3} & 1 \end{pmatrix}$

TABLE 1. Young’s natural, seminormal, and orthogonal form (denoted by R_{nat} , R_{semi} , and R_{orth} , respectively) for the two-dimensional irrep \square of the symmetric group S_3 .

where $\psi_{p,q}^d: \mathcal{B}_{p,q}^d \rightarrow \text{End}((\mathbb{C}^d)^{p+q})$ is a linear map from diagrams to matrices on $p+q$ qudits of dimension d . For example, the matrix representation of the diagram from eq. (1) has the following standard basis entries:

$$\langle x_1, \dots, x_5 | \psi_{3,2}^d \left(\begin{array}{c} \text{Diagram: 3 inputs, 2 outputs, crossing} \end{array} \right) | y_1, \dots, y_5 \rangle = \delta_{x_1, y_1} \delta_{x_2, y_3} \delta_{x_3, x_5} \delta_{x_4, y_5} \delta_{y_2, y_4}, \quad (3)$$

for any $x_1, \dots, x_5 \in [d]$ and $y_1, \dots, y_5 \in [d]$. In particular, note that

$$\text{SWAP}^\Gamma = \left(\begin{array}{c} \text{Diagram: two lines crossing} \end{array} \right)^\Gamma = \begin{array}{c} \text{Diagram: two lines crossing} \end{array} = d |\phi^+\rangle \langle \phi^+| \quad (4)$$

is proportional to the canonical maximally entangled state on two qudits (see also Table 2).

This interplay between permutations and entanglement is why the matrix algebra $\mathcal{A}_{p,q}^d$ and mixed Schur–Weyl duality is so relevant to quantum information. It appears in a variety of contexts, particularly in scenarios with multiple input and output systems such as quantum state purification [KW01b] and cloning [SIGA05; Fan+14; NPR21], port-based [MSSH18; SSMH17; Led20; Chr+21; SMK21] and multi-port-based teleportation [KMSH21; SMKH22; MSK21], and quantum algorithms [BLMMO21]. This symmetry also occurs in situations that involve the partial transpose on several systems, such as in entanglement detection [BCS20; BSH21], universality of qudit gate sets [SMZ22; DS22; SS22], and U_d -equivariant quantum circuits [HLM21; ZLLSK23]. It is also relevant in high-energy physics [KR07; Can11].

1.2. Historical context. The walled Brauer algebra $\mathcal{B}_{p,q}^d$ is a restricted version of the full Brauer algebra [Bra37], and a prominent example of a diagram algebra, which has been widely studied [Tur89; Koi89; Ben+94; Ben96; Nik07; Bul20] (see [Koe08] for a survey on Brauer and other diagram algebras). Mixed Schur–Weyl duality was established in [Koi89; Ben+94], where the matrix algebra $\mathcal{A}_{p,q}^d$ of partially transposed permutations was first introduced. Motivated by applications to quantum information, this algebra was subsequently studied in [MSK21; SMKH22]. In particular, the $q=1$ case was considered in [ZKW07; SHM13; MHS14; MSH18]. The characters of the walled Brauer algebra were first derived by Halverson [Hal96] (see also [Nik07]).

The representation theory of walled Brauer algebras has been strongly influenced by representation theory of symmetric group algebras, which correspond to the special case when either $p=0$ or $q=0$. The representation theory of the symmetric group is widely used and has a long history [Sag13; Rut48; CST10; How22]. In particular, there are three commonly used forms for irreducible representations of the symmetric group [Rut48] (see Table 1 for examples):

- (1) *Young’s natural form* provides invertible matrices with integer entries (i.e., in \mathbb{Z}),
- (2) *Young’s seminormal form* provides invertible matrices with rational entries (i.e., in \mathbb{Q}),
- (3) *Young’s orthogonal form* (also known as *Young–Yamanouchi basis*) provides real orthogonal matrices whose entries are square roots of rational numbers (i.e., in $\pm\sqrt{\mathbb{Q}_{\geq 0}}$).

The basis change between Young’s seminormal and orthogonal forms is diagonal and corresponds to normalization, while the basis change between seminormal and natural forms is triangular [AH21].

In the context of quantum information, Young’s orthogonal form is by far the most useful since it provides unitary matrices that can readily be used as operations in a quantum computer. In particular, irreps of this form are produced by the quantum Schur transform [Har05; Ber12]. Our goal is to extend Young’s orthogonal form from the symmetric group to the matrix algebra $\mathcal{A}_{p,q}^d$, and to derive the corresponding mixed Schur transform that decomposes $\mathcal{A}_{p,q}^d$ into irreps of this form.

Since our approach is based on a very general and well-established strategy that involves decomposing an algebra (or a group) into a chain of subalgebras (or subgroups), we will refer to the resulting basis as *Gelfand–Tsetlin basis*, a term that is commonly used for these types of constructions. Confusingly, this means that the basis we obtain can be referred to by three different names: “Young’s orthogonal form”, “Young–Yamanouchi basis”, and “Gelfand–Tsetlin basis”. We will use only the latter term throughout the rest of this paper.

1.3. Strategy. While the diagrammatic walled Brauer algebra $\mathcal{B}_{p,q}^d$ is well studied, its matrix representation $\mathcal{A}_{p,q}^d$ has received much less attention. A key difficulty in studying $\mathcal{A}_{p,q}^d$ is that

$$\mathcal{A}_{p,q}^d \cong \mathcal{B}_{p,q}^d / \ker(\psi_{p,q}^d) \quad (5)$$

according to eq. (2). While the linear map $\psi_{p,q}^d: \mathcal{B}_{p,q}^d \rightarrow \text{End}((\mathbb{C}^d)^{p+q})$ that turns diagrams into matrices has a simple description, see eqs. (3) and (48), its kernel $\ker(\psi_{p,q}^d)$ is non-trivial when $d < p + q$ and its basis has a rather complicated description. In addition, since $\mathcal{B}_{p,q}^d$ is not semisimple when $d < p + q - 1$ [CDDM08], it can be difficult to obtain results for $\mathcal{B}_{p,q}^d$ and then transfer them to $\mathcal{A}_{p,q}^d$ (which is always semisimple).

Our strategy hinges on the close connection between the walled Brauer algebra $\mathcal{B}_{p,q}^d$ and the group algebra $\mathbb{C}(S_p \times S_q)$ corresponding to its two symmetric subgroups. We will make use of the fact that $\mathcal{B}_{p,q}^d$ is generated by diagrams $\sigma_1, \dots, \sigma_{p+q-1}$ [Nik07] shown in eq. (41), where σ_i ($i \neq p$) are *transpositions* of consecutive systems i and $i + 1$ which generate $S_p \times S_q$, while the remaining generator σ_p *contracts* systems p and $p + 1$, e.g., see eq. (4) (see Definition 3.1 for more details). The matrix algebra $\mathcal{A}_{p,q}^d$ is generated by $\psi_{p,q}^d(\sigma_1), \dots, \psi_{p,q}^d(\sigma_{p+q-1})$.

1.4. Summary of our results. Our main technical result is Theorem 3.2, which provides an explicit construction of all irreducible representations of $\mathcal{A}_{p,q}^d$, the matrix algebra of partially transposed permutations on $p + q$ qudits. We provide a formula that allows to evaluate the irrep matrix entries on each of the generators, which by homomorphism and linearity fully determines the irrep on the rest of the algebra.

An important feature of our construction is that it provides irrep matrix entries in the Gelfand–Tsetlin basis. This basis has a recursive definition and hence is automatically adapted to a natural sequence of subalgebras obtained by including the generators σ_i one by one. This guarantees that the generators have a particularly sparse representation and gives a conceptually simple way to pinpoint their non-zero entries and describe their action. In addition, our basis coincides with the basis produced by the mixed quantum Schur transform. The conceptual simplicity of the Gelfand–Tsetlin basis together with its operational connection with the mixed quantum Schur transform is precisely what will allow us in Section 6 to derive an efficient quantum circuit for implementing the optimal port-based quantum teleportation protocol.

Theorem (Qualitative statement of Theorem 3.2). *When evaluated on one of the generators, any irreducible representation of the matrix algebra $\mathcal{A}_{p,q}^d$ has the following form:*

- *Transpositions σ_i ($i \neq p$) are represented by a direct sum of 1×1 and 2×2 blocks, where each 1×1 block is equal to ± 1 , while for each 2×2 block there is a constant $r \in \mathbb{Z}$ such that the block is equal to*

$$\begin{pmatrix} \frac{1}{r} & \sqrt{1 - \frac{1}{r^2}} \\ \sqrt{1 - \frac{1}{r^2}} & -\frac{1}{r} \end{pmatrix}, \quad (6)$$

which is an orthogonal reflection. The exact signs and values of r can be inferred from Young’s orthogonal form for symmetric groups.

- *The contraction σ_p is represented by a direct sum of rank-1 matrices with eigenvalue d .*

When $p = 0$ or $q = 0$, our formula reduces to the well-known Young’s orthogonal form for the symmetric group.

A concrete example of how all irreps of $\mathcal{A}_{3,2}^3$ look like in the Gelfand–Tsetlin basis is provided in Table 3. The main idea of the proof is that, thanks to this being the Gelfand–Tsetlin basis, we already know from Young’s orthogonal form how all generators (except for the contraction σ_p) are supposed to act. We made an educated guess for the matrix representation of σ_p and verified that it indeed works. This requires checking that the matrix representations of all generators satisfy the walled Brauer algebra relations stated in Definition 3.1.

As our second technical result, we investigate the mixed quantum Schur transform which can be used both to block diagonalize the matrix algebra $\mathcal{A}_{p,q}^d$ as well as to prepare the Gelfand–Tsetlin basis vectors. More specifically, in Theorem 4.1 of Section 4.3 we show that the rows of the mixed quantum Schur transform (or the Schur basis states) admit a matrix product state representation with bond dimension $(p + q)^{O(d^2)}$. This means that, for a constant local dimension d , we can compute the matrix entries of mixed Schur transform in polynomial time. In addition, Theorem 4.2 of Section 4.5 we provide an efficient quantum circuit with $\text{poly}(p + q, d, \log 1/\varepsilon)$ gates for computing the mixed Schur transform on a quantum computer. In particular, this transform achieves the Gelfand–Tsetlin basis from Theorem 3.2 on the walled Brauer algebra register.

1.4.1. *Application to SDP symmetry reduction.* Semidefinite optimization is an important tool in quantum information [ST21; Wat18]. When solving semidefinite optimization problems (SDPs), it is useful to take their symmetries into account, both in theory [BGSV12] and in practice [RMB21]. Eliminating irrelevant degrees of freedom, also known as *symmetry reduction*, can lead to significant computational savings and yield useful theoretical insights into the structure of solutions.

In quantum information, semidefinite optimization often intersects with Schur–Weyl duality due to the types of problems commonly investigated. If the SDP matrix variable, which typically represents a quantum state or a measurement operator, commutes with $U^{\otimes p}$, the problem can be significantly simplified by working in Schur basis. More generally, if the matrix variable, such as the Choi matrix of a quantum channel or superchannel, commutes with $U^{\otimes p} \otimes \bar{U}^{\otimes q}$, one should instead work in mixed Schur basis. We refer to this type of symmetry as *local unitary equivariance* since it most commonly occurs when considering the Choi matrix of a unitary-equivariant quantum channel (see Section 5.1 for more details). Recent examples where this symmetry occurs are quantum majority vote [BLMMO21], black-box transformations of quantum gates [QDSSM19b; QDSSM19a; QE21; YSM21; YSM22; Ebl+22], asymmetric cloning [NPR21; NPR23], entanglement witnesses [HKMV21], and monogamy of entanglement [All+23].

Our first application of the Gelfand–Tsetlin basis is for symmetry reduction of a general class of unitary-equivariant SDPs. Our main result in this regard is Theorem 5.2, which generalizes [GO22] from linear to semidefinite optimization with unitary symmetries.

Theorem (Qualitative statement of Theorem 5.2). *An SDP with a matrix variable $X \succeq 0$ subject to unitary equivariance $[X, U^{\otimes p} \otimes \bar{U}^{\otimes q}] = 0$ for all $U \in \mathcal{U}_d$, can be reduced from $d^{2(p+q)}$ variables to $\dim(\mathcal{A}_{p,q}^d)$ variables. This reduction can be computed in time polynomial in $\dim(\mathcal{A}_{p,q}^d)$.*

For example, in the regime where p and q are small constants while d is large (e.g., $p = 2$, $q = 3$, $d = 1000$), solving the SDP is clearly impossible by conventional methods since it has $1000^{10} = 10^{30}$ variables. In contrast, our method reduces it to a problem with only $(2 + 3)! = 5! = 120$ variables. When d is also small, even fewer variables suffice (e.g., 42 variables when $d = 2$, see Appendix E of [GO22]).

1.4.2. *Application to port-based teleportation.* Our second application of the Gelfand–Tsetlin basis is to port-based teleportation. In Theorem 6.1 we provide an efficient quantum circuit for port-based teleportation based on mixed quantum Schur transform. This is a long-standing open problem that has been open since the invention of port-based teleportation [IH08; IH09].

Together these two applications demonstrate the power of walled Brauer algebra techniques when applied to problems in quantum information, and suggests further possible applications of our Gelfand–Tsetlin basis and mixed quantum Schur transform. We expect it to be particularly useful for deriving quantum circuits for general unitary-equivariant quantum channels.

1.5. **Related work.** Young’s natural representation for the walled Brauer algebra has been constructed by Nikitin [Nik07], while Young’s orthogonal and seminormal forms for the full Brauer algebra are described in [Naz96] and [EG], respectively. In addition, [ST17] has obtained a seminormal form for the q -deformed version of the walled Brauer algebra. However, taking the “classical” $q \rightarrow 1$ limit of their construction and renormalizing the resulting basis vectors to obtain the corresponding orthogonal form is non-trivial. Moreover, their construction only works for semisimple walled Brauer algebras $\mathcal{B}_{p,q}^d$, so the problem of adapting their construction to $\mathcal{A}_{p,q}^d$ is still open. In the context of quantum information, the $q = 1$ case of $\mathcal{A}_{p,q}^d$ before our work was studied in [SHM13; MHS14; MSH18], and some aspects of the general q case were studied in [SMKH22].

While preparing our manuscript, we became aware of two simultaneous works [Ngu23; FTH23], which achieve similar results as ours. In particular, [Ngu23] constructs mixed quantum Schur transform in the same way as our Theorem 4.2, based on the original construction from [BCH06; Har05]. However, they have a number of different applications which do not intersect with our applications. The second work [FTH23] finds an efficient implementation of the pretty good measurement for the optimal port-based teleportation protocol by decomposing induced representations. They achieve a similar result as our Theorem 6.1, i.e., they construct a protocol with polynomial complexity. However, their approach is different from ours and is based on the other side of the Schur–Weyl duality: they induce from the symmetric group register, while we decompose a tensor product of unitary irreducible representations via the dual Clebsch–Gordan transform from our Theorem 4.2. Thus our approaches are complimentary to each other in a representation-theoretic sense.

Various applications of the quantum Schur transform were recently studied in a number of papers [HS18; HST19; ZLLSK23]. In [HS18; HST19], authors computed the matrix entries of the quantum Schur transform, although only for qubits. Ref. [ZLLSK23] studies how to define efficient ansatzes for variational quantum algorithms for problems with $U^{\otimes n}$ symmetry. We expect our work to be useful in extending their results to the setting of unitary-equivariance symmetry $U^{\otimes p} \otimes \bar{U}^{\otimes q}$.

In our previous work [GO22], we used the method developed in [DLS18] to compute the primitive central idempotents of $\mathcal{A}_{p,q}^d$, which is the same as determining the diagonal matrix units (or diagonal entries of irreps).

In this paper, we determine all irrep entries, including the off-diagonal ones. This immediately allows us to extend our previous application from linear to semidefinite programming with unitary symmetries.

2. PRELIMINARIES

2.1. Young diagrams and tableaux. A *partition* $\lambda \vdash p$ of an integer $p \geq 0$ is a tuple of integers $\lambda = (\lambda_1, \dots, \lambda_k)$ such that $\lambda_1 \geq \dots \geq \lambda_k \geq 0$ and $\lambda_1 + \dots + \lambda_k = p$. We denote by $\ell(\lambda) = \max\{k : \lambda_k > 0\}$ the *length* of λ . A partition $\lambda \vdash p$ can be graphically represented as a *Young diagram*—a collection of p cells arranged in k rows with λ_i of them in the i -th row. For example,

$$\begin{array}{|c|c|c|} \hline & & \\ \hline & & \\ \hline \end{array} \quad (7)$$

represents the partition $\lambda = (3, 1)$. We call $\mu = (\mu_1, \dots, \mu_{k'})$ a *subpartition* of $\lambda = (\lambda_1, \dots, \lambda_k)$, and write $\mu \subseteq \lambda$ if $k' \leq k$ and $\mu_i \leq \lambda_i$ for $i = 1, \dots, k'$. The *size* $|\lambda|$ of Young diagram denotes the number of boxes p .

Any cell $u \in \lambda$ of a Young diagram λ can be specified by its row and column coordinates i and j . The *content* of cell $u = (i, j)$ is

$$\text{cont}(u) := j - i. \quad (8)$$

For example, the cells of the Young diagram $(5, 3, 3)$ have the following content:

$$\begin{array}{|c|c|c|c|c|} \hline 0 & 1 & 2 & 3 & 4 \\ \hline -1 & 0 & 1 & & \\ \hline -2 & -1 & 0 & & \\ \hline \end{array}. \quad (9)$$

Note that content is constant on diagonals of λ and indicates how far each diagonal is from the main one. Content increases by one when going right or up, and decreases by one when going left or down. The *axial distance* (also known as *hook* or *Manhattan distance*) between two cells $u = (i, j)$ and $v = (i', j')$ in a Young diagram is

$$r(u, v) := \text{cont}(v) - \text{cont}(u). \quad (10)$$

For example, the axial distance from cell u to all other cells in the Young diagram $(5, 3, 3)$ is as follows:

$$\begin{array}{|c|c|c|c|c|} \hline -1 & u & 1 & 2 & 3 \\ \hline -2 & -1 & 0 & & \\ \hline -3 & -2 & -1 & & \\ \hline \end{array}. \quad (11)$$

For a Young diagram λ , a cell $u \in \lambda$ is called *removable* if the diagram λ/u obtained by removing the cell u from λ is a valid Young diagram. Similarly, a cell $u \notin \lambda$ is called *addable* if the diagram $\lambda \cup u$ obtained by adding the cell u to λ is a valid Young diagram. The set of all removable cells of λ is denoted by $\text{RC}(\lambda)$, while the set of all addable cells by $\text{AC}(\lambda)$. For example, the Young diagram $\lambda = (5, 3, 3)$ (shown in gray) has two removable cells (shown in white): $r_1 = (1, 5)$, $r_2 = (3, 3)$, and three addable cells: $a_1 = (1, 6)$, $a_2 = (2, 4)$, $a_3 = (4, 1)$:

$$\begin{array}{|c|c|c|c|c|c|} \hline & & & & r_1 & a_1 \\ \hline & & & & a_2 & \\ \hline & & & r_3 & & \\ \hline a_4 & & & & & \\ \hline \end{array}. \quad (12)$$

A *Young tableau* T of shape $\lambda \vdash p$ is a Young diagram with cells filled with some natural numbers. A *standard Young tableau* T of shape $\lambda \vdash p$ is obtained by filling the boxes of the Young diagram λ with symbols from $[p] := \{1, \dots, p\}$ strictly increasing across rows and down the columns. For example,

$$T_1 = \begin{array}{|c|c|c|} \hline 1 & 2 & 3 \\ \hline 4 & & \\ \hline \end{array}, \quad T_2 = \begin{array}{|c|c|c|} \hline 1 & 2 & 4 \\ \hline 3 & & \\ \hline \end{array}, \quad T_3 = \begin{array}{|c|c|c|} \hline 1 & 3 & 4 \\ \hline 2 & & \\ \hline \end{array} \quad (13)$$

are all standard Young tableaux of shape $\lambda = (3, 1)$. The set of all standard Young tableaux of a given shape λ is denoted as $\text{SYT}(\lambda)$. According to the well-known *hook length formula*,

$$|\text{SYT}(\lambda)| = \frac{(\lambda_1 + \dots + \lambda_d)!}{\prod_{u \in \lambda} h(u)} =: d_\lambda \quad (14)$$

where $h(u)$ denotes the *hook length* of cell u (the number of boxes to the right and below u , including u itself).

Notice that any standard Young tableau $T \in \text{SYT}(\lambda)$ can be represented as a sequence of $(p + 1)$ Young diagrams

$$T = (T^0, \dots, T^p), \quad (15)$$

such that $T^i \vdash i$, $T^i \subseteq T^{i+1}$, and $T^p = \lambda$. Indeed, T^i is obtained from the Young diagram $\lambda \vdash p$ by keeping only those boxes of T whose symbols are in $[i]$. For example, the Young tableau T_1 from eq. (13) is represented by the following sequence of Young diagrams (see also Fig. 1):

$$T_1 = \left(\emptyset, \begin{array}{|c|} \hline \square \\ \hline \end{array}, \begin{array}{|c|c|} \hline \square & \square \\ \hline \end{array}, \begin{array}{|c|c|c|} \hline \square & \square & \square \\ \hline \end{array}, \begin{array}{|c|c|c|} \hline \square & \square & \square \\ \hline \square & & \end{array} \right). \quad (16)$$

Consider a standard Young tableau $T \in \text{SYT}(\lambda)$ of shape $\lambda \vdash p$ and an arbitrary permutation $\pi \in S_p$. We will denote by πT the tableau obtained by permuting cell fillings of T according to π . For example, the Young tableaux T_1, T_2, T_3 presented in eq. (13) are related in the following way: $T_2 = (34)T_1$, $T_3 = (23)T_2 = (234)T_1$, where $(34), (23), (234) \in S_4$. Note that πT is not necessarily a standard tableau, e.g., consider $(14)T_1$.

Given a standard Young tableau T , we define

$$\text{cont}_i(T) := \text{cont}(T^i \setminus T^{i-1}). \quad (17)$$

This is simply the content of the cell of T containing i . Moreover, we define $r_i(T)$ to be the hook distance between cells containing i and $i+1$, i.e.,

$$r_i(T) := \text{cont}_{i+1}(T) - \text{cont}_i(T). \quad (18)$$

A *semistandard Young tableau* M of a shape λ and entries in $[d]$ is obtained by filling the boxes of a Young diagram λ with symbols from $[d]$ weakly increasing across the rows and strictly increasing down the columns. For example,

$$M_1 = \begin{array}{|c|c|c|} \hline 1 & 1 & 1 \\ \hline 2 & & \end{array}, \quad M_2 = \begin{array}{|c|c|c|} \hline 1 & 1 & 2 \\ \hline 2 & & \end{array}, \quad M_3 = \begin{array}{|c|c|c|} \hline 1 & 2 & 2 \\ \hline 2 & & \end{array} \quad (19)$$

are all semistandard Young tableaux of shape $\lambda = (3, 1)$ with entries in $[2]$. We will denote the set of all semistandard Young tableaux of shape λ and entries in $[d]$ by $\text{SSYT}(\lambda, d)$. According to the well-known *Weyl dimension formula* [Lou08, eq. (11.46)] and *hook-content formula*,

$$|\text{SSYT}(\lambda, d)| = \prod_{1 \leq i < j \leq d} \frac{\lambda_i - \lambda_j + j - i}{j - i} = \frac{\prod_{u \in \lambda} (d + \text{cont}(u))}{\prod_{u \in \lambda} h(u)} =: m_\lambda. \quad (20)$$

Recording the number of times each number appears in tableau M gives a sequence known as the *weight* of M , denoted as $w(M)$:

$$w(M)_i := \text{“the number of } i\text{'s in tableau } M\text{”}. \quad (21)$$

For example, the tableaux presented in eq. (19) have weights $(3, 1)$, $(2, 2)$, and $(1, 3)$, respectively. We can extend the notion of weight also to sequences of natural numbers. The *weight* $w(x_1, \dots, x_k)$ of a sequence x_1, \dots, x_k records the number of times each natural number appears in it. For example,

$$1, 2, 2, 2, \quad 2, 1, 2, 2, \quad 2, 2, 1, 2, \quad 2, 2, 2, 1 \quad (22)$$

are all sequences of weight $w(M) = (1, 3)$.

2.2. Bratteli diagram and Gelfand–Tsetlin basis. An algebra over \mathbb{C} is *semisimple* if it is isomorphic to a direct sum $\bigoplus_{i=1}^k \text{End}(\mathbb{C}^{n_i})$ of full matrix algebras, for some integers $k, n_1, \dots, n_k \geq 1$ [Cox12, Theorem 2.2.4]. Following [DLS18], we call a sequence

$$\mathcal{A}_0 \hookrightarrow \mathcal{A}_1 \hookrightarrow \dots \hookrightarrow \mathcal{A}_n \quad (23)$$

of finite-dimensional semisimple algebras over \mathbb{C} a *multiplicity-free family* if

- (a) $\mathcal{A}_0 \cong \mathbb{C}$,
- (b) each embedding $\mathcal{A}_i \hookrightarrow \mathcal{A}_{i+1}$ is unity-preserving¹, and
- (c) the restriction from \mathcal{A}_{i+1} to \mathcal{A}_i is multiplicity-free².

A canonical example of such family is the sequence $\mathbb{CS}_0 \hookrightarrow \mathbb{CS}_1 \hookrightarrow \dots \hookrightarrow \mathbb{CS}_n$ of symmetric group algebras, where \mathbb{CS}_i is embedded into \mathbb{CS}_{i+1} by acting trivially on the element $i+1$ [OV96; VO05]. Two other examples of such families are walled Brauer algebras $\mathcal{B}_{p,q}^d$ and partially transposed permutation matrix algebras $\mathcal{B}_{p,q}^d$ that will be particularly important to us (see Sections 3.1 and 3.2 for more details).

To any multiplicity-free family of algebras $\mathcal{A}_0 \hookrightarrow \mathcal{A}_1 \hookrightarrow \dots \hookrightarrow \mathcal{A}_n$ we can associate a *Bratteli diagram*. It is a directed acyclic simple graph (V, E) whose vertices correspond to simple modules of \mathcal{A}_i and edges show how they decompose when restricted to the previous subalgebra \mathcal{A}_{i-1} [Bra72]. More specifically, the vertices of the Bratteli diagram are divided into levels $i = 0, \dots, n$, i.e., $V = V_0 \sqcup V_1 \sqcup \dots \sqcup V_n$, where V_i denotes the set of vertices at *level* i . Furthermore, at level 0 the set $V_0 := \{\emptyset\}$ contains only the *root* \emptyset , while at levels $i = 1, \dots, n$ the set $V_i := \hat{\mathcal{A}}_i$ contains the labels of all non-isomorphic simple modules of \mathcal{A}_i . We will call the

¹It maps the unit (i.e., the identity matrix) of one algebra to the unit of the other algebra.

²This means that the restriction of any simple \mathcal{A}_{i+1} -module to \mathcal{A}_i is isomorphic to a direct sum of pairwise non-isomorphic simple \mathcal{A}_i -modules.

vertices at level n leaves. We draw an edge³ $\lambda \rightarrow \mu$ from vertex $\lambda \in \widehat{\mathcal{A}}_i$ to vertex $\mu \in \widehat{\mathcal{A}}_{i+1}$ if and only if the simple module V^λ corresponding to λ is isomorphic to a direct summand in $\text{Res}_{\mathcal{A}_i}^{\mathcal{A}_{i+1}} V^\mu$, the restriction of V^μ to the subalgebra \mathcal{A}_i , see Fig. 1.

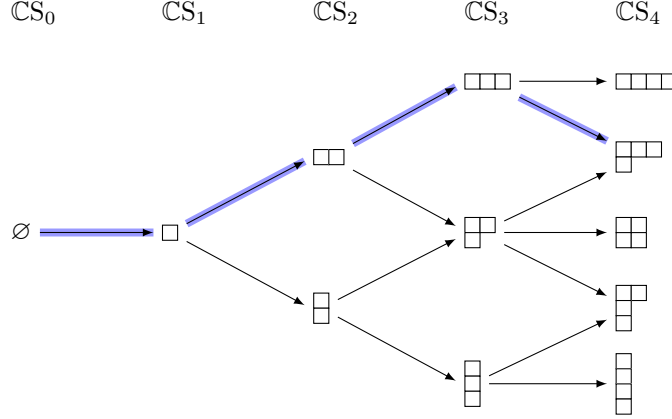


FIGURE 1. The Bratteli diagram for the family of symmetric group algebras $\mathbb{CS}_0 \hookrightarrow \mathbb{CS}_1 \hookrightarrow \mathbb{CS}_2 \hookrightarrow \mathbb{CS}_3 \hookrightarrow \mathbb{CS}_4$, also known as Young’s lattice. The vertices at level k are labelled by Young diagrams $\lambda \vdash k$ corresponding to all non-isomorphic irreducible representations of \mathbb{CS}_k . We have highlighted the path corresponding to sequence (16) and terminating at leaf $\lambda = (3, 1)$.

Paths⁴ in the Bratteli diagram play an important role in the representation theory of the corresponding algebras, so we will introduce some notation for them. If λ and μ are two vertices at levels $i < j$ of the Bratteli diagram, we will denote the set of all paths from λ to μ by

$$\text{Paths}_{i,j}(\lambda, \mu). \quad (24)$$

We will denote the set of all paths starting at the root \emptyset and terminating at vertex λ at level j by

$$\text{Paths}_j(\lambda) := \text{Paths}_{0,j}(\emptyset, \lambda). \quad (25)$$

When $j = n$, i.e., λ is a leaf, we will abbreviate this to

$$\text{Paths}(\lambda) := \text{Paths}_n(\lambda). \quad (26)$$

An arbitrary path $T = (T^0, \dots, T^n)$ in the Bratteli diagram can be *decomposed* at level $i \in \{0, \dots, n\}$ as $T = T_1 \circ T_2$ where $T_1 = (T^0, \dots, T^i)$ and $T_2 = (T^i, \dots, T^n)$ belong to $\text{Paths}_i(T^i)$ and $\text{Paths}_{i,n}(T^i, T^n)$, respectively.

An irreducible representation $\lambda \in \widehat{\mathcal{A}}_n$ of \mathcal{A}_n corresponds to a leaf λ of the Bratteli diagram. The basis for the representation space V^λ of λ is indexed by all paths from the root \emptyset to λ . We call this the *Gelfand–Tsetlin basis* for the multiplicity-free family $\mathcal{A}_0 \hookrightarrow \mathcal{A}_1 \hookrightarrow \dots \hookrightarrow \mathcal{A}_n$. Such basis can be obtained by choosing any leaf $\lambda \in \widehat{\mathcal{A}}_n$ and considering the restriction $\text{Res}_{\mathcal{A}_{n-1}}^{\mathcal{A}_n} V^\lambda$ of the corresponding simple \mathcal{A}_n -module V^λ to \mathcal{A}_{n-1} , which is multiplicity-free. This restriction can then be iterated further along any path in the Bratteli diagram towards the root \emptyset that corresponds to the one-dimensional algebra $\mathcal{A}_0 \cong \mathbb{C}$. Doing this along all $\text{Paths}(\lambda)$ connecting \emptyset and λ results in a decomposition of the chosen simple \mathcal{A}_n -module V^λ into one-dimensional simple \mathcal{A}_0 -modules. Repeating this procedure for all leaves $\lambda \in \widehat{\mathcal{A}}_n$ produces the full *Gelfand–Tsetlin basis* of $\bigoplus_{\lambda \in \widehat{\mathcal{A}}_n} V^\lambda$, which consists of all paths in the Bratteli diagram.

As an example, consider the sequence of symmetric group algebras

$$\mathbb{CS}_0 \hookrightarrow \mathbb{CS}_1 \hookrightarrow \dots \hookrightarrow \mathbb{CS}_p. \quad (27)$$

It is well-known that irreducible representations $\widehat{\mathbb{CS}}_i$ of the symmetric group algebra \mathbb{CS}_i (or equivalently the symmetric group S_i itself) are in one-to-one correspondence with Young diagrams $\lambda \vdash i$, and that the sequence (27) of subalgebras is multiplicity-free. Hence, the vertices of the corresponding Bratteli diagram are labelled by Young diagrams $\lambda \vdash i$. Moreover, two vertices $\mu \vdash (i-1)$ and $\lambda \vdash i$ are connected if μ is a sub-diagram of λ obtained by removing one box, see Fig. 1. As a consequence, the sequence (27) determines the Gelfand–Tsetlin basis of the module corresponding to any irreducible representation $\lambda \in \widehat{\mathbb{CS}}_p$, also known as the *Young–Yamanouchi basis* for symmetric group. Vectors of this basis are labelled by paths $T \in \text{Paths}(\lambda)$ ending at vertex λ in the Bratteli diagram. Notice that such paths are in one-to-one correspondence with the elements

³The notion of Bratteli diagram can be extended to sequences of algebras which are not necessarily multiplicity-free. In that case the corresponding graph is not simple anymore, and the number of edges connecting vertices λ and μ is equal to the number of direct summands in $\text{Res}_{\mathcal{A}_i}^{\mathcal{A}_{i+1}} V^\mu$ isomorphic to V^λ , i.e., the multiplicity of V^λ in the restriction of V^μ .

⁴By a “path” we always mean a *directed path*, i.e., a path that traverses edges only in the allowed direction (from lower to higher levels).

of $\text{SYT}(\lambda)$ since the i -th edge in the path indicates where the box containing i appears in the standard tableau. This implies that the dimension of $\text{irrep } \lambda \in \widehat{\text{CS}}_p$ is equal to $|\text{Paths}(\lambda)| = |\text{SYT}(\lambda)|$, i.e., the number of standard Young tableaux of shape λ . Recall that $S_p = \langle \sigma_1, \dots, \sigma_{p-1} \rangle$, i.e., S_p is generated by transpositions $\sigma_i = (i, i+1)$ that exchange two consecutive elements i and $i+1$. The action of these generators has a remarkably simple form in the Young–Yamanouchi basis. Indeed, consider a basis vector $|T\rangle \in V^\lambda$ where $T \in \text{SYT}(\lambda)$ in the representation space V^λ of $\text{irrep } \lambda$. Then σ_i acts on $|T\rangle$ in the following way:

$$\sigma_i |T\rangle = \frac{1}{r_i(T)} |T\rangle + \sqrt{1 - \frac{1}{r_i(T)^2}} |\sigma_i T\rangle \quad (28)$$

where $r_i(T)$ is the axial distance between cells containing i and $i+1$ in the Young tableau T , see eq. (18), and $\sigma_i T \in \text{SYT}(\lambda)$ is the tableau T with numbers i and $i+1$ exchanged, see Section 2.1. Note that $r_i(T) = \pm 1$ whenever $\sigma_i T$ is not a standard Young tableau, hence the coefficient in front of $|\sigma_i T\rangle$ vanishes. Our main technical result (see Theorem 3.2), generalizes eq. (28) to the matrix algebra $\mathcal{A}_{p,q}^d$ of partially transposed permutations.

2.3. Gelfand–Tsetlin patterns. A *Gelfand–Tsetlin pattern* M of shape λ and length d is represented by a triangular table with d rows and i integers in the i -th row (when counted from the bottom):

$$M = \begin{bmatrix} m_{1,d} & & m_{2,d} & & \cdots & & m_{d-1,d} & & m_{d,d} \\ & m_{1,d-1} & & \cdots & & & m_{d-1,d-1} & & \\ & & \ddots & & \vdots & & \ddots & & \\ & & & m_{1,2} & & m_{2,2} & & \ddots & \\ & & & & m_{1,1} & & & & \end{bmatrix} = \begin{bmatrix} \mathbf{m}_d \\ \mathbf{m}_{d-1} \\ \vdots \\ \mathbf{m}_2 \\ \mathbf{m}_1 \end{bmatrix}, \quad (29)$$

where $\mathbf{m}_j := (m_{1,j}, \dots, m_{j,j})$ denotes the j -th row of M . The entries $m_{i,j}$ of M are subject to the following constraints: the top row of M is equal to λ , i.e., $\mathbf{m}_d = (m_{1,d}, \dots, m_{d,d}) = (\lambda_1, \dots, \lambda_d)$, and all entries $m_{i,j}$ satisfy the so-called *interlacing* or *in-betweenness* condition:

$$m_{i,j} \geq m_{i,j-1} \geq m_{i+1,j} \quad \text{for all } 1 \leq i < j \leq d. \quad (30)$$

We will write $\mathbf{m}_{j-1} \sqsubseteq \mathbf{m}_j$ as a shorthand for the interlacing relations (30) between vectors \mathbf{m}_{j-1} and \mathbf{m}_j . We will denote the set of all Gelfand–Tsetlin patterns of shape λ and length d by $\text{GT}(\lambda, d)$.

For any partition λ of length d , the Gelfand–Tsetlin patterns $\text{GT}(\lambda, d)$ are in one-to-one correspondence with semistandard Young tableaux $\text{SSYT}(\lambda, d)$:

$$|\text{GT}(\lambda, d)| = |\text{SSYT}(\lambda, d)| = m_\lambda. \quad (31)$$

Indeed, for any tableau $T \in \text{SSYT}(\lambda, d)$ let $m_{i,j}$ be the number of symbols from $[j]$ in the i -th row of T . Equivalently, $\mathbf{m}_j \subseteq \lambda$ is the shape of the subtableau of T formed by entries less or equal to j . Then eq. (29) constitutes the Gelfand–Tsetlin pattern of tableau T . For example, the Gelfand–Tsetlin patterns corresponding to the semistandard Young tableaux in eq. (19) are

$$M_1 = \begin{bmatrix} 3 & & 1 \\ & 3 & \\ & & 1 \end{bmatrix}, \quad M_2 = \begin{bmatrix} 3 & & 1 \\ & 2 & \\ & & 1 \end{bmatrix}, \quad M_3 = \begin{bmatrix} 3 & & 1 \\ & 1 & \\ & & 1 \end{bmatrix}, \quad (32)$$

which are in fact all Gelfand–Tsetlin patterns $\text{GT}(\lambda, d)$ of shape $\lambda = (3, 1)$ and length $d = 2$. Conversely, given any Gelfand–Tsetlin pattern M , the corresponding semistandard tableau T has shape $\lambda = \mathbf{m}_1$ given by the first row of M , while the filling of the i -th row of T can be deduced from the i -th diagonal of M . Indeed, $m_{i,j} - m_{i,j-1}$ is the number of j 's in the i -th row of T .

The *weight* of Gelfand–Tsetlin pattern M consists of differences of consecutive row sums:

$$w(M) := (w(\mathbf{m}_1), w(\mathbf{m}_2) - w(\mathbf{m}_1), \dots, w(\mathbf{m}_d) - w(\mathbf{m}_{d-1})) \quad \text{where} \quad w(\mathbf{m}_j) := \sum_{i=1}^j m_{i,j}. \quad (33)$$

Notice that the weight of a Gelfand–Tsetlin pattern coincides with the weight (21) of the corresponding semistandard Young tableau. For example, the patterns (32) have weights $(3, 1)$, $(2, 2)$, and $(1, 3)$, respectively.

2.4. Mixed Young diagrams and tableaux. In this section, we define combinatorial notions analogous to Young diagrams and tableaux that will be used in Section 4 to describe mixed Schur–Weyl duality and mixed quantum Schur transform. First, let us first describe three equivalent ways of representing a pair of Young diagrams.

A *mixed Young diagram* of length d is a pair of Young diagrams $\lambda = (\lambda_l, \lambda_r)$ of total length at most d : $\ell(\lambda_l) + \ell(\lambda_r) \leq d$. Equivalently, we can represent λ by combining the diagrams λ_l and λ_r into a single *staircase* $\tilde{\lambda} \in \mathbb{Z}^d$ obtained by subtracting from $\lambda_l = (\lambda_{l,1}, \dots, \lambda_{l,d})$ the reverse of $\lambda_r = (\lambda_{r,1}, \dots, \lambda_{r,d})$ [Ste87]:

$$\tilde{\lambda} := (\lambda_{l,1} - \lambda_{r,d}, \lambda_{l,2} - \lambda_{r,d-1}, \dots, \lambda_{l,d} - \lambda_{r,1}). \quad (34)$$

Intuitively, the staircase $\tilde{\lambda}$ corresponds to rotating the diagram λ_r by 180 degrees and attaching it at the bottom of λ_l (see Fig. 2). Since $\ell(\lambda_l) + \ell(\lambda_r) \leq d$, this operation is reversible and one can easily recover λ_l and λ_r from the staircase $\tilde{\lambda}$. Finally, a third way of representing the same concept is via *walled concatenation* $(\hat{\lambda}, s)$ where $s := \lambda_{r,1}$ and $\hat{\lambda}$ is a Young diagram of shape

$$\hat{\lambda} := \lambda_{r,1} + \tilde{\lambda} = (\lambda_{r,1} + \lambda_{l,1} - \lambda_{r,d}, \lambda_{r,1} + \lambda_{l,2} - \lambda_{r,d-1}, \dots, \lambda_{r,1} + \lambda_{l,d-1} - \lambda_{r,2}, \lambda_{l,d}). \quad (35)$$

This diagram corresponds to shifting the staircase $\tilde{\lambda}$ to the right by $\lambda_{r,1}$ boxes so that all its entries become non-negative. Equivalently, we can obtain $\hat{\lambda}$ by adding $\lambda_{r,1}$ columns of d boxes on the left of λ_l and then removing the diagram λ_r (rotated by 180 degrees) from the bottom of these columns (see Fig. 2). This process is reversible, so we can easily convert $(\hat{\lambda}, s)$ back into the pair of diagrams (λ_l, λ_r) or the staircase $\tilde{\lambda}$. Mixed Young diagrams, walled concatenations, and staircases are three equivalent ways of thinking about the same combinatorial object, see Fig. 2. Throughout the paper we will use the same symbol λ to denote either of these three concepts, depending on the convenience in a given context.

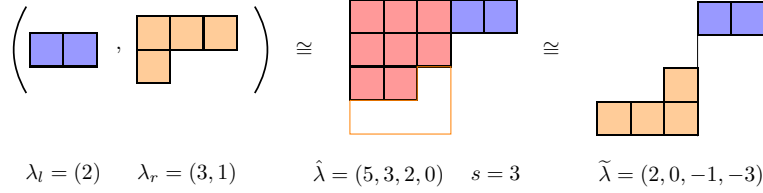


FIGURE 2. Three equivalent ways of representing a pair of Young diagrams: as a mixed Young diagram $\lambda = (\lambda_l, \lambda_r)$, as a staircase $\tilde{\lambda}$, or as a walled concatenation $(\hat{\lambda}, \lambda_{r,1})$. Here the total length of all tableaux is $d = 4$.

Gelfand–Tsetlin patterns (29) generalize straightforwardly to mixed Young diagrams simply by allowing the entries $m_{i,j}$ of the pattern to be negative. In particular, the first row $\mathbf{m}_d = (m_{1,d}, \dots, m_{d,d})$ of a Gelfand–Tsetlin pattern does not have to be a partition but may also be a staircase. Formally, for any mixed Young diagram λ we let $\text{GT}(\lambda, d) := \text{GT}(\tilde{\lambda}, d)$, i.e., Gelfand–Tsetlin patterns of shape λ are defined as those of the corresponding staircase $\tilde{\lambda}$.⁵ Equivalently, one can replace the staircase $\tilde{\lambda}$ by the walled concatenation $\hat{\lambda}$ and consider the set $\text{GT}(\hat{\lambda}, d)$ instead. Indeed, there is a simple bijection between the sets $\text{GT}(\tilde{\lambda}, d)$ and $\text{GT}(\hat{\lambda}, d)$: for any $M \in \text{GT}(\tilde{\lambda}, d)$ one can construct the corresponding $M' \in \text{GT}(\hat{\lambda}, d)$ by subtracting $\tilde{\lambda}_d = m_{d,d}$ from each entry $m_{i,j}$ of the pattern M . In particular, this implies that

$$|\text{GT}(\tilde{\lambda}, d)| = |\text{GT}(\hat{\lambda}, d)| = m_{\hat{\lambda}}, \quad (36)$$

where $m_{\hat{\lambda}}$ can be computed using eq. (20).

Recall from Section 2.3 that for any Young diagram λ , the Gelfand–Tsetlin patterns $\text{GT}(\lambda, d)$ are in one-to-one correspondence with semistandard Young tableaux $\text{SSYT}(\lambda, d)$. Similarly, for any staircase $\tilde{\lambda}$, one can interpret $\text{GT}(\tilde{\lambda}, d)$ as *mixed semistandard Young tableaux*.

Recall from eq. (15) that a sequence of Young diagrams can be interpreted as a standard Young tableau. Similarly, for any shape $\lambda = (\lambda_l, \lambda_r)$, where $\lambda_l \vdash p - k$ and $\lambda_r \vdash q - k$ for some $p, q \geq 0$ and $k \geq 0$ such that $0 \leq k \leq \min(p, q)$, we define a *mixed standard Young tableau* T of length d as a sequence $(T^0, T^1, T^2, \dots, T^{p+q})$ of mixed Young diagrams such that each T^i has length d and

- (1) $T^0 := (\emptyset, \emptyset)$ and $T^{p+q} := \lambda = (\lambda_l, \lambda_r)$,
- (2) if $p \geq i \geq 1$ then $T_l^{i-1} \subseteq T_l^i$ with $|T_l^{i-1}| + 1 = |T_l^i|$ and $T_r^{i-1} = T_r^i = \emptyset$,
- (3) if $p + q \geq i > p$ then either
 - (a) $T_l^i \subseteq T_l^{i-1}$ with $|T_l^i| + 1 = |T_l^{i-1}|$ and $T_r^{i-1} = T_r^i$, or
 - (b) $T_r^{i-1} \subseteq T_r^i$ with $|T_r^{i-1}| + 1 = |T_r^i|$ and $T_l^{i-1} = T_l^i$.

Such sequence corresponds to a path in a certain Bratteli diagram (see Section 3.3 for more details).

Similar to eqs. (13) and (16), we can translate a sequence T of mixed Young diagrams into what is essentially a pair of standard tableaux, thus justifying calling T a *mixed standard Young tableau*. The first p steps of this translation build up the left tableau following the same procedure as described in Section 2.1. The remaining steps either build up the right tableau in the same way or add secondary entries to the left tableau indicating at which steps the corresponding boxes are removed. For example, when $p = 3$, $q = 2$, and $k = 1$, the sequence

$$T = ((\emptyset, \emptyset), (\square, \emptyset), (\square\square, \emptyset), (\square\square\square, \emptyset), (\square\square, \emptyset), (\square\square, \square)) \quad (37)$$

⁵This is a slight abuse of notation, as λ in $\text{GT}(\lambda, d)$ may be either a single Young diagram or a pair of Young diagrams. However, it will always be clear from context what kind of object λ is. Furthermore, both notions agree when the right diagram in a pair of diagrams is empty: $\text{GT}((\lambda_l, \emptyset), d) = \text{GT}(\lambda_l, d)$ for any Young diagram λ_l . Alternatively, one can always think of λ as a staircase, in which case no ambiguity arises.

corresponds to the following pair of tableau:

$$T = \left(\begin{array}{|c|c|c|} \hline 1 & 2 & 3,4 \\ \hline \end{array}, \begin{array}{|c|} \hline 5 \\ \hline \end{array} \right). \quad (38)$$

This is a mixed Young tableau of shape $\lambda = ((2), (1))$ since the left tableau has only two boxes remaining. Similar to Section 2.1, for any permutation $\pi \in S_p \times S_q$ we will write πT to denote the tableau obtained by permuting the cell fillings of T according to π .

3. REPRESENTATION THEORY OF PARTIALLY TRANSPOSED PERMUTATION MATRIX ALGEBRA

3.1. Walled Brauer algebra $\mathcal{B}_{p,q}^d$. Let $p, q \geq 0$ be integers and $d \in \mathbb{C}$ arbitrary⁶. The *walled Brauer algebra* $\mathcal{B}_{p,q}^d$ consists of formal complex linear combinations of diagrams, where each diagram has two rows of $p + q$ nodes each and a vertical *wall* between the first p and the last q nodes [Tur89; Koi89; Ben+94; Ben96; Nik07; Bul20]. All nodes are connected in pairs, and any two connected nodes are either on the same side of the wall and in different rows, or the other way around. For example, the following diagram

$$p = 3 \quad q = 2 \quad (39)$$

belongs to $\mathcal{B}_{3,2}^d$. The addition in $\mathcal{B}_{p,q}^d$ is defined by simply adding the respective coefficients in the two formal linear combinations. Multiplication of two diagrams corresponds to their *concatenation* by identifying the bottom row of the first diagram with the top row of the second diagram. Any loops that may have appeared in this process are erased and the resulting diagram is multiplied by the scalar $d^{\#\text{loops}}$:

$$\rho = \sigma = \rho \sigma = d \cdot \quad (40)$$

where parameter d of a walled Brauer algebra $\mathcal{B}_{p,q}^d$ explicitly appear. Multiplication of diagrams extends by linearity to multiplication in a walled Brauer algebra $\mathcal{B}_{p,q}^d$.

Note that the group algebra of the permutation group $S_p \times S_q$ forms a subalgebra of the walled Brauer algebra $\mathcal{B}_{p,q}^d$ consisting only of those diagrams where no edge goes across the wall. In fact, the two algebras are isomorphic when $p = 0$ or $q = 0$, i.e., $\mathbb{C}S_p \cong \mathcal{B}_{p,0}^d \cong \mathcal{B}_{0,p}^d$ for any value of d . The walled Brauer algebra $\mathcal{B}_{p,q}^d$ itself is a subalgebra of the so-called full *Brauer algebra* \mathcal{B}_{p+q}^d that is defined similarly but without the wall and with no restrictions on which pairs of nodes can be connected [Bra37]. This algebra was originally introduced by Brauer [Bra37] for studying Schur–Weyl-like dualities of orthogonal and symplectic groups.

The walled Brauer algebra $\mathcal{B}_{p,q}^d$ is generated by *transpositions* σ_i that swap the i -th and $(i + 1)$ -th node of the two rows, where $i \in \{1, \dots, p + q - 1\} \setminus \{p\}$, and a *contraction* σ_p between the p -th and $(p + 1)$ -th node within each row. For example, $\mathcal{B}_{2,2}^d$ is generated by

$$\begin{aligned} \sigma_1 &= \\ \sigma_2 &= \\ \sigma_3 &= \end{aligned} \quad (41)$$

One can also define $\mathcal{B}_{p,q}^d$ abstractly in terms of relations between its generators [Bul20; BS12; Nik07].

⁶We will later require $d \geq 2$ to be an integer as well.

Definition 3.1. Let $p, q \geq 0$ be integers and $d \in \mathbb{C}$. The walled Brauer algebra $\mathcal{B}_{p,q}^d$ is a finite-dimensional associative algebra over \mathbb{C} generated by $\sigma_1, \dots, \sigma_{p+q-1}$ subject to the following relations:

$$(a) \sigma_i^2 = 1 \ (i \neq p), \quad (b) \sigma_i \sigma_{i+1} \sigma_i = \sigma_{i+1} \sigma_i \sigma_{i+1} \ (i \neq p-1, p), \quad (c) \sigma_i \sigma_j = \sigma_j \sigma_i \ (|i-j| > 1), \quad (42)$$

$$(d) \sigma_p^2 = d \sigma_p, \quad (e) \sigma_p \sigma_{p \pm 1} \sigma_p = \sigma_p, \quad (f) \sigma_p \sigma_i = \sigma_i \sigma_p \ (i \neq p \pm 1), \quad (43)$$

$$(g) \sigma_p \sigma_{p+1} \sigma_{p-1} \sigma_p \sigma_{p-1} = \sigma_p \sigma_{p+1} \sigma_{p-1} \sigma_p \sigma_{p+1}, \quad (44)$$

$$(h) \sigma_{p-1} \sigma_p \sigma_{p+1} \sigma_{p-1} \sigma_p = \sigma_{p+1} \sigma_p \sigma_{p+1} \sigma_{p-1} \sigma_p. \quad (45)$$

We can embed the walled Brauer algebra $\mathcal{B}_{i,0}^d$ into $\mathcal{B}_{i+1,0}^d$ by making adding a new pair of nodes on the left-hand side of the wall, which are connected by a vertical line. Similarly, we can embed $\mathcal{B}_{p,j}^d$ into $\mathcal{B}_{p,j+1}^d$ by adding a new pair of nodes on the right-hand side of the wall. This produces the following sequence of inclusions among walled Brauer algebras:

$$\mathcal{B}_{0,0}^d \hookrightarrow \mathcal{B}_{1,0}^d \hookrightarrow \dots \hookrightarrow \mathcal{B}_{p,0}^d \hookrightarrow \mathcal{B}_{p,1}^d \hookrightarrow \dots \hookrightarrow \mathcal{B}_{p,q}^d. \quad (46)$$

This is a multiplicity-free family when the underlying algebras are semisimple.

There exist special elements inside $\mathcal{B}_{p,q}^d$ called *Jucys–Murphy elements*, which are given by

$$J_k := \begin{cases} 0 & \text{if } k = 1, \\ \sum_{i=1}^{k-1} (i, k) & \text{if } 2 \leq k \leq p, \\ \sum_{i=p+1}^{k-1} (i, k) - \sum_{i=1}^p \overline{(i, k)} + d & \text{if } p+1 \leq k \leq p+q, \end{cases} \quad (47)$$

where (i, k) is the transposition of elements i and k , and $\overline{(i, k)} := (i, p-1)(p, k)\sigma_p(i, p-1)(p, k)$ is the contraction between i and k . These elements are important in the representation theory of $\mathcal{B}_{p,q}^d$ [BS12; SS15; JK20] and the related matrix algebra $\mathcal{A}_{p,q}^d$ [GO22] defined in the next section.

3.2. Matrix algebra $\mathcal{A}_{p,q}^d$ of partially transposed permutations. Let us fix a local dimension $d \geq 2$. Let $V_d^p := (\mathbb{C}^d)^{\otimes p}$ denote the tensor product space of p qudits, and let $V_d^{p,q} := V_d^p \otimes (V_d^q)^*$. The walled Brauer algebra has a natural matrix representation $\psi_{p,q}^d: \mathcal{B}_{p,q}^d \rightarrow \text{End}(V_d^{p,q})$ in which the generators $\sigma_i, \dots, \sigma_{p+q-1} \in \mathcal{B}_{p,q}^d$ act on strings $x_1, \dots, x_{p+q} \in [d]$ as follows:

$$\psi_{p,q}^d(\sigma_i) |x_1, \dots, x_{p+q}\rangle := \begin{cases} |x_1, \dots, x_{i+1}, x_i, \dots, x_{p+q}\rangle, & i \neq p, \\ |x_1, \dots, x_{p-1}\rangle \otimes \delta_{x_p, x_{p+1}} \sum_{k=1}^d |k, k\rangle \otimes |x_{p+2}, \dots, x_{p+q}\rangle, & i = p. \end{cases} \quad (48)$$

One can check that $\psi_{p,q}^d$ preserves all relations in Definition 3.1. By multiplying the generators and using linearity, the action (48) can be extended to the entire walled Brauer algebra $\mathcal{B}_{p,q}^d$.

The image of $\psi_{p,q}^d$ is a quotient algebra over the two-sided ideal $\ker(\psi_{p,q}^d)$ of $\mathcal{B}_{p,q}^d$:

$$\mathcal{A}_{p,q}^d := \psi_{p,q}^d(\mathcal{B}_{p,q}^d) \cong \mathcal{B}_{p,q}^d / \ker(\psi_{p,q}^d), \quad (49)$$

which we call the *matrix algebra of partially transposed permutations*. It is important to make a distinction between the algebras $\mathcal{A}_{p,q}^d$ and $\mathcal{B}_{p,q}^d$. When the local dimension d is small, i.e., $d < p+q$, those two algebras are not isomorphic. As a finite-dimensional star matrix algebra, $\mathcal{A}_{p,q}^d$ is always semisimple [Eti+11]. On the other hand, $\mathcal{B}_{p,q}^d$ is not semisimple for integer $d < p+q-1$ [CDDM08].

As an example, consider the walled Brauer algebras $\mathcal{B}_{2,0}^d$ and $\mathcal{B}_{1,1}^d$, which are both generated by one generator, σ_1 , which is a transposition in the first case and a contraction in the second. The image of σ_1 under the map $\psi_{p,q}^d$ is shown in Table 2.

3.3. Representation theory of the algebra $\mathcal{A}_{p,q}^d$. In this section, we describe the representation theory of the matrix algebra $\mathcal{A}_{p,q}^d$ of partially transposed permutations [GO22]. For this purpose, we will employ the notions of the Bratteli diagram and Gelfand–Tsetlin basis introduced in Section 2.2.

First, similar to the so-called Okounkov–Vershik approach, we consider the following sequence of algebra inclusions:

$$\mathcal{A}_{0,0}^d \hookrightarrow \mathcal{A}_{1,0}^d \hookrightarrow \dots \hookrightarrow \mathcal{A}_{p,0}^d \hookrightarrow \mathcal{A}_{p,1}^d \hookrightarrow \dots \hookrightarrow \mathcal{A}_{p,q}^d, \quad (50)$$

where each inclusion corresponds to tensoring the previous algebra with the identity matrix I_d on the right or, equivalently, applying $\psi_{p,q}^d$ onto eq. (46). All algebras in this sequence are semisimple, and their inclusions are multiplicity-free [Eti+11]. For convenience, we will sometimes use the following single-subscript notation:

$$\mathcal{A}_0^d \hookrightarrow \mathcal{A}_1^d \hookrightarrow \dots \hookrightarrow \mathcal{A}_{p+q}^d \quad (51)$$

where the algebras \mathcal{A}_k^d are defined as follows:

$$\mathcal{A}_k^d := \begin{cases} \mathbb{C} & \text{if } k = 0, \\ \mathcal{A}_{k,0}^d & \text{if } 1 \leq k \leq p, \\ \mathcal{A}_{p,k-p}^d & \text{if } p+1 \leq k \leq p+q. \end{cases} \quad (52)$$

	Algebra $\mathcal{B}_{2,0}^d$	Algebra $\mathcal{B}_{1,1}^d$
Diagram of the generator	$\sigma_1 = \begin{array}{c} \text{---} \diagup \text{---} \\ \text{---} \diagdown \text{---} \end{array}$ (transposition)	$\sigma_1 = \begin{array}{c} \text{---} \diagup \text{---} \\ \text{---} \diagdown \text{---} \\ \text{---} \diagup \text{---} \\ \text{---} \diagdown \text{---} \end{array}$ (contraction)
Action in $\mathcal{A}_{p,q}^d$	$\psi_{2,0}^d(\sigma_1): i\rangle j\rangle \mapsto j\rangle i\rangle$	$\psi_{1,1}^d(\sigma_1): i\rangle j\rangle \mapsto \delta_{i,j} \sum_{k=1}^d k\rangle k\rangle$
Matrix representation when $d = 2$	$\psi_{2,0}^2(\sigma_1) = \begin{pmatrix} 1 & 0 & 0 & 0 \\ 0 & 0 & 1 & 0 \\ 0 & 1 & 0 & 0 \\ 0 & 0 & 0 & 1 \end{pmatrix}$	$\psi_{1,1}^2(\sigma_1) = \begin{pmatrix} 1 & 0 & 0 & 1 \\ 0 & 0 & 0 & 0 \\ 0 & 0 & 0 & 0 \\ 1 & 0 & 0 & 1 \end{pmatrix}$

TABLE 2. Comparison of algebras $\mathcal{B}_{2,0}^d$ and $\mathcal{B}_{1,1}^d$. They both have a single generator σ_1 which is a transposition and a contraction, respectively. The corresponding matrix algebras $\mathcal{A}_{2,0}^d$ and $\mathcal{A}_{1,1}^d$ are two-dimensional and spanned by the identity matrix and $\psi_{p,q}^d(\sigma_1)$.

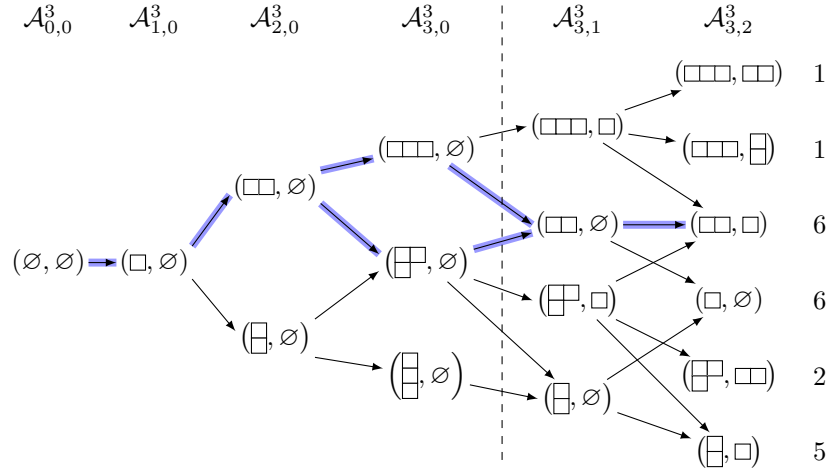


FIGURE 3. The Brattelli diagram associated with the family (50) of partially transposed permutation matrix algebras when $p = 3$, $q = 2$, and local dimension $d = 3$. For a chosen path $T = ((\emptyset, \emptyset), (\square, \emptyset), (\square, \square), (\square, \square, \emptyset), (\square, \square, \emptyset), (\square, \square, \emptyset))$, we have highlighted in blue the set $\mathcal{M}(T)$ of all paths that agree with T everywhere except for level p . For each leaf, we have indicated the number of paths from the root to that leaf, which coincides with the dimension of the corresponding irrep.

The irreducible representations of $\mathcal{A}_{p,q}^d$ are labelled by the following set of mixed Young diagrams (λ_l, λ_r) :

$$\widehat{\mathcal{A}}_{p,q}^d := \left\{ \lambda = (\lambda_l, \lambda_r) : 0 \leq k \leq \min(p, q), \lambda_l \vdash p - k, \lambda_r \vdash q - k, \ell(\lambda_l) + \ell(\lambda_r) \leq d \right\}. \quad (53)$$

The Brattelli diagram corresponding to the sequence (50) is as follows [BO20]. Its levels are labelled by $0, \dots, p + q$. The vertices at level $s + t$, where (s, t) ranges over subscripts in eq. (50), are labelled by $\widehat{\mathcal{A}}_{s,t}^d$. An edge $\lambda \rightarrow \mu$ between $\lambda = (\lambda_l, \lambda_r) \in \widehat{\mathcal{A}}_{s,t}^d$ and $\mu = (\mu_l, \mu_r) \in \widehat{\mathcal{A}}_{s',t'}^d$ is present if and only if λ and μ are in consecutive levels, i.e., $s' + t' = s + t + 1$, and

- (1) if $s \leq p$, the diagram μ can be obtained from λ by adding one cell to λ_l ,
- (2) if $s > p$, the diagram μ can be obtained from λ by either adding one cell to λ_r or removing one cell from λ_l .

This is equivalent to saying that $\text{Paths}(\lambda)$ in this Brattelli diagram correspond precisely to the set of mixed standard Young tableaux of shape λ (see Section 2.4). For example, Fig. 3 shows the Brattelli diagram for the sequence (50) ending with algebra $\mathcal{A}_{3,2}^3$.

For any $\lambda \in \widehat{\mathcal{A}}_{p,q}^d$, we will denote the corresponding irrep by

$$\psi_\lambda: \mathcal{A}_{p,q}^d \rightarrow \text{End}(V_\lambda^{\mathcal{A}_{p,q}^d}) \quad \text{where} \quad V_\lambda^{\mathcal{A}_{p,q}^d} := \mathbb{C}^{\text{Paths}(\lambda)}. \quad (54)$$

Our main technical result (see Theorem 3.2 below) provides an explicit formula for $\psi_\lambda(\sigma_i)$, for any generator σ_i of $\mathcal{A}_{p,q}^d$. This effectively describes how the matrix algebra $\mathcal{A}_{p,q}^d$ acts on the Gelfand–Tsetlin basis vectors $|T\rangle$, where T is any root–leaf path in the corresponding Brattelli diagram.

Before presenting our formula, we introduce some auxiliary notation. Consider a path $T = (T^0, \dots, T^{p+q}) \in \text{Paths}(\lambda)$. Similar to eq. (17), we define the *walled content* of a cell containing i in T as

$$\text{wcont}_i(T) := \begin{cases} \text{cont}(T_l^i \setminus T_l^{i-1}) & \text{if } i \leq p, \\ \text{cont}(T_r^i \setminus T_r^{i-1}) + d & \text{if } i > p \text{ and } T_l^i = T_l^{i-1}, \\ -\text{cont}(T_l^{i-1} \setminus T_l^i) & \text{if } i > p \text{ and } T_r^i = T_r^{i-1}. \end{cases} \quad (55)$$

This definition is chosen so that $\text{wcont}_i(T)$ matches the spectrum of Jucys–Murphy elements in Lemma B.7. For example, the path T given in eqs. (37) and (38) has the following values of walled content: $\text{wcont}_1(T) = 0$, $\text{wcont}_2(T) = 1$, $\text{wcont}_3(T) = 2$, $\text{wcont}_4(T) = -2$, $\text{wcont}_5(T) = d$. We define the *walled axial distance* between cells containing i and $i + 1$ in $T \in \text{Paths}(\lambda)$ as

$$r_i(T) := \text{wcont}_{i+1}(T) - \text{wcont}_i(T). \quad (56)$$

The walled axial distance has a simple combinatorial interpretation. Indeed, $r_i(T)$ is the axial distance between cells containing i and $i + 1$ in a staircase representation \hat{T} of a mixed Young diagram T , see Fig. 2 and eq. (38).

Furthermore, we denote by

$$\mathcal{M}(T) := \begin{cases} \{(T^0, \dots, T^{p-1}, \mu, T^{p+1}, \dots, T^{p+q}) \in \text{Paths}(T^{p+q}) \mid \mu \in \hat{\mathcal{A}}_{p,0}^d\} & \text{if } T^{p-1} = T^{p+1}, \\ \emptyset & \text{otherwise} \end{cases} \quad (57)$$

the set of all paths in the Bratteli diagram differing from T only at the p -th level (see Fig. 3 for an example). For a given path T , we call the cell

$$a_T := \begin{cases} T_l^p \setminus T_l^{p-1} & \text{if } T^{p-1} = T^{p+1}, \\ \emptyset & \text{otherwise,} \end{cases} \quad (58)$$

a *mobile element*⁷, where T_l^k denotes the left diagram in $T^k = (T_l^k, T_r^k)$. For a mixed Young diagram (λ_l, λ_r) , we define the sets of *removable/addable cells* based on the left tableau, i.e., $\text{RC}((\lambda_l, \lambda_r)) := \text{RC}(\lambda_l)$ and $\text{AC}((\lambda_l, \lambda_r)) := \text{AC}(\lambda_l)$. With this notation at hand, we can state our main technical result.

Theorem 3.2 (Gelfand–Tsetlin basis for $\mathcal{A}_{p,q}^d$). *For any $\lambda \in \hat{\mathcal{A}}_{p,q}^d$, the following map $\psi_\lambda: \mathcal{A}_{p,q}^d \rightarrow \text{End}(\mathbb{C}^{\text{Paths}(\lambda)})$ is an irreducible representation of $\mathcal{A}_{p,q}^d$. Given a generator σ_i of $\mathcal{A}_{p,q}^d$, $i = 1, \dots, p + q - 1$, the matrix $\psi_\lambda(\sigma_i)$ acts on the Gelfand–Tsetlin basis vectors $|T\rangle$ with $T \in \text{Paths}(\lambda)$ as follows:*

$$\psi_\lambda(\sigma_i) |T\rangle = \frac{1}{r_i(T)} |T\rangle + \sqrt{1 - \frac{1}{r_i(T)^2}} |\sigma_i T\rangle, \quad \text{for } i \neq p, \quad (59)$$

$$\psi_\lambda(\sigma_p) |T\rangle = c(T) |v_T\rangle, \quad |v_T\rangle := \sum_{T' \in \mathcal{M}(T)} c(T') |T'\rangle, \quad \text{for } i = p, \quad (60)$$

where $r_i(T)$ is the walled axial distance defined in eq. (56), $\sigma_i T$ denotes the mixed standard Young tableau T with cell fillings permuted according to σ_i (see Section 2.4), and the coefficient $c(T) \in \mathbb{R}$ is given by

$$c(T) := \sqrt{\frac{(d + \text{cont}(a_T)) \prod_{c \in \text{RC}(T^{p-1})} (\text{cont}(a_T) - \text{cont}(c))}{\prod_{a \in \text{AC}(T^{p-1}) \setminus a_T} (\text{cont}(a_T) - \text{cont}(a))}} \quad (61)$$

where a_T is the mobile element of T , and RC/AC are the sets of removable/addable cells.

Remark 3.3. Due to Lemmas B.1 and B.2 the coefficient $c(T)$ presented in Theorem 3.2 has the following combinatorial expression:

$$c(T) = \sqrt{\frac{m_{T^p}}{m_{T^{p-1}}}}, \quad (62)$$

where m_λ is the dimension of the irreducible representation of the unitary group U_d corresponding to the Young diagram λ . It is well-known that the dimension m_λ equals the number of semistandard Young tableaux $\text{SSYT}(\lambda, d)$ of shape λ and entries in $[d]$, see eq. (20).

We delegate the proof of Theorem 3.2 to Appendix B. Table 3 gives an example of how Theorem 3.2 can be used to compute all irreps of $\mathcal{A}_{3,2}^3$ using the Bratteli diagram shown in Fig. 3. Moreover, we provide a code in *Wolfram Mathematica* to generate the Gelfand–Tsetlin basis for arbitrary $\mathcal{A}_{p,q}^d$ [GBO23].

⁷The terms *mobile cell* and *mobile element* are from [ST17].

	σ_1	σ_2	σ_3	σ_4
$(\square\square\square, \square)$	(1)	(1)	(0)	(1)
$(\square\square\square, \square)$	(1)	(1)	(0)	(-1)
$(\square\square, \square)$	$\begin{pmatrix} -1 & 0 & 0 & 0 & 0 & 0 \\ 0 & -1 & 0 & 0 & 0 & 0 \\ 0 & 0 & 1 & 0 & 0 & 0 \\ 0 & 0 & 0 & 1 & 0 & 0 \\ 0 & 0 & 0 & 0 & 1 & 0 \\ 0 & 0 & 0 & 0 & 0 & 1 \end{pmatrix}$	$\begin{pmatrix} \frac{1}{2} & 0 & \frac{\sqrt{3}}{2} & 0 & 0 & 0 \\ 0 & \frac{1}{2} & 0 & \frac{\sqrt{3}}{2} & 0 & 0 \\ \frac{\sqrt{3}}{2} & 0 & -\frac{1}{2} & 0 & 0 & 0 \\ 0 & \frac{\sqrt{3}}{2} & 0 & -\frac{1}{2} & 0 & 0 \\ 0 & 0 & 0 & 0 & 1 & 0 \\ 0 & 0 & 0 & 0 & 0 & 1 \end{pmatrix}$	$\begin{pmatrix} 0 & 0 & 0 & 0 & 0 & 0 \\ 0 & 0 & 0 & 0 & 0 & 0 \\ 0 & 0 & \frac{4}{3} & 0 & \frac{2\sqrt{5}}{3} & 0 \\ 0 & 0 & 0 & 0 & 0 & 0 \\ 0 & 0 & \frac{2\sqrt{5}}{3} & 0 & \frac{5}{3} & 0 \\ 0 & 0 & 0 & 0 & 0 & 0 \end{pmatrix}$	$\begin{pmatrix} \frac{1}{2} & \frac{\sqrt{3}}{2} & 0 & 0 & 0 & 0 \\ \frac{\sqrt{3}}{2} & -\frac{1}{2} & 0 & 0 & 0 & 0 \\ 0 & 0 & \frac{1}{2} & \frac{\sqrt{3}}{2} & 0 & 0 \\ 0 & 0 & \frac{\sqrt{3}}{2} & -\frac{1}{2} & 0 & 0 \\ 0 & 0 & 0 & 0 & \frac{1}{5} & \frac{2\sqrt{6}}{5} \\ 0 & 0 & 0 & 0 & \frac{2\sqrt{6}}{5} & -\frac{1}{5} \end{pmatrix}$
(\square, \emptyset)	$\begin{pmatrix} -1 & 0 & 0 & 0 & 0 & 0 \\ 0 & -1 & 0 & 0 & 0 & 0 \\ 0 & 0 & -1 & 0 & 0 & 0 \\ 0 & 0 & 0 & 1 & 0 & 0 \\ 0 & 0 & 0 & 0 & 1 & 0 \\ 0 & 0 & 0 & 0 & 0 & 1 \end{pmatrix}$	$\begin{pmatrix} -1 & 0 & 0 & 0 & 0 & 0 \\ 0 & \frac{1}{2} & 0 & \frac{\sqrt{3}}{2} & 0 & 0 \\ 0 & 0 & \frac{1}{2} & 0 & \frac{\sqrt{3}}{2} & 0 \\ 0 & \frac{\sqrt{3}}{2} & 0 & -\frac{1}{2} & 0 & 0 \\ 0 & 0 & \frac{\sqrt{3}}{2} & 0 & -\frac{1}{2} & 0 \\ 0 & 0 & 0 & 0 & 0 & 1 \end{pmatrix}$	$\begin{pmatrix} \frac{1}{3} & \frac{2\sqrt{2}}{3} & 0 & 0 & 0 & 0 \\ \frac{2\sqrt{2}}{3} & \frac{8}{3} & 0 & 0 & 0 & 0 \\ 0 & 0 & 0 & 0 & 0 & 0 \\ 0 & 0 & 0 & 0 & 0 & 0 \\ 0 & 0 & 0 & \frac{4}{3} & \frac{2\sqrt{5}}{3} & 0 \\ 0 & 0 & 0 & \frac{2\sqrt{5}}{3} & \frac{5}{3} & 0 \end{pmatrix}$	$\begin{pmatrix} -1 & 0 & 0 & 0 & 0 & 0 \\ 0 & \frac{1}{2} & \frac{\sqrt{3}}{2} & 0 & 0 & 0 \\ 0 & \frac{\sqrt{3}}{2} & -\frac{1}{2} & 0 & 0 & 0 \\ 0 & 0 & 0 & \frac{1}{2} & \frac{\sqrt{3}}{2} & 0 \\ 0 & 0 & 0 & \frac{\sqrt{3}}{2} & -\frac{1}{2} & 0 \\ 0 & 0 & 0 & 0 & 0 & 1 \end{pmatrix}$
$(\square\square, \square)$	$\begin{pmatrix} -1 & 0 \\ 0 & 1 \end{pmatrix}$	$\begin{pmatrix} \frac{1}{2} & \frac{\sqrt{3}}{2} \\ \frac{\sqrt{3}}{2} & -\frac{1}{2} \end{pmatrix}$	$\begin{pmatrix} 0 & 0 \\ 0 & 0 \end{pmatrix}$	$\begin{pmatrix} 1 & 0 \\ 0 & 1 \end{pmatrix}$
(\square, \square)	$\begin{pmatrix} -1 & 0 & 0 & 0 & 0 \\ 0 & -1 & 0 & 0 & 0 \\ 0 & 0 & -1 & 0 & 0 \\ 0 & 0 & 0 & 1 & 0 \\ 0 & 0 & 0 & 0 & 1 \end{pmatrix}$	$\begin{pmatrix} -1 & 0 & 0 & 0 & 0 \\ 0 & \frac{1}{2} & 0 & \frac{\sqrt{3}}{2} & 0 \\ 0 & 0 & \frac{1}{2} & 0 & \frac{\sqrt{3}}{2} \\ 0 & \frac{\sqrt{3}}{2} & 0 & -\frac{1}{2} & 0 \\ 0 & 0 & \frac{\sqrt{3}}{2} & 0 & -\frac{1}{2} \end{pmatrix}$	$\begin{pmatrix} \frac{1}{3} & \frac{2\sqrt{2}}{3} & 0 & 0 & 0 \\ \frac{2\sqrt{2}}{3} & \frac{8}{3} & 0 & 0 & 0 \\ 0 & 0 & 0 & 0 & 0 \\ 0 & 0 & 0 & 0 & 0 \\ 0 & 0 & 0 & 0 & 0 \end{pmatrix}$	$\begin{pmatrix} 1 & 0 & 0 & 0 & 0 \\ 0 & \frac{1}{4} & \frac{\sqrt{15}}{4} & 0 & 0 \\ 0 & \frac{\sqrt{15}}{4} & -\frac{1}{4} & 0 & 0 \\ 0 & 0 & 0 & \frac{1}{4} & \frac{\sqrt{15}}{4} \\ 0 & 0 & 0 & \frac{\sqrt{15}}{4} & -\frac{1}{4} \end{pmatrix}$

TABLE 3. Example of Theorem 3.2 in action: the matrices $\psi_\lambda(\sigma_i)$ in the Gelfand–Tsetlin basis for all irreps ψ_λ and generators σ_i of the matrix algebra $\mathcal{A}_{3,2}^3$. Rows and columns correspond to irrep labels $\lambda = (\lambda_l, \lambda_r)$ and generators σ_i , respectively. Note that irreps with $|\lambda_l| = 3$ and $|\lambda_r| = 2$ vanish on the contraction σ_3 since they are irreps of $S_3 \times S_2$. The Bratteli diagram for $\mathcal{A}_{3,2}^3$ is shown in Fig. 3.

4. MIXED QUANTUM SCHUR TRANSFORM

4.1. Mixed Schur–Weyl duality. As before, let $V_d^p := (\mathbb{C}^d)^{\otimes p}$ and $V_d^{p,q} := V_d^p \otimes (V_d^q)^*$. Consider the natural action $\phi_{p,q}^d: U_d \rightarrow \text{End}(V_d^{p,q})$ of the unitary group U_d on $V_d^{p,q}$ given by

$$\phi_{p,q}^d(U) |x_1, \dots, x_{p+q}\rangle = (U^{\otimes p} \otimes \bar{U}^{\otimes q}) |x_1, \dots, x_{p+q}\rangle \quad (63)$$

where $U \in U_d$, \bar{U} is the complex conjugate of U , and $x_1, \dots, x_{p+q} \in [d]$. This action is relevant in several contexts in quantum information, such as unitary-equivariant quantum channels with p input and q output qudits (see Section 5.1). The action (63) commutes with the aforementioned action $\psi_{p,q}^d: \mathcal{B}_{p,q}^d \rightarrow \text{End}(V_d^{p,q})$ from eq. (48) which defines the algebra $\mathcal{A}_{p,q}^d$ of partially transposed permutations on $V_d^{p,q}$.⁸

The actions $\psi_{p,q}^d$ and $\phi_{p,q}^d$ of the matrix algebra $\mathcal{A}_{p,q}^d$ and the unitary group U_d commute, i.e.,

$$[\psi_{p,q}^d(\sigma), \phi_{p,q}^d(U)] = 0, \quad \text{for all } \sigma \in \mathcal{A}_{p,q}^d \text{ and } U \in U_d. \quad (64)$$

Moreover, the space $V_d^{p,q}$ decomposes into a direct sum of irreducible modules of both actions:

$$V_d^{p,q} \cong \bigoplus_{\lambda \in \hat{\mathcal{A}}_{p,q}^d} V_\lambda^{\mathcal{A}_{p,q}^d} \otimes V_\lambda^{U_d} \quad \text{where } V_\lambda^{\mathcal{A}_{p,q}^d} := \mathbb{C}^{\text{Paths}(\lambda)} \text{ and } V_\lambda^{U_d} := \mathbb{C}^{\text{GT}(\lambda,d)}. \quad (65)$$

Here the direct sum ranges over all irreducible representations λ of $\mathcal{A}_{p,q}^d$, see eq. (53), and the spaces $V_\lambda^{\mathcal{A}_{p,q}^d}$ and $V_\lambda^{U_d}$ correspond to irreducible representations of $\mathcal{A}_{p,q}^d$ and U_d , respectively. We will denote their dimensions by

$$d_\lambda := \dim V_\lambda^{\mathcal{A}_{p,q}^d} = |\text{Paths}(\lambda)|, \quad (66)$$

$$m_\lambda := \dim V_\lambda^{U_d} = |\text{GT}(\lambda,d)|. \quad (67)$$

Both these irrep dimensions implicitly depend on the local dimension d .⁹ By comparing the dimensions on both sides of eq. (65) we obtain a non-trivial combinatorial identity

$$d^{p+q} = \sum_{\lambda \in \hat{\mathcal{A}}_{p,q}^d} d_\lambda m_\lambda, \quad (68)$$

⁸This is a consequence of the fact that the maximally entangled state $\frac{1}{\sqrt{d}} \sum_{k \in [d]} |k, k\rangle$ is invariant under $U \otimes \bar{U}$ for any $U \in U_d$. On the other side, the permutation of registers between spaces V_d^p and $(V_d^p)^*$ does not commute with action eq. (63).

⁹For d_λ the d -dependence is more subtle since it results from truncating the Bratteli diagram. Recall from eq. (53) that for small values of d some vertices are removed from the Bratteli diagram, which can result in fewer paths reaching a given leaf. This phenomenon does not occur when $q = 0$, hence in the regular Schur–Weyl duality the S_p irrep dimension d_λ does not depend on d .

which is a consequence of the Robinson–Schensted–Knuth correspondence for mixed tensors [Ste87, Section 4].

Equation (65) is known as *mixed Schur–Weyl duality* and is usually expressed in the following more abstract way: the algebras generated by the actions $\psi_{p,q}^d$ and $\phi_{p,q}^d$ of $\mathcal{A}_{p,q}^d$ and U_d on $V_d^{p,q}$ are complete mutual centralizers of each other within $\text{End}(V_d^{p,q})$ [Koi89; Ben+94], see also [GO22]. The decomposition (65) follows from the double centralizer theorem [Eti+11, Theorem 4.54] applied to this pair of algebras.

4.2. Mixed Schur transform. We would like to understand in more detail the basis change (65) that simultaneously block-diagonalizes both actions. This is a unitary transformation

$$U_{\text{Sch}}(p, q): V_d^{p,q} \rightarrow \bigoplus_{\lambda \in \hat{\mathcal{A}}_{p,q}^d} V_{\lambda}^{\mathcal{A}_{p,q}^d} \otimes V_{\lambda}^{U_d} \quad (69)$$

known as *mixed Schur transform* [GO22]. It maps the computational basis to a new basis composed of irreducible representations of $\mathcal{A}_{p,q}^d$ and U_d :

$$U_{\text{Sch}}(p, q) \psi_{p,q}^d(\sigma) U_{\text{Sch}}(p, q)^{\dagger} = \bigoplus_{\lambda \in \hat{\mathcal{A}}_{p,q}^d} \psi_{\lambda}(\sigma) \otimes I_{m_{\lambda}}, \quad (70)$$

$$U_{\text{Sch}}(p, q) \phi_{p,q}^d(U) U_{\text{Sch}}(p, q)^{\dagger} = \bigoplus_{\lambda \in \hat{\mathcal{A}}_{p,q}^d} I_{d_{\lambda}} \otimes \phi_{\lambda}(U), \quad (71)$$

where $\psi_{p,q}^d$ and $\phi_{p,q}^d$ are defined in eqs. (48) and (63), ψ_{λ} is described in Theorem 3.2, and ϕ_{λ} is an

Recall from eq. (65) that we can label the standard bases of $V_{\lambda}^{\mathcal{A}_{p,q}^d}$ and $V_{\lambda}^{U_d}$ by paths $T \in \text{Paths}(\lambda)$ and Gelfand–Tsetlin patterns $M \in \text{GT}(\lambda, d)$, respectively:

$$V_{\lambda}^{\mathcal{A}_{p,q}^d} := \text{span}_{\mathbb{C}}\{|T\rangle : T \in \text{Paths}(\lambda)\}, \quad (72)$$

$$V_{\lambda}^{U_d} := \text{span}_{\mathbb{C}}\{|M\rangle : M \in \text{GT}(\lambda, d)\}. \quad (73)$$

When $q = 0$ we can equivalently think of T and M as a standard and a semistandard Young tableau, respectively (see Sections 2.1 and 2.3). For general values of p, q , one can interpret T as a mixed standard Young tableau (see Section 2.4) while M can still be interpreted as a semistandard tableau by adding an appropriate constant to all entries of the Gelfand–Tsetlin pattern so that they become non-negative. Note that the irrep label $\lambda \in \hat{\mathcal{A}}_{p,q}^d$ is implicit in both T and M . Indeed, it can be recovered from the final vertex of the path T as well as from the first row of the pattern M . Hence, we can treat the output space in eq. (69) as a formal linear span of all pairs (T, M) :

$$\bigoplus_{\lambda \in \hat{\mathcal{A}}_{p,q}^d} V_{\lambda}^{\mathcal{A}_{p,q}^d} \otimes V_{\lambda}^{U_d} = \text{span}_{\mathbb{C}}\{|(T, M)\rangle : \lambda \in \hat{\mathcal{A}}_{p,q}^d, T \in \text{Paths}(\lambda), M \in \text{GT}(\lambda, d)\}. \quad (74)$$

Note that the output space of $U_{\text{Sch}}(p, q)$ does *not* have a tensor product structure, i.e., one should not treat $|(T, M)\rangle$ as $|T\rangle \otimes |M\rangle$. Nevertheless, for each individual λ the corresponding subspace $\mathbb{C}^{d_{\lambda}} \otimes \mathbb{C}^{m_{\lambda}}$ is indeed a tensor product.

We would like to find an efficient way of computing the mixed Schur transform matrix entries

$$\langle (T, M) | U_{\text{Sch}}(p, q) | x_1, \dots, x_{p+q} \rangle. \quad (75)$$

Here the rows are labelled by pairs (T, M) , where $T \in \text{Paths}(\lambda)$ and $M \in \text{GT}(\lambda, d)$ for all choices of $\lambda \in \hat{\mathcal{A}}_{p,q}^d$, while the columns are labelled by strings $x_1, \dots, x_{p+q} \in [d]$.^{10,11} The matrix entries (75) can be arranged into a matrix as follows:

$$U_{\text{Sch}}(p, q) = \sum_{\lambda \in \hat{\mathcal{A}}_{p,q}^d} \sum_{T \in \text{Paths}(\lambda)} \sum_{M \in \text{GT}(\lambda, d)} \sum_{x_1, \dots, x_{p+q} \in [d]} \langle (T, M) | U_{\text{Sch}}(p, q) | x_1, \dots, x_{p+q} \rangle \cdot |(T, M)\rangle \langle x_1, \dots, x_{p+q} |. \quad (76)$$

¹⁰Note that eq. (69) is a passive transformation, as a change of coordinates system from the computational basis vectors into the basis labelled by tuples (T, M) . As the number of such tuples matches the dimension of $V_d^{p,q}$ space, it can be seen as a transformation of $V_d^{p,q}$ onto itself, after applying any bijection between tuples (T, M) and computational basis vectors. As such, the Schur transform is a unitary transformation (also active transformation).

¹¹Note that Schur transform, defined as a transformation (69) which simultaneously decomposes $V_d^{p,q}$ into irreducible modules of $\mathcal{A}_{p,q}^d$ and U_d is not uniquely defined. Indeed, arbitrary change of basis within modules $V_{\lambda}^{\mathcal{A}_{p,q}^d}$ and $V_{\lambda}^{U_d}$ does not affect decomposition (69). On the other hand, such a change of basis within modules is the only degree of freedom for the Schur transform. In this paper, we present the most common form of Schur transform related to a Gelfand–Tsetlin basis corresponding to a sequence of algebras (50) for $\mathcal{A}_{p,q}^d$ and sequence $U_1 \hookrightarrow \dots \hookrightarrow U_d$ for unitary group $U(d)$. Moreover, for $d = 2$, it can be seen as a consecutive composition of spin- $\frac{1}{2}$ particles into a system with well-defined global spin.

In particular, the mixed quantum Schur transform of any standard basis vector $|x_1, \dots, x_{p+q}\rangle$ is

$$U_{\text{Sch}}(p, q) |x_1, \dots, x_{p+q}\rangle = \sum_{\lambda \in \hat{\mathcal{A}}_{p,q}^d} \sum_{T \in \text{Paths}(\lambda)} \sum_{M \in \text{GT}(\lambda, d)} \langle (T, M) | U_{\text{Sch}}(p, q) |x_1, \dots, x_{p+q}\rangle \cdot |(T, M)\rangle, \quad (77)$$

while the Schur basis vectors $\langle (T, M) |$ can be expressed as

$$\langle (T, M) | = \sum_{x_1, \dots, x_{p+q} \in [d]} \langle (T, M) | U_{\text{Sch}}(p, q) |x_1, \dots, x_{p+q}\rangle \cdot \langle x_1, \dots, x_{p+q} |. \quad (78)$$

The most common way of implementing the regular $q = 0$ Schur transform is by a sequence of Clebsch–Gordan transforms [Har05; BCH06; KS18]. Since this approach can be generalized to any $q \geq 0$ in a straightforward way, we can derive an explicit formula for the matrix entries of the mixed quantum Schur transform by inductively decomposing it as a sequence of Clebsch–Gordan transforms.

We start with a single qudit in state $|x_1\rangle$. At each step $k = 2, \dots, p+q$ we use the Clebsch–Gordan transform $\text{CG}^k \in U_d$ to couple the output state from the previous iteration with an additional qudit in state $|x_k\rangle$. The input and output spaces of CG^k can be decomposed as follows:

$$\text{CG}^k : \left(\bigoplus_{\lambda \in \hat{\mathcal{A}}_{k-1}^d} V_{\lambda}^{\mathcal{A}_{k-1}^d} \otimes V_{\lambda}^{U_d} \right) \otimes \mathbb{C}^d \rightarrow \bigoplus_{\mu \in \hat{\mathcal{A}}_k^d} V_{\mu}^{\mathcal{A}_k^d} \otimes V_{\mu}^{U_d}, \quad (79)$$

where we are using the single-subscript convention (52) for the sequence of algebras \mathcal{A}_k^d from eq. (51). For any path $T = (T^0, \dots, T^{k-1})$ and pattern $M \in \text{GT}(T^{k-1}, d)$ the action of CG^k is defined as

$$\text{CG}^k \left(|(T, M)\rangle \otimes |x_k\rangle \right) := \sum_{\mu: T^{k-1} \rightarrow \mu} \sum_{\substack{N \in \text{GT}(\mu, d) \\ w(N) = w(M) + w(x_k)}} c_{N, M}^{x_k} |(T \circ \mu, N)\rangle, \quad (80)$$

where $T^{k-1} \rightarrow \mu$ means that μ can be reached from T^{k-1} by one step in the Bratteli diagram, and $c_{N, M}^{x_k}$ are the so-called *Clebsch–Gordan coefficients* (see Appendix A for an explicit formula). The mixed quantum Schur transform $U_{\text{Sch}}(p, q)$ is given by a cascade of $p + q - 1$ Clebsch–Gordan transforms:

$$U_{\text{Sch}}(p, q) = \text{CG}^{p+q} \cdot (\text{CG}^{p+q-1} \otimes I) \cdots (\text{CG}^3 \otimes I^{\otimes p+q-3}) \cdot (\text{CG}^2 \otimes I^{\otimes p+q-2}). \quad (81)$$

In particular, the usual Schur transform satisfies $U_{\text{Sch}}(k, 0) = \text{CG}^k (U_{\text{Sch}}(k-1, 0) \otimes I)$ where $k = 2, \dots, p$.

Let us use eq. (81) to derive an explicit formula for the matrix entries of the mixed quantum Schur transform. For an arbitrary path $T = (T^0, \dots, T^{p+q}) \in \text{Paths}(\lambda)$ and Gelfand–Tsetlin pattern $M \in \text{GT}(\lambda, d)$, we get from eqs. (80) and (81) that

$$\langle (T, M) | U_{\text{Sch}}(p, q) |x_1, \dots, x_{p+q}\rangle = \langle M | C_{T^{p+q}T^{p+q-1}}^{x_{p+q}} \cdots C_{T^2T^1}^{x_2} |x_1\rangle \quad (82)$$

where $|M\rangle$ is a Gelfand–Tsetlin basis vector of the unitary group irrep corresponding to the staircase λ , and $C_{T^kT^{k-1}}^{x_k}$ for $k = 2, \dots, p+q$ are rectangular matrices with rows labelled by $N \in \text{GT}(T^k, d)$ and columns labelled by $M \in \text{GT}(T^{k-1}, d)$, with the corresponding matrix entry equal to the Clebsch–Gordan coefficient:

$$\langle N | C_{T^kT^{k-1}}^{x_k} | M \rangle := c_{N, M}^{x_k}. \quad (83)$$

Hence, according to eq. (82), any matrix entry of $U_{\text{Sch}}(p, q)$ can be computed by applying a sequence of matrices onto $|x_1\rangle$. The complexity of this computation depends on the dimensions of the matrices $C_{T^kT^{k-1}}^{x_k}$.

In practice, one can take advantage of the fact that the matrices $C_{T^kT^{k-1}}^{x_k}$ are block-diagonal. By tracking which blocks contribute non-trivially to a given $\langle (T, M) |$, eq. (82) can be modified as follows:

$$\langle (T, M) | U_{\text{Sch}}(p, q) |x_1, \dots, x_{p+q}\rangle = \langle M | C_{T^{p+q}T^{p+q-1}}^{x_{p+q}, w(x_{p+q-1}, \dots, x_1)} C_{T^{p+q-1}T^{p+q-2}}^{x_{p+q-1}, w(x_{p+q-2}, \dots, x_1)} \cdots C_{T^2T^1}^{x_2} |x_1\rangle, \quad (84)$$

where $C_{T^kT^{k-1}}^{x_k, w(x_{k-1}, \dots, x_1)}$ are submatrices of $C_{T^kT^{k-1}}^{x_k}$ with rows labelled only by $N \in \text{GT}(T^k, d)$ of weight $w(N) = w(x_k, \dots, x_1)$ and columns labelled only by $M \in \text{GT}(T^{k-1}, d)$ of weight $w(M) = w(x_{k-1}, \dots, x_1)$.

4.3. MPS representation of mixed Schur basis vectors. Notice that eq. (82) presents the Schur basis vectors $|(T, M)\rangle$ as matrix product states (MPS) with bond dimensions given by $D_k := |\text{GT}(T^k, d)|$, see Fig. 4. For fixed local dimension d , bond dimensions D_k are upper-bounded by $(p+q)^{O(d^2)}$.¹² Note that the length of

¹²This can be easily seen by counting the number of Gelfand–Tsetlin patterns $\text{GT}(T^k, d)$. Indeed, for any pair of Young diagrams $\lambda = (\lambda_l, \lambda_r)$ satisfying $\ell(\lambda_l) + \ell(\lambda_r) \leq d$, and of size $|\lambda_l| \leq p$, $|\lambda_r| \leq q$, a corresponding set of Gelfand–Tsetlin patterns $\text{GT}(\lambda, d)$ consists of patterns (29) with $\frac{d(d+1)}{2}$ entries m_{ij} , see eq. (34). Notice that $m_{1d} = \lambda_{l,1}$ and $m_{dd} = -\lambda_{r,1}$. Obviously, $|\lambda_{l,1}| \leq |\lambda| \leq p$, and $|\lambda_{r,1}| \leq |\lambda| \leq q$. Therefore, $m_{1d} \leq p$ and $m_{dd} \geq -q$. It is easy to see, that all entries m_{ij} of the Gelfand–Tsetlin pattern are bounded by $m_{dd} \leq m_{ij} \leq m_{1d}$, hence for arbitrary entry of the pattern m_{ij} , we have $-q \leq m_{ij} \leq p$. As the number of entries is $\frac{d(d+1)}{2}$, the size of the set $\text{GT}(\lambda, d)$ can be upper bound by $(p+q)^{O(d^2)}$.

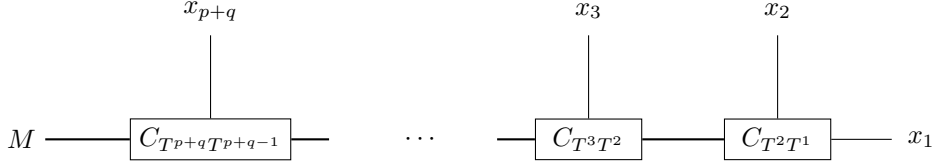


FIGURE 4. Tensor network representation of $U_{\text{Sch}}^\dagger(p, q)|(T, M)\rangle$ from eq. (82) as a matrix product state. Tensors $C_{T^k T^{k-1}}$ have three indices. The matrices $C_{T^k T^{k-1}}^{x_k}$ from eq. (83) are obtained from $C_{T^k T^{k-1}}$ by fixing the index corresponding to x_k . Indices $x_k \in [d]$ indicate the computational basis states $|x_k\rangle$. The bond dimensions $D_k = |\text{GT}(T^k, d)|$ are equal to the number of Gelfand–Tsetlin patterns of a shape T^k . Asymptotically the maximal value of D_k for different k is upper bounded by $(p+q)^{O(d^2)}$.

an MPS is given by $(p+q)$, and bond dimensions D_k are upper bounded by $(p+q)^{O(d^2)}$.¹³ As a consequence, for fixed local dimension d the computational complexity of computing $\langle (T, M) | U_{\text{Sch}}(p, q) | x_1, \dots, x_{p+q} \rangle$ is upper bounded by

$$(p+q)^{O(d^2)}. \quad (85)$$

Not that the complexity of computing the entries of matrices $C_{T^k T^{k-1}}^{x_k}$ (see Appendix A) is absorbed into the above bound. Thus, we have established the following result.

Theorem 4.1 (MPS representation of mixed Schur basis vectors). *The Schur basis states $|(T, M)\rangle$ (or rows of mixed quantum Schur transform $U_{\text{Sch}}(p, q)$) admit a matrix product state representation with bond dimension $(p+q)^{O(d^2)}$. Hence, the matrix entries $\langle (T, M) | U_{\text{Sch}}(p, q) | x_1, \dots, x_{p+q} \rangle$ of mixed Schur transform U_{Sch} can be computed in time $(p+q)^{O(d^2)}$. In particular, for constant local dimension d , this is polynomial in the system size $p+q$.*

Moreover, notice that eq. (84) provides a more refined approach for computing entries of vectors $|(T, M)\rangle$ in the computational basis. Although it is no longer an MPS, as the choice of consecutive matrices $C_{T^k T^{k-1}}^{x_k, w(x_{k-1}, \dots, x_1)}$ does not depend on x_k only. notice that matrices in this product are of the size given by $|\{M \in \text{GT}(T^k, d) : w(M) = w(x_1, \dots, x_k)\}|$ the number of Gelfand–Tsetlin patterns with a given weight $w(x_1, \dots, x_k)$. This number is known as a *Kostka number* $K_{T^k, w(x_1, \dots, x_k)}$ depending on two integer partitions T^k and $w(x_1, \dots, x_k)$. Clearly the size of those matrices is smaller than in eq. (82), however, we did not find an improvement in the asymptotic upper bound. As previously, $K_{T^k, w(x_1, \dots, x_k)}$ can be upper bounded by $(p+q)^{O(d^2)}$, which leads to the same upper bound (85).

4.4. Mixed Schur transform achieves the Gelfand–Tsetlin basis. By construction [VK92], the Clebsch–Gordan transform eq. (80) achieves the Gelfand–Tsetlin basis of the unitary group on the unitary group registers $V_\lambda^{\text{U}^d}$ in eq. (69). As a consequence, the same holds true also for the mixed Schur transform (81). However, it is also true that the mixed Schur transform yields the Gelfand–Tsetlin basis of the algebra $\mathcal{A}_{p,q}^d$ in the relevant register $V_\lambda^{\mathcal{A}_{p,q}^d}$.

Because the Clebsch–Gordan transform CG^k from eqs. (79) and (80) acts only on the unitary irrep registers upon adding a qudit \mathbb{C}^d , we get for every $\sigma \in \mathcal{A}_{k-1}^d$

$$\text{CG}^k \left(\left(\bigoplus_{\mu \in \hat{\mathcal{A}}_{k-1}^d} \psi_\mu(\sigma) \otimes I_\mu^{\text{U}^d} \right) \otimes I \right) \text{CG}^{k\dagger} = \bigoplus_{\lambda \in \hat{\mathcal{A}}_k^d} \left(\bigoplus_{\substack{\mu \in \hat{\mathcal{A}}_{k-1}^d \\ \mu : \mu \rightarrow \lambda}} \psi_\mu(\sigma) \right) \otimes I_\lambda^{\text{U}^d}. \quad (86)$$

We see that the CG^k does not change the action inside the registers $V_\lambda^{\mathcal{A}_{k-1}^d}$, meaning that it is naturally implementing a subalgebra-adapted basis, namely a Gelfand–Tsetlin basis. However, there is still a degree of freedom of choosing phases for the Gelfand–Tsetlin basis vectors. In [Jor09; Har05] it was argued, that our choice of the Clebsch–Gordan transforms CG^k implements exactly the same Gelfand–Tsetlin basis in $\mathcal{A}_{p,q}^d$ register of the mixed Schur–Weyl duality as in Theorem 3.2 for permutations σ_i , $i \neq p$. For the contraction generator $\sigma_p \in \mathcal{A}_{p,q}^d$ we numerically observe the same correspondence. This, in principle, can be proved by directly contracting two tensor networks from Fig. 4 corresponding to two different paths $S, T \in \text{Paths}(\lambda)$ for every $\lambda \in \hat{\mathcal{A}}_{p,q}^d$.

¹³In principle, for $d > p+q$, the scaling should be $(p+q)^{O((p+q)^2)}$ by adapting a strategy outlined in [Har05]. Indeed, in such case, any semistandard Young tableau $M \in \text{SSYT}(\lambda, d)$ of size $|\lambda| = p+q$ and with letters in $[d]$ has effectively at most $p+q$ different symbols. Therefore, it can be encoded as $M' \in \text{SSYT}(\lambda, n)$ by some encoding function $f_{\text{enc}} : [n] \rightarrow [d]$ which takes the values of the original tableau M .

The knowledge of explicit action of the generators of $\mathcal{A}_{p,q}^d$ in the Gelfand–Tsetlin basis is useful for quantum computing applications. For example, it yields the efficient quantum circuit for port-based teleportation, see Section 6. Equation (81) suggests not only a way of classically computing the matrix entries of the mixed quantum Schur transform unitary but also a quantum circuit for implementing the corresponding isometry (we will use the same notation for both). In the next section, we describe a quantum circuit which implements the needed basis transformation.

4.5. Quantum circuit for mixed Schur transform. In this section, we describe a quantum circuit that implements the mixed quantum Schur transform isometry $U_{\text{Sch}}(p, q)$:

$$U_{\text{Sch}}(p, q): (\mathbb{C}^d)^{p+q} \rightarrow \underbrace{\mathbb{C}^{|\hat{\mathcal{A}}_2^d|} \otimes \dots \otimes \mathbb{C}^{|\hat{\mathcal{A}}_{p+q-1}^d|}}_T \otimes \underbrace{\mathbb{C}^{|\hat{\mathcal{A}}_{p+q}^d|} \otimes \mathbb{C}^{|\hat{\mathcal{U}}_{d-1}^{p+q}|} \otimes \dots \otimes \mathbb{C}^{|\hat{\mathcal{U}}_1^{p+q}|}}_M, \quad (87)$$

where the first $p + q - 1$ registers of the output correspond to a path $T \in \text{Paths}(\lambda)$ labelling corresponding irreps of \mathcal{A}_k^d , the last d registers correspond to a Gelfand–Tsetlin pattern $M \in \text{GT}(\lambda, d)$ for some $\lambda \in \hat{\mathcal{A}}_{p,q}^d$ and $\hat{\mathcal{U}}_k^{p+q}$ is a set of staircases of bounded size, labelling the irreps of the group U_k . The last vertex T^{p+q} of the path T coincides with the top row \mathbf{m}_d of the Gelfand–Tsetlin pattern M , i.e., $T^{p+q} = \mathbf{m}_d = \lambda$; this explains the overlap between T and M in eq. (87).

More precisely, for every integer $n \in [p + q]$ and $k \in [d]$ we define the set $\hat{\mathcal{U}}_k^n$ of staircases labelling some irreps of U_k as

$$\hat{\mathcal{U}}_k^n := \begin{cases} \{\lambda \in \hat{\mathcal{U}}_k \mid |\lambda| \leq n\} & n < p + q \text{ or } k < d, \\ \hat{\mathcal{A}}_{p+q}^d & n = p + q \text{ and } k = d. \end{cases} \quad (88)$$

The output is eq. (87) of the quantum mixed Schur transform has tensor product structure for both path $T \in \text{Paths}(\lambda)$ and the Gelfand–Tsetlin pattern $M \in \text{GT}(\lambda, d)$. The natural way of interpreting the rows of a general Gelfand–Tsetlin pattern $M = (\mathbf{m}_d, \mathbf{m}_{d-1}, \mathbf{m}_{d-2}, \dots, \mathbf{m}_1) \in \text{GT}(\mathbf{m}_d, d)$ is to use the staircase notation for each row. This means that one should think of the quantum states $|T\rangle$ and $|M\rangle$ as follows:

$$|T\rangle = |T^2\rangle \otimes |T^3\rangle \otimes \dots \otimes |T^{p+q-1}\rangle \otimes |T^{p+q}\rangle, \quad (89)$$

$$|M\rangle = |\mathbf{m}_d\rangle \otimes |\mathbf{m}_{d-1}\rangle \otimes \dots \otimes |\mathbf{m}_2\rangle \otimes |\mathbf{m}_1\rangle. \quad (90)$$

Note that we suppress the registers corresponding to $|T^0\rangle$ and $|T^1\rangle$ of the path $T \in \text{Paths}(\lambda)$ since they are always one-dimensional. Moreover, it is useful to define a shorthand notation $M_{(k)}$ to indicate only the bottom k rows of the Gelfand–Tsetlin pattern M and the corresponding quantum state for any $k \in [d]$ as

$$|M_{(k)}\rangle := |\mathbf{m}_k\rangle \otimes |\mathbf{m}_{k-1}\rangle \otimes \dots \otimes |\mathbf{m}_1\rangle. \quad (91)$$

Our construction is a slight modification of the original quantum Schur transform [BCH06; Har05] for the classical Schur–Weyl duality (i.e., the $q = 0$ case of our formalism). It involves a cascade of Clebsch–Gordan isometries CG_d^+ (see Fig. 5), where each isometry implements one of the unitary Clebsch–Gordan transforms CG^k from eq. (79). The only modification we make to the original construction is to replace CG_d^+ by a similarly defined *dual Clebsch–Gordan isometry* CG_d^- in the second half of the circuit (see Fig. 6). This immediately leads to the following result which agrees with [BCH06; Har05] in the $q = 0$ case.

Theorem 4.2 (Mixed quantum Schur transform). *The mixed quantum Schur transform isometry (see Fig. 6) for block-diagonalizing the algebra $\mathcal{A}_{p,q}^d$ has a quantum circuit with $\text{poly}(d, p + q, \log 1/\epsilon)$ gates, where ϵ is the desired error, d is the local dimension, and p and q are the parameters of $\mathcal{A}_{p,q}^d$.*

The main new building block of the mixed quantum Schur transform circuit is the dual Clebsch–Gordan isometry CG_d^- . It can be obtained by a small modification of the usual CG_d^+ isometry, which can be taken directly from [BCH06; Har05]. While both isometries have the same structure, their representation-theoretic interpretation is slightly different: CG_d^+ is used when $k \leq p$ to add a new box to T_l^{k-1} producing a new diagram T_l^k , while CG_d^- is used when $k > p$ either to remove a box from T_l^{k-1} or to add a box to T_r^{k-1} . In the staircase notation from Section 2.4, this is equivalent to adding a box to the staircase T^{k-1} when $k \leq p$ and removing a box when $k > p$. We describe efficient quantum circuits for both isometries in a unified way in Section 4.6. Their complexity is $\text{poly}(d, \log(p + q), \log 1/\epsilon)$, which leads to the $(p + q)\text{poly}(d, \log(p + q), \log 1/\epsilon)$ complexity for the mixed quantum Schur transform $U_{\text{Sch}}(p, q)$.

4.6. Quantum circuit for Clebsch–Gordan transforms. In this section, we describe a recursive quantum circuit of complexity $\text{poly}(d, \log(p + q), \log 1/\epsilon)$ for the (dual) Clebsch–Gordan isometry CG_d^\pm . The only difference between CG_d^- and CG_d^+ is the formulas for their matrix entries and the labelling scheme of their input and output basis vectors. Our construction is based on [BCH06; Har05] and can be seen as a consequence of the fact

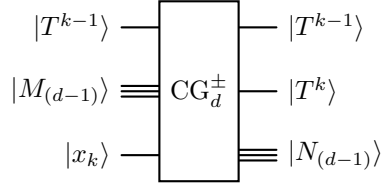


FIGURE 5. Input and output registers of the Clebsch–Gordan isometry CG_d^\pm which appears in Fig. 6. Here T^{k-1} and T^k denote the incoming and outgoing unitary group irreps (they are denoted by λ and μ in eq. (79)). Moreover, T^{k-1} is the first row of a Gelfand–Tsetlin pattern M of length d whose remaining rows $M_{(d-1)}$ are encoded by the tensor product state $|M_{(d-1)}\rangle := |\mathbf{m}_{d-1}\rangle \cdots |\mathbf{m}_1\rangle$. Similarly, T^k is the first row of a Gelfand–Tsetlin pattern N of length d whose remaining rows $N_{(d-1)}$ are encoded by $|N_{(d-1)}\rangle := |\mathbf{n}_{d-1}\rangle \cdots |\mathbf{n}_1\rangle$.

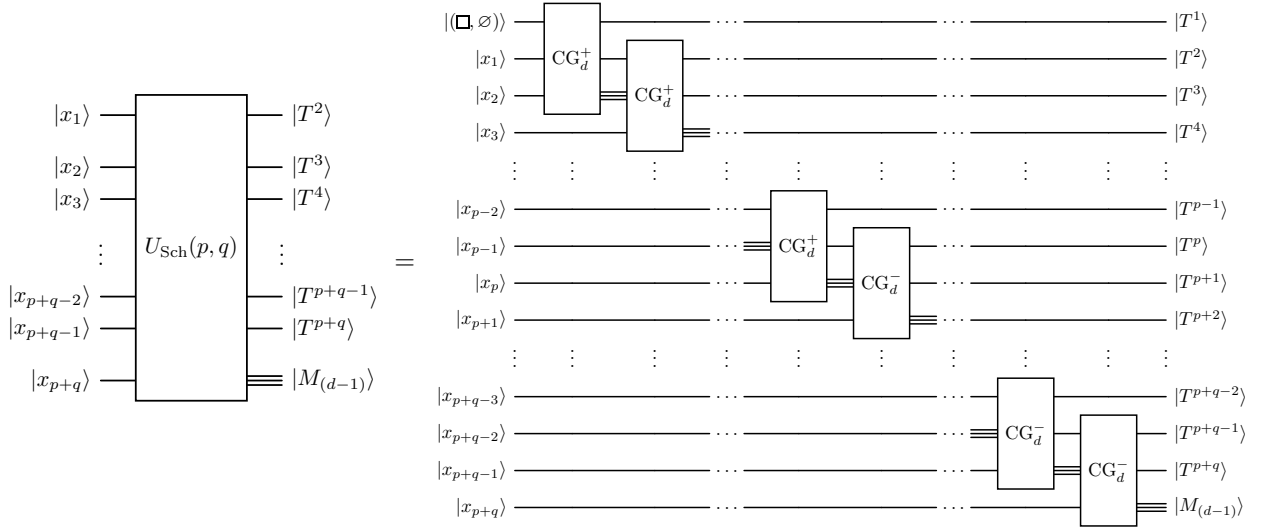


FIGURE 6. Schematic depiction of the mixed quantum Schur transform $U_{\text{Sch}}(p, q)$ and its implementation by a cascade of Clebsch–Gordan transforms CG_d^\pm . Note that we switch from CG_d^+ to CG_d^- starting at input $|x_{p+1}\rangle$. Since the topmost register on the right is one-dimensional, i.e., its input and output values are fixed to $|T^1\rangle = |(\square, \emptyset)\rangle$, we suppress it in $U_{\text{Sch}}(p, q)$.

that both the usual and the dual Clebsch–Gordan coefficients can be expressed as products of *reduced Wigner coefficients*¹⁴, see Appendix A.

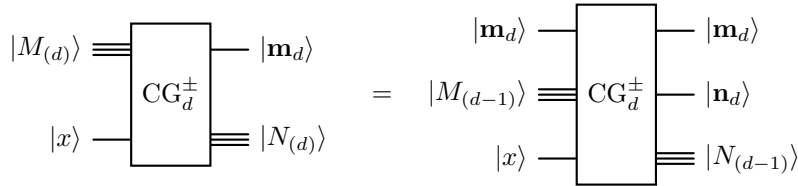


FIGURE 7. Input and output registers of the quantum gate CG_d^\pm that implements the CG^k transform from eq. (79). Here $\mathbf{m}_d, \mathbf{n}_d$ denote the top rows of the Gelfand–Tsetlin patterns M and N , indicating irrep labels. We denote the last $d-1$ rows of M by $M_{(d-1)}$ and encode it as a tensor product state: $|M_{(d-1)}\rangle = |\mathbf{m}_{d-1}\rangle \cdots |\mathbf{m}_1\rangle$.

Let us fix an arbitrary level $k = 2, \dots, p+q$ in the Bratteli diagram of $\mathcal{A}_{p,q}^d$, which is the same as fixing a position in the cascade of Clebsch–Gordan transforms in Fig. 6. Then for any $x \in [d]$ and $\mathbf{n}_d, \mathbf{m}_d \in \widehat{\mathcal{U}}_d^n$, we define

$$C_{\mathbf{n}_d, \mathbf{m}_d}^{x, \pm} |M_{(d-1)}\rangle := \sum_{N \in \text{GT}(\mathbf{n}_d, d)} c_{N, M}^{x, \pm} |N_{(d-1)}\rangle \quad (92)$$

¹⁴In [BCH06; Har05] this fact is proved based on the Wigner–Eckart theorem. In our approach, the starting point is the fact that Clebsch–Gordan coefficients can be expressed as products of reduced Wigner coefficients, see [VK92]. Consequently, we try to keep the notation from [VK92], see Appendix A.

where $c_{N,M}^{x,\pm}$ are defined in Appendix A and \pm refers to either dual or direct Clebsch–Gordan coefficients. The operators $C_{\mathbf{n}_d, \mathbf{m}_d}^{x,\pm}$ defined above are essentially the same as classical matrices $C_{T^j, T^{j-1}}^{x,j}$ defined in eq. (83). Now we can define quantum Clebsch–Gordan transforms CG_d^\pm , which are quantum analogues of CG^k from eq. (79), as

$$\text{CG}_d^\pm |M_{(d)}\rangle |x\rangle := |\mathbf{m}_d\rangle \sum_{\mathbf{n}_d : \mathbf{m}_d \rightarrow \pm \mathbf{n}_d} |\mathbf{n}_d\rangle (C_{\mathbf{n}_d, \mathbf{m}_d}^{x,\pm} |M_{(d-1)}\rangle), \quad (93)$$

where the notation $\mathbf{n}_d : \mathbf{m}_d \rightarrow \pm \mathbf{n}_d$ means that we obtain a staircase \mathbf{n}_d by either adding or removing a box from the staircase \mathbf{m}_d , depending on the chosen CG_d^\pm Clebsch–Gordan transform. More explicitly, we can write

$$\text{CG}_d^\pm = \sum_{x \in [d]} \sum_{\mathbf{m}_d, \mathbf{n}_d \in \widehat{\mathcal{U}}_d^{p+q}} \sum_{\substack{M \in \text{GT}(\mathbf{m}_d, d) \\ N \in \text{GT}(\mathbf{n}_d, d)}} c_{N_{(d)}, M_{(d)}}^{x,\pm} |\mathbf{m}_d, \mathbf{n}_d, N_{(d-1)}\rangle \langle \mathbf{m}_d, M_{(d-1)}, x|. \quad (94)$$

Our goal is to recursively implement CG_d^\pm in terms of CG_{d-1}^\pm . Using eq. (94) we can easily write the Clebsch–Gordan transform for $d-1$:

$$\text{CG}_{d-1}^\pm = \sum_{x \in [d-1]} \sum_{\mathbf{m}_{d-1}, \mathbf{n}_{d-1} \in \widehat{\mathcal{U}}_{d-1}^{p+q}} \sum_{\substack{M \in \text{GT}(\mathbf{m}_{d-1}, d-1) \\ N \in \text{GT}(\mathbf{n}_{d-1}, d-1)}} c_{N_{(d-1)}, M_{(d-1)}}^{x,\pm} |\mathbf{m}_{d-1}, \mathbf{n}_{d-1}, N_{(d-2)}\rangle \langle \mathbf{m}_{d-1}, M_{(d-2)}, x|. \quad (95)$$

Recall from Appendix A that for every $k \in [d]$ and Gelfand–Tsetlin patterns of length $k-1$,

$$c_{N_{(k-1)}, M_{(k-1)}}^{k,\pm} := \delta_{N_{(k-1)}, M_{(k-1)}}. \quad (96)$$

Moreover, for any symbol $x \in [k]$, staircases $\mathbf{m}_k, \mathbf{n}_k \in \widehat{\mathcal{U}}_k^{p+q}$, and Gelfand–Tsetlin patterns $M \in \text{GT}(\mathbf{m}_k, k)$, $N \in \text{GT}(\mathbf{n}_k, k)$ the following recursive identity holds:

$$c_{N_{(k)}, M_{(k)}}^{x,\pm} = (z^\pm)^{\mathbf{m}_k, \mathbf{n}_k}_{\mathbf{m}_{k-1}, \mathbf{n}_{k-1}} \cdot c_{N_{(k-1)}, M_{(k-1)}}^{x,\pm}. \quad (97)$$

Moreover, note that

$$\begin{aligned} & |\mathbf{m}_d, \mathbf{n}_d, N_{(d-1)}\rangle \langle \mathbf{m}_d, M_{(d-1)}, x| \\ &= |\mathbf{m}_d, \mathbf{n}_d, \mathbf{n}_{d-1}, N_{(d-2)}\rangle \langle \mathbf{m}_d, \mathbf{m}_{d-1}, M_{(d-2)}, x| \end{aligned} \quad (98)$$

$$= (|\mathbf{m}_d, \mathbf{n}_d, \mathbf{n}_{d-1}\rangle \langle \mathbf{m}_d, \mathbf{m}_{d-1}, \mathbf{n}_{d-1}| \otimes I) \cdot (I \otimes |\mathbf{m}_{d-1}, \mathbf{n}_{d-1}, N_{(d-2)}\rangle \langle \mathbf{m}_{d-1}, M_{(d-2)}, x|), \quad (99)$$

which implies

$$\begin{aligned} & c_{N_{(d)}, M_{(d)}}^{x,\pm} |\mathbf{m}_d, \mathbf{n}_d, N_{(d-1)}\rangle \langle \mathbf{m}_d, M_{(d-1)}, x| \\ &= ((z^\pm)^{\mathbf{m}_d, \mathbf{n}_d}_{\mathbf{m}_{d-1}, \mathbf{n}_{d-1}} |\mathbf{m}_d, \mathbf{n}_d, \mathbf{n}_{d-1}\rangle \langle \mathbf{m}_d, \mathbf{m}_{d-1}, \mathbf{n}_{d-1}| \otimes I) \cdot \\ & \quad \cdot (c_{N_{(d-1)}, M_{(d-1)}}^{x,\pm} I \otimes |\mathbf{m}_{d-1}, \mathbf{n}_{d-1}, N_{(d-2)}\rangle \langle \mathbf{m}_{d-1}, M_{(d-2)}, x|). \end{aligned} \quad (100)$$

Together, these observations allow us rewrite eq. (94) as

$$\text{CG}_d^\pm = \sum_{x \in [d]} \sum_{\mathbf{m}_d, \mathbf{n}_d \in \widehat{\mathcal{U}}_d^{p+q}} \sum_{\substack{M \in \text{GT}(\mathbf{m}_d, d) \\ N \in \text{GT}(\mathbf{n}_d, d)}} |\mathbf{m}_d, \mathbf{n}_d, N_{(d-1)}\rangle \langle \mathbf{m}_d, M_{(d-1)}, x| \quad (101)$$

$$= \sum_{x \in [d]} \sum_{\substack{\mathbf{m}_d, \mathbf{n}_d \in \widehat{\mathcal{U}}_d^{p+q} \\ \mathbf{m}_{d-1}, \mathbf{n}_{d-1} \in \widehat{\mathcal{U}}_{d-1}^{p+q}}} \sum_{\substack{M \in \text{GT}(\mathbf{m}_{d-1}, d-1) \\ N \in \text{GT}(\mathbf{n}_{d-1}, d-1)}} ((z^\pm)^{\mathbf{m}_d, \mathbf{n}_d}_{\mathbf{m}_{d-1}, \mathbf{n}_{d-1}} |\mathbf{m}_d, \mathbf{n}_d, \mathbf{n}_{d-1}\rangle \langle \mathbf{m}_d, \mathbf{m}_{d-1}, \mathbf{n}_{d-1}| \otimes I) \cdot \quad (102)$$

$$\cdot (c_{N_{(d-1)}, M_{(d-1)}}^{x,\pm} I \otimes |\mathbf{m}_{d-1}, \mathbf{n}_{d-1}, N_{(d-2)}\rangle \langle \mathbf{m}_{d-1}, M_{(d-2)}, x|)$$

$$= \left(\sum_{\substack{\mathbf{m}_d, \mathbf{n}_d \in \widehat{\mathcal{U}}_d^{p+q} \\ \mathbf{m}_{d-1}, \mathbf{n}_{d-1} \in \widehat{\mathcal{U}}_{d-1}^{p+q}}} (z^\pm)^{\mathbf{m}_d, \mathbf{n}_d}_{\mathbf{m}_{d-1}, \mathbf{n}_{d-1}} |\mathbf{m}_d, \mathbf{n}_d, \mathbf{n}_{d-1}\rangle \langle \mathbf{m}_d, \mathbf{m}_{d-1}, \mathbf{n}_{d-1}| \otimes I \right) \cdot \quad (103)$$

$$\cdot \left(I \otimes \sum_{x \in [d]} \sum_{\mathbf{m}_{d-1}, \mathbf{n}_{d-1} \in \widehat{\mathcal{U}}_{d-1}^{p+q}} \sum_{\substack{M \in \text{GT}(\mathbf{m}_{d-1}, d-1) \\ N \in \text{GT}(\mathbf{n}_{d-1}, d-1)}} c_{N_{(d-1)}, M_{(d-1)}}^{x,\pm} |\mathbf{m}_{d-1}, \mathbf{n}_{d-1}, N_{(d-2)}\rangle \langle \mathbf{m}_{d-1}, M_{(d-2)}, x| \right)$$

$$= (C_d^\pm \otimes I) \cdot (I \otimes \widehat{\text{CG}}_{d-1}^\pm), \quad (104)$$

where we introduced the following two operators

$$C_d^\pm := \sum_{\substack{\mathbf{m}_d, \mathbf{n}_d \in \widehat{U}_d^{p+q} \\ \mathbf{m}_{d-1}, \mathbf{n}_{d-1} \in \widehat{U}_{d-1}^{p+q}}} (z^\pm)^{\mathbf{m}_d, \mathbf{n}_d}_{\mathbf{m}_{d-1}, \mathbf{n}_{d-1}} |\mathbf{m}_d, \mathbf{n}_d, \mathbf{n}_{d-1}\rangle \langle \mathbf{m}_d, \mathbf{m}_{d-1}, \mathbf{n}_{d-1}|, \quad (105)$$

$$\begin{aligned} \widetilde{CG}_{d-1}^\pm &:= \sum_{x \in [d]} \sum_{\mathbf{m}_{d-1}, \mathbf{n}_{d-1} \in \widehat{U}_{d-1}^{p+q}} \sum_{\substack{M \in \text{GT}(\mathbf{m}_{d-1}, d-1) \\ N \in \text{GT}(\mathbf{n}_{d-1}, d-1)}} c_{N_{(d-1)}, M_{(d-1)}}^{x, \pm} |\mathbf{m}_{d-1}, \mathbf{n}_{d-1}, N_{(d-2)}\rangle \langle \mathbf{m}_{d-1}, M_{(d-2)}, x| \\ &= CG_{d-1}^\pm + \sum_{\mathbf{m}_{d-1} \in \widehat{U}_{d-1}^{p+q}} \sum_{M \in \text{GT}(\mathbf{m}_{d-1}, d-1)} |\mathbf{m}_{d-1}, \mathbf{m}_{d-1}, M_{(d-2)}\rangle \langle \mathbf{m}_{d-1}, M_{(d-2)}, d|, \end{aligned} \quad (106)$$

where the last term corresponds to $x = d$. We can translate eq. (104) into a quantum circuit shown in Fig. 8. This procedure can be continued recursively on the parameter d .

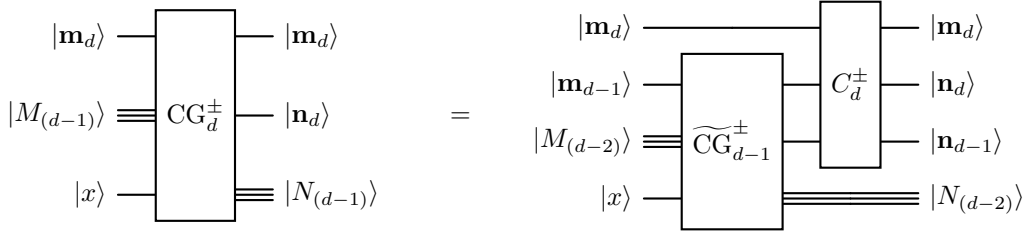


FIGURE 8. Recursive implementation of CG_d^\pm . The registers $|M_{(d-1)}\rangle$ and $|N_{(d-1)}\rangle$ on the left-hand side should be understood as tensor products $|M_{(d-1)}\rangle = |\mathbf{m}_{d-1}\rangle |M_{(d-2)}\rangle$ and $|N_{(d-1)}\rangle = |\mathbf{n}_{d-1}\rangle |N_{(d-2)}\rangle$.

Note from eq. (105) that C_d^\pm is a controlled operation acting on the middle register:

$$C_d^\pm = \sum_{\mathbf{m}_d \in \widehat{U}_d^{p+q}} \sum_{\mathbf{n}_{d-1} \in \widehat{U}_{d-1}^{p+q}} |\mathbf{m}_d\rangle \langle \mathbf{m}_d| \otimes C_{\mathbf{m}_d, \mathbf{n}_{d-1}}^\pm \otimes |\mathbf{n}_{d-1}\rangle \langle \mathbf{n}_{d-1}|, \quad (107)$$

where we define $C_{\mathbf{m}_d, \mathbf{n}_{d-1}}^\pm$ as

$$C_{\mathbf{m}_d, \mathbf{n}_{d-1}}^\pm := \sum_{\mathbf{m}_{d-1} \in \widehat{U}_{d-1}^{p+q}} \sum_{\mathbf{n}_d \in \widehat{U}_d^{p+q}} (z^\pm)^{\mathbf{m}_d, \mathbf{n}_d}_{\mathbf{m}_{d-1}, \mathbf{n}_{d-1}} |\mathbf{n}_d\rangle \langle \mathbf{m}_{d-1}|. \quad (108)$$

We can think of C_d^\pm as the quantum circuit shown in Fig. 9. Crucially, the $C_{\mathbf{m}_d, \mathbf{n}_{d-1}}^\pm$ operator is essentially a $d \times d$ matrix since most of the coefficients $(z^\pm)^{\mathbf{m}_d, \mathbf{n}_d}_{\mathbf{m}_{d-1}, \mathbf{n}_{d-1}}$ are zero, see Appendix A. The operator $C_{\mathbf{m}_d, \mathbf{n}_{d-1}}^\pm$ admits an efficient implementation as a quantum circuit because the reduced Wigner coefficients $(z^\pm)^{\mathbf{m}_d, \mathbf{n}_d}_{\mathbf{m}_{d-1}, \mathbf{n}_{d-1}}$ are efficiently computable, see eqs. (169) to (172).

From these formulas, we see that computing the reduced Wigner coefficients has complexity $\text{poly}(d, \log(p+q))$. Therefore, the complexity of implementing the operator C_d^\pm to accuracy ϵ is $\text{poly}(d, \log(p+q), \log(1/\epsilon))$. This is the same complexity as in [BCH06; Har05].

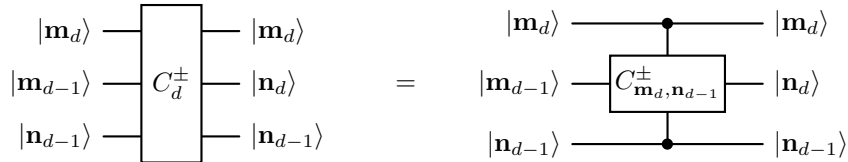


FIGURE 9. Circuit for the C_d^\pm operator from eq. (105).

5. UNITARY-EQUIVARIANT SDPS

5.1. Unitary-equivariant quantum channels. A quantum channel $\Phi: \text{End}(V^p) \rightarrow \text{End}(V^q)$ is *locally* U_d -equivariant or simply *unitary-equivariant* if

$$\Phi(U^{\otimes p} \rho U^{\dagger \otimes p}) = U^{\otimes q} \Phi(\rho) U^{\dagger \otimes q} \quad (109)$$

for every $U \in U_d$ and quantum state ρ . A convenient way of representing any quantum channel is by its *Choi matrix*. In particular, for a quantum channel $\Phi: \text{End}(V^p) \rightarrow \text{End}(V^q)$, its Choi matrix $X^\Phi \in \text{End}(V_d^{p,q})$ is defined as

$$X^\Phi := \sum_{\substack{i_1, \dots, i_p \in [d] \\ j_1, \dots, j_p \in [d]}} |i_1, \dots, i_p\rangle \langle j_1, \dots, j_p| \otimes \Phi(|i_1, \dots, i_p\rangle \langle j_1, \dots, j_p|) \quad (110)$$

where the sum runs over the computational basis of V_d^p . Recall that the action of Φ on state ρ can be recovered from its Choi matrix X^Φ via $\Phi(\rho) = \text{Tr}_{V_d^p}[X^\Phi(\rho^\top \otimes I_{V_d^q})]$. Furthermore, a given matrix $X \in \text{End}(V_d^{p,q})$ describes a quantum channel if and only if $X \succeq 0$ and $\text{Tr}_{V_d^q}(X) = I_{V_d^p}$ [Wat18].

Let $X^\Phi \in \text{End}(V_d^{p,q})$ be the Choi matrix of a channel Φ . Then Φ is unitary-equivariant if and only if

$$[X^\Phi, U^{\otimes p} \otimes \bar{U}^{\otimes q}] = 0, \quad (111)$$

for all $U \in U_d$ [GO22]. Thanks to Schur's lemma, applying the mixed quantum Schur transform (69) decomposes X^Φ as follows:

$$U_{\text{Sch}}(p, q) X^\Phi U_{\text{Sch}}^\dagger(p, q) = \bigoplus_{\lambda \in \hat{\mathcal{A}}_{p,q}^d} \sum_{T, S \in \text{Paths}(\lambda)} x_{TS} |T\rangle \langle S| \otimes I_{m_\lambda} \quad (112)$$

where m_λ is the dimension of the λ -irrep of U_d , $I_{m_\lambda} = \sum_{M \in \text{GT}(\lambda, d)} |M\rangle \langle M|$ is the identity matrix on the unitary irrep register λ , and

$$\mathcal{E}_{TS} := U_{\text{Sch}}^\dagger(p, q) \left(\bigoplus_{\mu \in \hat{\mathcal{A}}_{p,q}^d} \delta_{\lambda\mu} |T\rangle \langle S| \otimes I_{m_\lambda} \right) U_{\text{Sch}}(p, q) \quad (113)$$

is the so-called *matrix unit* algebra $\mathcal{A}_{p,q}^d$ corresponding to the pair of paths $T, S \in \text{Paths}(\lambda)$. These matrix units form a basis of $\mathcal{A}_{p,q}^d$ and span the whole algebra:

$$\mathcal{A}_{p,q}^d = \text{span} \left\{ \mathcal{E}_{TS} \mid \lambda \in \hat{\mathcal{A}}_{p,q}^d, S, T \in \text{Paths}(\lambda) \right\} \quad (114)$$

Notice that the trace of a matrix unit for $T, S \in \text{Paths}(\lambda)$ is

$$\text{Tr}(\mathcal{E}_{TS}) = \delta_{TS} m_\lambda, \quad (115)$$

and their product satisfies

$$\mathcal{E}_{ST} \cdot \mathcal{E}_{T'S'} = \delta_{TT'} \mathcal{E}_{SS'}. \quad (116)$$

5.2. Full trace. In this section, we present methods to efficiently compute the trace $\text{Tr}(YX)$ of the product of two matrices X and Y , where X is of the form (112), i.e.,

$$X = \sum_{\lambda \in \hat{\mathcal{A}}_{p,q}^d} \sum_{S, T \in \text{Paths}(\lambda)} x_{ST} \mathcal{E}_{ST}, \quad (117)$$

and Y is assumed to be of one of three special forms: either corresponding to a matrix unit, to an entry in the matrix written in the computational basis or corresponding to a walled Brauer diagram. Those methods will be crucial for semi-definite optimization problems over unitary equivariant quantum channels.

5.2.1. Firstly, assume that matrix Y is also a matrix unit, i.e. $Y = \mathcal{E}_{S,T}$ for some $\mathcal{E}_{S,T} \in \mathcal{E}$ with $S, T \in \text{Paths}(\lambda)$. $X = \sum_{S', T'} x_{S', T'} \mathcal{E}_{S', T'}$. As the matrix X is of the form (117), by elementary properties of matrix units, we have

$$\text{Tr}(YX) = \sum_{T', S'} x_{T', S'} \text{Tr}(\mathcal{E}_{S, T} \mathcal{E}_{T', S'}) = x_{T, S} \cdot m_\lambda. \quad (118)$$

Hence, the computational complexity of computing all coefficients in front of $x_{T, S}$ of this operation equals the complexity of the computation of the number m_λ , which is $O((p+q) \log^2(p+q+d))$.

5.2.2. Secondly, assume that matrix Y is written in the computational basis and has only a single non-zero entry, i.e. $Y = |I\rangle \langle J|$ for some $I = i_1, \dots, i_{p+q}$ and $J = j_1, \dots, j_{p+q}$. In order to compute the trace $\text{Tr}(YX)$, we need to re-write the entries of matrix (117) into computational basis by applying Schur transform:

$$\text{Tr}(|I\rangle \langle J| X) = \langle J| X |I\rangle = \sum_{\lambda \in \hat{\mathcal{A}}_{p,q}^d} \sum_{S, T \in \text{Paths}(\lambda)} x_{TS} \sum_{M \in \text{GT}(\lambda, d)} \langle J| U_{\text{Sch}}^\dagger(p, q) |(T, M)\rangle \langle (S, M)| U_{\text{Sch}}(p, q) |I\rangle \quad (119)$$

Using previously derived form of Schur transform (84), the computation of $\langle (T, M)| U_{\text{Sch}}(p, q) |I\rangle = \langle I| U_{\text{Sch}}^\dagger(p, q) |(T, M)\rangle$ is reduced to the multiplication of Clebsch–Gordan matrices:

$$\langle I| U_{\text{Sch}}^\dagger(p, q) |(T, M)\rangle = \begin{cases} \langle M| C_{T^{p+q} T^{p+q-1}}^{i_{p+q}, w(i_{p+q-1}, \dots, i_1)} \dots C_{T^2 T^1}^{i_2} |i_1\rangle & w(I) = w(M), \\ 0 & w(I) \neq w(M), \end{cases} \quad (120)$$

where $|M\rangle$ is a Gelfand–Tsetlin basis vector for the irreducible representation of a unitary group corresponding to λ . Notice that $\sum_{M \in \text{GT}(\lambda, d)} |M\rangle \langle M| = I_{m_\lambda}$, hence we can rewrite (119) as

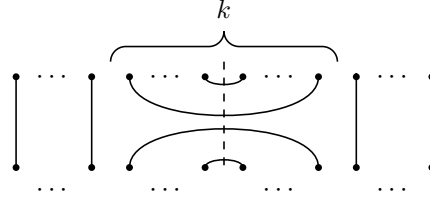
$$\langle J|X|I\rangle = \begin{cases} \sum_{S,T} x_{S,T} \langle j_1 | (C_{S^2 S^1}^{i_2})^\dagger \cdots (C_{S^{p+q} S^{p+q-1}}^{j_{p+q}, w(j_{p+q-1}, \dots, j_1)})^\dagger C_{T^{p+q} T^{p+q-1}}^{i_{p+q}, w(i_{p+q-1}, \dots, i_1)} \cdots C_{T^2 T^1}^{i_2} | i_1 \rangle & w(I) = w(J), \\ 0 & w(I) \neq w(J). \end{cases} \quad (121)$$

As it we demonstrated in Section 4.3, matrices in the above equation have dimensions given by Kostka numbers $K_{T^{(k)}, w(i_k, \dots, i_1)}$ and $K_{S^{(k)}, w(j_k, \dots, j_1)}$ respectively, and computation of complexity of computing (121) is given by $(p+q)^{O(d^2)}$.

5.2.3. Lastly, assume that the matrix Y is an image of a single Brauer diagram $\pi \in \mathcal{B}_{p,q}^d$, i.e. $Y = \psi_{p,q}^d(\pi) \in \mathcal{A}_{p,q}^d$. In order to compute trace $\text{Tr}(\psi_{p,q}^d(\pi)X)$, we shall compute matrix entries of $\psi_{p,q}^d(\pi)$ in the Gelfand–Tsetlin basis of all irreducible representations of $\mathcal{A}_{p,q}^d$. For that purpose, we shall present diagram $\pi \in \mathcal{B}_{p,q}^d$ in terms of generators $\sigma_i \in \mathcal{B}_{p,q}^d$ of the walled Brauer algebra $\mathcal{B}_{p,q}^d$. Assume that diagram π has exactly k contractions. By applying certain permutations $\sigma_l^u, \sigma_l^d \in S_p$ and $\sigma_r^u, \sigma_r^d \in S_q$ acting on the left and rights sides of the diagram π , it can be represented as

$$\pi = (\sigma_l^u \otimes \sigma_r^u) \bar{\sigma}_k (\sigma_l^d \otimes \sigma_r^d) \quad (122)$$

where $\bar{\sigma}_k := \prod_{i=0}^{k-1} \overline{(p-i, p+1+i)}$ is represented by the diagram with k contractions located near the wall, i.e.



As $\sigma_l^u, \sigma_l^d \in S_p$ they might be written as a product of at most p^2 generators σ_i of the algebra $\mathcal{B}_{p,q}^d$. Similarly, $\sigma_r^u, \sigma_r^d \in S_q$ can be written as a product of q^2 generators σ_i of the algebra $\mathcal{B}_{p,q}^d$. Furthermore, the diagram $\bar{\sigma}_k$ can be decomposed into generators σ_i of the algebra $\mathcal{B}_{p,q}^d$ as follows:

$$\bar{\sigma}_k = (\sigma_p \sigma_{p+1} \cdots \sigma_{p-k+1} \cdots \sigma_{p-1} \sigma_{p+k-1}) \cdots (\sigma_p \sigma_{p+1} \sigma_{p+2} \sigma_{p-1} \sigma_{p-2}) (\sigma_p \sigma_{p+1} \sigma_{p-1}) \sigma_p \quad (124)$$

which is of the length given by k^2 . Altogether, the decomposition of an arbitrary diagram π into generators of the algebra $\mathcal{B}_{p,q}^d$ requires $O((p+q)^2)$ multiplications of these generators. We shall multiply those generators separately in the Gelfand–Tsetlin basis for each irreducible representation related to $\lambda \in \hat{\mathcal{A}}_{p,q}^d$. Such a multiplication has a complexity $O(d_\lambda^3)$, where d_λ is a dimension of irreducible representation corresponding to λ . Due to the fact [GO22]

$$\dim \mathcal{A}_{p,q}^d = \sum_{\lambda \in \hat{\mathcal{A}}_{p,q}^d} d_\lambda^2, \quad (125)$$

complexity of computing the aforementioned product of generators is $O((\dim \mathcal{A}_{p,q}^d)^{3/2})$ ¹⁵. Combining everything together, the total complexity of computing all matrix units of $\psi_{p,q}^d(\pi)$, i.e. computing $\psi(\pi)_{S,T} := \text{Tr}(\psi_{p,q}^d(\pi) \mathcal{E}_{S,T})$ is $O((p+q)^2 (\dim \mathcal{A}_{p,q}^d)^{3/2})$. Note that having the matrix units of $\psi_{p,q}^d(\pi)$ allows us to write

$$\text{Tr}(YX) = \text{Tr}(\psi_{p,q}^d(\pi)X) = \sum_{\lambda \in \hat{\mathcal{A}}_{p,q}^d} \sum_{S,T \in \text{Paths}(\lambda)} \psi(\pi)_{S,T} \text{Tr}(\mathcal{E}_{S,T}X) = \sum_{\lambda \in \hat{\mathcal{A}}_{p,q}^d} \sum_{S,T \in \text{Paths}(\lambda)} \psi(\pi)_{S,T} \cdot x_{T,S} \cdot m_\lambda. \quad (126)$$

5.3. **Partial trace.** In this section, we present methods to efficiently compute the partial trace $\text{Tr}_S(XY)$ of a product of two matrices where X is presented as a linear combination of matrix units (117), and Y is also of one of the special form. For simplicity, we assume that traced out systems are always the last system, i.e. we compute $\text{Tr}_{S_k}(X)$ for the sets $S_k := \{k+1, \dots, p+q\}$ for arbitrary k such that $1 \leq k \leq p+q-1$. In that case,

¹⁵It seems, that the factor $\frac{3}{2}$ in this estimation could be dropped by applying Fast Fourier Transform (FFT). Indeed, FFT was successfully adapted to the setting of finite groups and some finite-dimensional semisimple algebras [MRW18a; MRW18b] and could be easily adapted for the full walled Brauer algebra $\mathcal{B}_{p,q}^d$, when it is semisimple. However, for the algebra of partially transposed permutations $\mathcal{A}_{p,q}^d$, it is not clear to us how to present the set of vectors which span the entire algebra $\mathcal{A}_{p,q}^d$. The non-triviality of the ideal $\ker(\psi_{p,q}^d)$ makes the adaptation of [MRW18a; MRW18b] highly nontrivial, so we leave it for future work.

we use the following general result by Ram and Wenzl [RW92], which we adopt to our setting of algebras $\mathcal{A}_{p,q}^d$.¹⁶

Lemma 5.1 ([RW92]). *Consider any irreducible representation $\lambda \in \mathcal{A}_{p,q}^d$, two paths $S, T \in \text{Paths}(\lambda)$ and a corresponding matrix unit $\mathcal{E}_{S,T}$. One can decompose paths S, T with respect to the last system, i.e. write $S = \bar{S} \circ \lambda$ and $T = \bar{T} \circ \lambda$, and $\bar{S} \in \text{Paths}_{p+q-1}(\mu)$ and $\bar{T} \in \text{Paths}_{p+q-1}(\mu')$ where $S^{p+q-1} = \mu$ and $T^{p+q-1} = \mu'$. The partial trace of the last system for the matrix unit $\mathcal{E}_{S,T}$ reads:*

$$\text{Tr}_{p+q} \mathcal{E}_{S,T} = \begin{cases} \frac{m_\lambda}{m_\mu} \mathcal{E}_{\bar{S}, \bar{T}} & \mu = \mu', \\ 0 & \mu \neq \mu'. \end{cases} \quad (127)$$

For simplicity of the notation, in this subsection, we rewrite the sequence of inclusions (50) in the following way:

$$\mathcal{A}_0^d \hookrightarrow \mathcal{A}_1^d \hookrightarrow \dots \hookrightarrow \mathcal{A}_{p+q-1}^d \hookrightarrow \mathcal{A}_{p+q}^d, \quad (128)$$

i.e. $\mathcal{A}_k^d := \mathcal{A}_{k,0}^d$ for $k \leq p$ and $\mathcal{A}_k^d := \mathcal{A}_{p,k-p}^d$ for $k \geq p$. As previously, we assume that matrix X is of the form (112), and matrix Y is of one of the special forms: either identity matrix, or corresponding to a matrix unit, or corresponding to a walled Brauer diagram.

5.3.1. Firstly, assume that $Y = I$ is an identity matrix. Applying Lemma 5.1 recursively, we have

$$\text{Tr}_{S_k}(X) = \sum_{\lambda \in \hat{\mathcal{A}}_{p,q}^d} \sum_{S, T \in \text{Paths}(\lambda)} x_{S,T} \text{Tr}_k \text{Tr}_{k+1} \dots \text{Tr}_{p+q} \mathcal{E}_{S,T} \quad (129)$$

$$= \sum_{\lambda \in \hat{\mathcal{A}}_{p,q}^d} \sum_{\mu \in \hat{\mathcal{A}}_k^d} \sum_{\substack{S, T \in \text{Paths}(\lambda) \\ S^k = T^k = \mu \\ \forall i \geq k : S^i = T^i}} x_{S,T} \frac{m_\lambda}{m_\mu} \mathcal{E}_{\bar{S}, \bar{T}}, \quad (130)$$

where $\bar{S} \in \text{Paths}_k(\mu)$, $\bar{T} \in \text{Paths}_k(\mu)$ are truncations of $S, T \in \text{Paths}(\lambda)$ to the first k subsystems.

5.3.2. Secondly, assume that matrix $Y = \mathcal{E}_{S', T'}$ is a matrix unit. By elementary properties of matrix units and by applying Lemma 5.1 recursively, we have

$$\text{Tr}_{S_k}(\mathcal{E}_{S', T'} X) = \sum_{\lambda \in \hat{\mathcal{A}}_{p,q}^d} \sum_{T \in \text{Paths}(\lambda)} x_{T', T} \text{Tr}_{S_k}(\mathcal{E}_{S', T}) = \sum_{\lambda \in \hat{\mathcal{A}}_{p,q}^d} \sum_{\substack{T \in \text{Paths}(\lambda) \\ T^k = \mu \\ \forall i \geq k : T^i = S'^i}} x_{T', T} \frac{m_\lambda}{m_\mu} \mathcal{E}_{\bar{S}', \bar{T}} \quad (131)$$

where $\bar{S}' \in \text{Paths}_k(\mu)$, $\bar{T} \in \text{Paths}_k(\mu)$ are truncations of $S', T \in \text{Paths}(\lambda)$ respectively to the first k subsystems.

5.3.3. Lastly, assume that the matrix Y is an image of a single Brauer diagram $\pi \in \mathcal{B}_{p,q}^d$, i.e. $Y = \psi_{p,q}^d(\pi) \in \mathcal{A}_{p,q}^d$. As In Section 5.2.3, we shown how to compute all matrix units of $\psi_{p,q}^d(\pi)$, i.e. computing $\psi(\pi)_{S,T} := \text{Tr}(\psi_{p,q}^d(\pi) \mathcal{E}_{S,T})$ in time $O((p+q)^2 (\dim \mathcal{A}_{p,q}^d)^{3/2})$. Having done it, we can use the same method as in Section 5.3.2:

$$\begin{aligned} \text{Tr}_{S_k}(YX) &= \text{Tr}_{S_k}(\psi_{p,q}^d(\pi) X) = \sum_{\lambda \in \hat{\mathcal{A}}_{p,q}^d} \sum_{S, T \in \text{Paths}(\lambda)} \psi_{p,q}^d(\pi)_{S,T} \text{Tr}_{S_k}(\mathcal{E}_{S,T} X) \\ &= \sum_{\lambda \in \hat{\mathcal{A}}_{p,q}^d} \sum_{S, T \in \text{Paths}(\lambda)} \psi_{p,q}^d(\pi)_{S,T} \sum_{\lambda \in \hat{\mathcal{A}}_{p,q}^d} \sum_{\mu \in \hat{\mathcal{A}}_k^d} \sum_{\substack{T' \in \text{Paths}(\lambda) \\ S^k = T'^k = \mu \\ \forall i \geq k : T'^i = S^i}} x_{T, T'} \frac{m_\lambda}{m_\mu} \mathcal{E}_{\bar{S}, \bar{T}'} \end{aligned} \quad (132)$$

in order to compute the partial trace.

5.4. Unitary-equivariant SDPs. Semidefinite programming is an important subfield of optimization [WSV12] that has numerous applications in quantum information theory [ST21; Wat18]. A particularly common class of semidefinite programs (SDPs) that occur in quantum information is one where the matrix variable X has a continuous unitary symmetry group:

$$[X, U^{\otimes p} \otimes \bar{U}^{\otimes q}] = 0, \quad \forall U \in \text{U}_d. \quad (133)$$

¹⁶In fact, it should be possible to adapt the same result for computing the partial trace over all types of subsystems $S \subset [p+q]$. Indeed, one can "SWAP" given two subsystems using, so-called, $6j$ -symbol. In that way, subsystems in S can be effectively swapped to the last positions. We leave for future work the details of such procedure.

For example, this occurs when X describes a unitary-equivariant quantum channel with p inputs and q outputs, each of dimension d (see Section 5.1 for more details). We will focus on the following general class of SDPs with this symmetry:

$$\begin{aligned} \max_X \quad & \text{Tr}(CX) \\ \text{s.t.} \quad & \text{Tr}(A_k X) \leq b_k, \quad \forall k \in [m_1], \\ & \text{Tr}_{S_{i_k}}(D_k X) = B_k, \quad \forall k \in [m_2], \\ & [X, U^{\otimes p} \otimes \bar{U}^{\otimes q}] = 0, \quad \forall U \in \text{U}_d, \\ & X \succeq 0, \end{aligned} \tag{134}$$

Here m_1 and m_2 denote the number of inequality and equality constraints, respectively. The matrices A_k, D_k, C are Hermitian, and we consider only a specific choice of the sets S_{i_k} , namely $S_{i_k} := \{i_k, \dots, p+q\}$, furthermore, we assume that matrices D_k are written as linear combinations of matrix units (112).

Our goal is to devise a symmetry reduction procedure that translates the above SDP into one where the irrelevant degrees of freedom in the matrix X variable are eliminated. Thanks to mixed Schur–Weyl duality, the unitary equivariance constrain (133) on matrix X implies that it can be written as a linear combination of the matrix units (117) of the matrix algebra $\mathcal{A}_{p,q}^d$, i.e.,

$$X = \sum_{S,T} x_{ST} \mathcal{E}_{ST} = \sum_{\lambda \in \hat{\mathcal{A}}_{p,q}^d} \sum_{S,T \in \text{Paths}(\lambda)} x_{ST} \mathcal{E}_{ST}. \tag{135}$$

By rewriting the constraints in (134) into the mixed Schur basis, we can translate the input problem in eq. (134) into the following equivalent SDP problem:

$$\begin{aligned} \max_{x_{ST}} \quad & f_C(x_{ST}) \\ \text{s.t.} \quad & f_{A_k}(x_{ST}) \leq b_k, \quad \forall k \in [m_1], \\ & g_{D_k, B_k}^{i_k, T_{i_k}, S_{i_k}}(x_{ST}) = 0, \quad \forall k \in [m_2], \\ & X_\lambda \succeq 0, \end{aligned} \tag{136}$$

where $T_{i_k}, S_{i_k} \in \text{Paths}_{i_k}(\mu)$ for some $\mu \in \mathcal{A}_{p,q}^d$, and $X_\lambda := \sum_{S,T \in \text{Paths}(\lambda)} x_{ST} \mathcal{E}_{ST}$, and $f_C, f_{A_k}, g_{D_k, B_k}^{i_k, T_{i_k}, S_{i_k}}$ are some affine functions depending on indicated matrices. The above optimisation problem has $\dim(\mathcal{A}_{p,q}^d) = \sum_{\lambda \in \hat{\mathcal{A}}_{p,q}^d} d_\lambda^2$ degrees of freedom. For comparison, the original optimization problem has $d^{2(p+q)}$ degrees of freedom. In order to make the optimization problem trackable, we make some further assumptions on the form and sparseness of matrices A_k, C, D_k, B_k in the original problem. Hence, we analyze some particular cases in which the aforementioned matrices are given in one of the following forms:

- (1) they are arbitrary linear combinations of matrix units of $\mathcal{A}_{p,q}^d$,
- (2) they are sparse linear combinations of computational basis matrix units,
- (3) they are sparse linear combinations of diagrams that span $\mathcal{B}_{p,q}^d$.

Firstly, notice that if all matrices C, A_k, D_k, B_k are written as a linear combination of matrix units \mathcal{E}_{ST} , the optimization problem (134) can be rewritten to the form (136) trivially.

Furthermore, we can use the methods presented in Sections 5.2 and 5.3 to efficiently compute the (partial) traces of products of matrices of different forms. Indeed, by summarizing results from Sections 5.2 and 5.3, we obtain the following generalization of the main result of [GO22] from linear to semidefinite programming.

Theorem 5.2. *The computational complexity of rewriting the input SDP (134) with $d^{2(p+q)}$ variables to the reduced SDP (136) with $\dim(\mathcal{A}_{p,q}^d)$ variables is*

- $O(s)$ if C, A_k, D_k, B_k are given as s -sparse linear combinations of matrix units \mathcal{E}_{ST} of $\mathcal{A}_{p,q}^d$, or are the identity matrix,
- $s \cdot (p+q)^{O(d^2)}$ if C, A_k, D_k, B_k are given as s -sparse linear combinations of computational basis matrix units, while the matrices D_k are linear combinations of matrix units,
- $O(s(p+q)^2(\dim \mathcal{A}_{p,q}^d)^{3/2})$ if C, A_k, D_k, B_k are s -sparse linear combinations of diagrams in $\mathcal{B}_{p,q}^d$.

In the first two cases, the complexity scales polynomially in the system size $p+q$ when the local dimension d is constant. In the third case, the complexity scales in $\dim(\mathcal{A}_{p,q}^d)$ as opposed to $\dim(\mathcal{B}_{p,q}^d) = (p+q)!$, which can make a significant difference for small values of the local dimensions d (see [GO22] for more discussion). Note that scaling in $\dim(\mathcal{A}_{p,q}^d)$ versus $\dim(\mathcal{B}_{p,q}^d)$ results from writing the matrix variable as a formal linear combination of matrix units \mathcal{E}_{ST} instead of walled Brauer algebra diagrams.

Theorem 5.2 can be applied to a number of important optimization problems in quantum information which are all of the form (134): optimization over PPT-extendible channels [HSW22], SDP relaxation hierarchy for bilinear optimization [BBFS22] for approximate quantum error correction [CTV23], optimization over quantum combs [QDSSM19a; QDSSM19b; YSM21; QE21; GO22], unitary-equivariant Boolean functions [Buh+16],

monogamy of entanglement [All+23], and many others (see [GO22] for an extensive list of references). In most of these settings, there are additional discrete symmetries as well, which can be utilized together with unitary-equivariance to simplify the problem even further. We leave finding efficient ways of combining these symmetries with unitary equivariance for future work.

6. EFFICIENT QUANTUM CIRCUIT FOR OPTIMAL PORT-BASED TELEPORTATION

Quantum teleportation is a cornerstone of quantum information [Ben+93]. However, one drawback of the original teleportation protocol is that the receiving party needs to perform a correction operation on the received state. *Port-based teleportation* (PBT) gets around this limitation [IH08; IH09]. In PBT, Alice and Bob share an entangled resource state distributed evenly among p quantum systems called *ports* on each side. To teleport an unknown quantum state, Alice measures it together with her share of the ports. The measurement outcome, which she communicates to Bob, indicates to which of Bob's ports the state has teleported to. Bob does not need to perform any correction but simply discard the remaining ports.

Port-based teleportation possesses the crucial feature of unitary equivariance, meaning it remains effective when Bob applies the same unitary operation to his port systems before the protocol starts. However, due to finite resources [NC97], unitarily equivariant PBT protocols can only achieve approximate teleportation. Nevertheless, certain PBT protocols become asymptotically faithful as the number of ports increases [BK11; MSSH18; Chr+21]. PBT has diverse applications in non-local quantum computation and quantum communication [BK11; Buh+16; May22], channel discrimination [PLLP19], channel simulation [PBP21], and holography in high-energy physics [May19; May22]. PBT has also been extended to multi-port teleportation [SMKH22; KMSH21; MSK21]. The resource requirements for PBT have been studied further in [SMK22; SS23].

Usually, two types of PBT protocols are considered: probabilistic exact and deterministic inexact. The optimal entanglement fidelity for deterministic protocol is related to the success probability in probabilistic version [Led20]. Typical resource states considered for PBT are either p maximally entangled pairs of states or a nontrivial optimized state (which achieves the best possible optimal entanglement fidelity) [SSMH17; MSSH18].

It turns out that the same *pretty good measurement* measurement is optimal for both cases [SSMH17; MSSH18; Led20]. We denote this positive operator-valued measure (POVM) by $E = \{E_k\}_{k=0}^p$. Denote Alice's ports by A_1, \dots, A_p . The input register $p+1$ on Alice's side is for the state $|\psi\rangle \in \mathbb{C}^d$ to be teleported to Bob. Alice measures all her registers and if she obtains outcome $k \in [p]$, then this is the number of the port where Bob should find the teleported state $|\psi\rangle$. Otherwise, upon measuring $k=0$ she aborts the protocol (for probabilistic exact PBT) or sends a random classical outcome $k \in [p]$ to Bob (deterministic inexact PBT). The optimal POVM E is given by [SSMH17; MSSH18; Led20]

$$E_k = \rho^{-1/2} \rho_k \rho^{-1/2} \text{ for every } k \in [p], \quad E_0 = I - \sum_{k=1}^p E_k. \quad (137)$$

Here ρ^{-1} should be understood as the generalized inverse of $\rho := \sum_{k=1}^p \rho_k$ where

$$\rho_k := \psi_{p,q}^d(\pi^k \sigma_p \pi^{-k}), \quad (138)$$

where $\psi_{p,q}^d$ denotes the map defined in eq. (48), $\pi := \sigma_1 \sigma_2 \dots \sigma_{p-2} \sigma_{p-1}$ is the cyclic shift permutation, and σ_p the contraction between systems p and $p+1$.

While the form of the optimal measurement is known, an efficient quantum circuit for implementing it was not known until our work. Our main result is

Theorem 6.1. *The pretty good measurement E for the port-based teleportation protocol from eq. (137) can be implemented by a quantum circuit with gate complexity $\text{poly}(p, d)$, where p is the number of ports and d is the dimension of the teleported quantum state.*

The proof is explained in detail in the next two sections. Our construction provides the first efficient implementation of the optimal measurement E as a quantum circuit of gate complexity $\text{poly}(p, d)$. This is an exponential improvement over a trivial implementation which has complexity $\text{poly}(d^p)$.

The setting of port-based teleportation is naturally suited to the use of representation theory of the algebra $\mathcal{A}_{p,1}^d$. It is also natural to work in the mixed Schur basis, which can be achieved by applying the mixed quantum Schur transform from Section 4.5.¹⁷

¹⁷Starting from now on, for brevity we will not mention explicitly the matrix representation of the walled Brauer algebra $\psi_{p,q}^d$ and we assume that we are working in the mixed Schur basis, i.e., when using, for example, a diagram $\sigma \in \mathcal{B}_{p,q}^d$ it should be understood as $U_{\text{Sch}} \psi_{p,q}^d(\sigma) U_{\text{Sch}}^\dagger$. Moreover, we ignore multiplicity registers $V_\lambda^{\text{U}^d}$ corresponding to unitary group irreps in the mixed Schur–Weyl duality, i.e., we write all expressions in the Gelfand–Tsetlin basis from Theorem 3.2.

6.1. Naimark’s dilation. Before we present our circuit, we need to explain how to dilate the POVM E to a projective measurement Π (projection-valued measure or PVM for short). That, in principle, is possible for any POVM due to the Naimark’s dilation theorem. However, a simple and efficient dilation is not obvious to achieve and implement in general. After we explain how to construct such dilation explicitly, we present a construction of an efficient circuit for E in the next section.

Note that the unnormalized state ρ coincides with the shifted Jucys–Murphy element $d - J_{p+1}$ of $\mathcal{A}_{p,1}^d$, so its spectrum can be easily obtained, see Lemma B.7. More concretely, ρ is diagonal in the Gelfand–Tsetlin basis and due to Lemma B.7:

$$\rho = \sum_{\substack{\lambda \in \hat{\mathcal{A}}_{p,1}^d \\ \lambda_r = \emptyset}} \rho_\lambda, \quad \rho_\lambda := \sum_{T \in \text{Paths}(\lambda)} (d + \text{cont}(T^p \setminus \lambda_l)) |T\rangle \langle T|. \quad (139)$$

Note that ρ is zero on irreps λ for which $\lambda_r \neq \emptyset$.¹⁸ Also note that due to Theorem 3.2 the generator σ_p in the Gelfand–Tsetlin basis can be written as

$$\sigma_p = \sum_{\substack{\lambda \in \hat{\mathcal{A}}_{p,1}^d \\ \lambda_r = \emptyset}} \sum_{S \in \text{Paths}_{p-1}(\lambda)} |v_{S,\lambda}\rangle \langle v_{S,\lambda}|, \quad \text{where } |v_{S,\lambda}\rangle := \sum_{T \in \mathcal{M}(S,\lambda)} c(T) |T\rangle \quad (140)$$

where $c(T) = \sqrt{\frac{m_{T^p}}{m_{T^{p-1}}}}$ and we define for $S \in \text{Paths}_{p-1}(\lambda)$:

$$\mathcal{M}(S,\lambda) := \left\{ T \in \text{Paths}(\lambda) \mid \exists \mu \in \hat{\mathcal{A}}_{p,0}^d : T = (S^0, S^1, \dots, S^{p-2}, \lambda, \mu, \lambda) \right\}. \quad (141)$$

Note that $\mathcal{M}(S,\lambda)$ is in bijection with a subset $\text{AC}_d(\lambda) \subseteq \text{AC}(\lambda)$ of addable boxes to $\lambda \vdash p-1$ formally defined as

$$\text{AC}_d(\lambda) := \{a \in \text{AC}(\lambda) \mid \ell(\lambda \cup a) \leq d\}. \quad (142)$$

Now we can rewrite E_p in the Gelfand–Tsetlin basis as follows:

$$E_p = \rho^{-1/2} \sigma_p \rho^{-1/2} = \sum_{\substack{\lambda \in \hat{\mathcal{A}}_{p,1}^d : \lambda_r = \emptyset \\ S \in \text{Paths}_{p-1}(\lambda)}} \rho_\lambda^{-1/2} |v_{S,\lambda}\rangle \langle v_{S,\lambda}| \rho_\lambda^{-1/2} = \sum_{\substack{\lambda \in \hat{\mathcal{A}}_{p,1}^d : \lambda_r = \emptyset \\ S \in \text{Paths}_{p-1}(\lambda)}} |w_{S,\lambda}\rangle \langle w_{S,\lambda}|, \quad (143)$$

with

$$|w_{S,\lambda}\rangle := \sum_{T \in \mathcal{M}(S,\lambda)} \sqrt{\frac{d_{T^p}}{p \cdot d_{T^{p-1}}}} |T\rangle = \sum_{a \in \text{AC}_d(\lambda)} \sqrt{\frac{d_{\lambda \cup a}}{p \cdot d_\lambda}} |S \circ (\lambda \cup a) \circ \lambda\rangle, \quad (144)$$

where we used Theorem 3.2 and Lemmas B.1 and B.2. Since ρ commutes with $\mathcal{A}_{p,0}^d$, the other POVM elements E_k for $k \in [p]$ can be written as

$$E_k = \rho^{-1/2} \pi^k \sigma_p \pi^{-k} \rho^{-1/2} = \pi^k E_p \pi^{-k}. \quad (145)$$

We will denote the restriction of E_k to irrep $\lambda \in \hat{\mathcal{A}}_{p,1}^d$ by E_k^λ .

Note that for any irrep $\lambda \in \hat{\mathcal{A}}_{p,1}^d$ with $\lambda_r = \emptyset$ and every path $T \in \text{Paths}(\lambda)$ the dimensions d_{T^p} and $d_{T^{p-1}}$ coincide with the dimensions of the corresponding irreps of the symmetric groups S_p and S_{p-1} , respectively. Now recall that the Bratteli diagram of the symmetric group is the *Young lattice* or *Young graph* [Sag13], and the following identity holds for every $\lambda \vdash p-1$ [Sta13] in the Young lattice:

$$p \cdot d_\lambda = \sum_{a \in \text{AC}(\lambda)} d_{\lambda \cup a}, \quad (146)$$

where the notation $\lambda \cup a$ denotes the Young diagram in the Young lattice obtained by adding a box a to λ , and d_λ is the dimension of the symmetric group irrep λ .¹⁹

The main observation of this section is that for a Young diagram $\lambda \vdash p-1$, we have $\text{AC}_d(\lambda) = \text{AC}(\lambda)$ if $\lambda_d = 0$ and $\text{AC}_d(\lambda) \neq \text{AC}(\lambda)$ if $\lambda_d > 0$. In particular, when $\lambda_d = 0$ this implies that

$$\| |w_{S,\lambda}\rangle \|^2 = \sum_{T \in \mathcal{M}(S,\lambda)} \frac{d_{T^p}}{p \cdot d_{T^{p-1}}} = \sum_{a \in \text{AC}_d(\lambda)} \frac{d_{\lambda \cup a}}{p \cdot d_\lambda} = \sum_{a \in \text{AC}(\lambda)} \frac{d_{\lambda \cup a}}{p \cdot d_\lambda} = 1, \quad (147)$$

so E_p^λ is an orthogonal projector. Since the cyclic shift π acts unitarily, all E_i^λ are orthogonal projectors as well. Because E^λ provides a resolution of the identity in the irreducible representation λ , the POVM E^λ restricted to the irreducible representation λ with $\lambda_d = 0$ is actually a PVM on that irreducible representation. We will replace E^λ by Π^λ from now on to indicate that E^λ is actually a PVM.

¹⁸Therefore our convention, from now on, is that we will drop subscript l from λ_l and will refer to it simply by λ . Moreover, all vertices μ in all levels up to p in the Bratteli diagram do have the property $\mu_r = \emptyset$, so a similar convention applies to all such μ .

¹⁹The dimension d_λ can be both understood as the number of paths from the root to a vertex λ in the Young lattice as well as in the Bratteli diagram of $\mathcal{A}_{p,0}^d$, since up to level p the Bratteli diagram is a subset of the full Young lattice and the procedure of adding a cell is monotonic with respect to the number of rows in λ along a given path in the Young lattice.

However, for the irreps λ with $\lambda_d > 0$ the POVM E^λ is not a PVM because $\text{AC}(\lambda) = \text{AC}_d(\lambda) \sqcup \{(d+1, 1)\}$ and the vectors $|w_{S,\lambda}\rangle$ are not normalized anymore:

$$\|w_{S,\lambda}\|^2 = \sum_{T \in \mathcal{M}(S,\lambda)} \frac{d_{T^p}}{p \cdot d_{T^{p-1}}} = \sum_{a \in \text{AC}_d(\lambda)} \frac{d_\mu}{p \cdot d_\lambda} = \left(\sum_{a \in \text{AC}(\lambda)} \frac{d_\mu}{p \cdot d_\lambda} \right) - \frac{d_{\lambda \cup (d+1,1)}}{p \cdot d_\lambda} = 1 - \frac{d_{\lambda \cup (d+1,1)}}{p \cdot d_\lambda} < 1, \quad (148)$$

where $\lambda \cup (d+1, 1)$ denotes the Young diagram obtained from λ by adding a cell with coordinates $(d+1, 1)$, so that $\ell(\lambda \cup (d+1, 1)) = d+1$. The vertex corresponding to this Young diagram does not exist in the Bratteli diagram of $\mathcal{A}_{p,1}^d$. Fortunately, eq. (148) suggests immediately how to construct a Naimark's dilation Π^λ of E^λ for λ with $\lambda_d > 0$. For this construction, one needs to modify the Bratteli diagram of $\mathcal{A}_{p,1}^d$ by adding certain vertices to each level of the diagram. Then the set of all paths in this modified Bratteli diagram will define a new basis for the Naimark dilated Hilbert space.

More concretely, to each level $k \leq p$ of the Bratteli diagram of $\mathcal{A}_{p,1}^d$ we add all possible vertices labelled by all Young diagrams $\nu \vdash k$ such that $\nu_{d+1} = 1$ (if such Young diagrams exist for a given level k). An edge between a pair of Young diagrams in two consecutive levels is added if the latter diagram can be obtained by adding a cell to the previous one. This procedure ensures that all the levels up to p of the new Bratteli diagram form a subset of the Young lattice, such that for every vertex at level p the irrep dimensions still satisfy eq. (146). The basis for the Naimark dilated Hilbert space consists of all paths in this modified Bratteli diagram, which we denote by $\widetilde{\text{Paths}}$ which we formally define as follows. For every $\lambda \in \widehat{\mathcal{A}}_{p,1}^d$, if $\lambda_r = \emptyset$ we define

$$\widetilde{\text{Paths}}(\lambda) := \left\{ T = (T^1, \dots, T^p, \lambda) \in \widehat{\mathcal{A}}_{1,0}^{d+1} \times \dots \times \widehat{\mathcal{A}}_{p,0}^{d+1} \times \widehat{\mathcal{A}}_{p,1}^d \mid T \text{ satisfies eq. (150)} \right\}, \quad (149)$$

where

$$T_{l,d+1}^k \leq 1 \quad \forall k \in [p], \quad \text{and} \quad T^k \setminus T^{k-1} \in \text{AC}(T^{k-1}) \quad \forall k \in [p], \quad \text{and} \quad T^p \setminus \lambda \in \text{RC}(T^p). \quad (150)$$

If $\lambda_r \neq \emptyset$ then

$$\widetilde{\text{Paths}}(\lambda) := \text{Paths}(\lambda). \quad (151)$$

The full modified Bratteli diagram can be thought of as a disjoint union of modified sets of paths for every $\lambda \in \widehat{\mathcal{A}}_{p,1}^d$:

$$\widetilde{\text{Paths}} := \bigsqcup_{\lambda \in \widehat{\mathcal{A}}_{p,1}^d} \widetilde{\text{Paths}}(\lambda). \quad (152)$$

The action of the generators $\sigma_1, \dots, \sigma_{p-1}$ of S_p in this modified Bratteli diagram is given by Theorem 3.2 when $\lambda_r \neq \emptyset$, and by the trivial generalization of these formulas to all paths in $\widetilde{\text{Paths}}(\lambda)$ if $\lambda_r = \emptyset$. For this new Bratteli diagram, we define the dilated versions $|\widetilde{w}_{S,\lambda}\rangle$ of vectors $|w_{S,\lambda}\rangle$, for $S \in \widetilde{\text{Paths}}_{p-1}(\lambda)$ as follows:

$$|\widetilde{w}_{S,\lambda}\rangle := \sum_{T \in \widetilde{M}(S,\lambda)} \sqrt{\frac{d_{T^p}}{p \cdot d_{T^{p-1}}}} |T\rangle, \quad (153)$$

where $\widetilde{M}(S,\lambda)$ is defined in the same way as the set $\mathcal{M}(S,\lambda)$, but for the dilated Bratteli diagram $\widetilde{\text{Paths}}$, i.e., for every $S \in \widetilde{\text{Paths}}_{p-1}(\lambda)$:

$$\widetilde{M}(S,\lambda) := \left\{ T \in \widetilde{\text{Paths}}(\lambda) \mid \exists \mu \in \widehat{\mathcal{A}}_{p,0}^{d+1} : T = (S^0, S^1, \dots, S^{p-2}, \lambda, \mu, \lambda), \mu_{d+1} \leq 1 \right\}. \quad (154)$$

Note that $\widetilde{M}(S,\lambda)$ is in bijection now with the set $\text{AC}(\lambda)$ and we can rewrite $|\widetilde{w}_{S,\lambda}\rangle$ as

$$|\widetilde{w}_{S,\lambda}\rangle = \sum_{a \in \text{AC}(\lambda)} \sqrt{\frac{d_{\lambda \cup a}}{p \cdot d_\lambda}} |S \circ (\lambda \cup a) \circ \lambda\rangle, \quad (155)$$

Therefore in the dilated space since eq. (146) holds and all vertices $\lambda \cup a$, which can be obtained from a vertex λ at level $p-1$ by adding a box a , exist then

$$\| \widetilde{w}_{S,\lambda} \|^2 = \sum_{T \in \widetilde{M}(S,\lambda)} \frac{d_{T^p}}{p \cdot d_{T^{p-1}}} = \sum_{a \in \text{AC}(\lambda)} \frac{d_{\lambda \cup a}}{p \cdot d_\lambda} = 1. \quad (156)$$

Consequently, in the dilated space our POVM E^λ is actually a PVM, which we denote by Π^λ . From now on assume that we work in the dilated space and we want to implement the PVM $\Pi = \{\Pi_k\}_{k=0}^p$, where for every $k \in [p]$:

$$\Pi_k = \sum_{\substack{\lambda \in \widehat{\mathcal{A}}_{p,1}^d \\ \lambda_r = \emptyset}} \Pi_k^\lambda, \quad \Pi_k^\lambda := \pi^k \Pi_p^\lambda \pi^{-k} = \sum_{S \in \widetilde{\text{Paths}}_{p-1}(\lambda)} \pi^k |\widetilde{w}_{S,\lambda}\rangle \langle \widetilde{w}_{S,\lambda}| \pi^{-k}, \quad \Pi_0 = I - \sum_{k=1}^p \Pi_k. \quad (157)$$

We have provided a *Wolfram Mathematica* notebook implementing our construction in [GBO23].

6.2. Efficient quantum circuit for the pretty good measurement. Using the results of Section 6.1, our task now is to implement the PVM Π from eq. (157). To explain our construction, let us illustrate the main idea in a simpler example, so first we reformulate the problem in a more abstract language for a simplified setting of rank 1 projectors.

Suppose we have the ability to implement $n + 1$ orthogonal vectors $|x_k\rangle$ for $k \in \{0, \dots, n\}$ via some easy-to-implement unitaries U_k starting from known basis vector $|0\rangle$ as $|x_k\rangle = U_k|0\rangle$. Assume, that we also know that these vectors comprise a PVM $X = \{|x_k\rangle\langle x_k|\}_{k=0}^n$. We can implement PVM X via the following two ideas:

(1) Define a unitary V as

$$V := \sum_{k=0}^n \omega_{n+1}^k |x_k\rangle\langle x_k| \quad (158)$$

where ω_{n+1} is root of unity of order $n + 1$. Note, that we can implement the unitary V efficiently if we have easy-to-implement unitaries U_k via the following circuit:

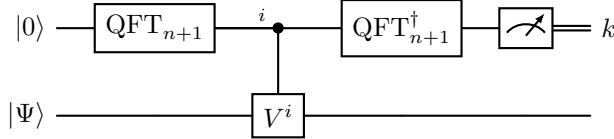
$$\text{---} [V] \text{---} = \text{---} [U_1^\dagger] \text{---} [\omega_{n+1}] \text{---} [U_1] \text{---} [U_2^\dagger] \text{---} [\omega_{n+1}^2] \text{---} [U_2] \text{---} \dots \text{---} [U_n^\dagger] \text{---} [\omega_{n+1}^n] \text{---} [U_n] \text{---},$$

where $[\omega_{n+1}^k]$ represents the gate $\omega_{n+1}^k |0\rangle\langle 0| + |0^\perp\rangle\langle 0^\perp|$.

(2) Note that implementing V^i is easy:

$$\text{---} [V^i] \text{---} = \text{---} [U_1^\dagger] \text{---} [\omega_{n+1}^i] \text{---} [U_1] \text{---} [U_2^\dagger] \text{---} [\omega_{n+1}^{2i}] \text{---} [U_2] \text{---} \dots \text{---} [U_n^\dagger] \text{---} [\omega_{n+1}^{ni}] \text{---} [U_n] \text{---}.$$

Therefore we can use the standard phase estimation circuit to measure a given state $|\Psi\rangle$ with respect to the PVM X as follows:



The above ideas are trivially extended to higher-rank PVMs. Now before presenting our circuit for Π from eq. (157), we need to define a unitary W , which can be used to prepare states $|\tilde{w}_{S,\lambda}\rangle = |S\rangle|\tilde{w}_\lambda\rangle$ for every $\lambda \in \widehat{\mathcal{A}}_{p,1}^d$ with $\lambda_r = \emptyset$ and $S \in \widehat{\text{Paths}}_{p-1}(\lambda)$, where we denote

$$|\tilde{w}_\lambda\rangle := \sum_{a \in \text{AC}(\lambda)} \sqrt{\frac{d_{\lambda \cup a}}{p \cdot d_\lambda}} |\lambda \cup a\rangle. \quad (159)$$

Now we define W as a unitary, which prepares $|\tilde{w}_\lambda\rangle$ conditioned on $|\lambda\rangle$:

$$W := \sum_{\lambda} W_\lambda \otimes |\lambda\rangle\langle \lambda|, \quad W_\lambda |0\rangle := |\tilde{w}_\lambda\rangle \quad (160)$$

W_λ is a rotation matrix of size at most $(d + 1) \times (d + 1)$ with easy-to-compute coefficients determined from eq. (159) and Lemma B.1.

Assume we start at the state $|S\rangle|0\rangle|\lambda\rangle := |S^0\rangle|S^1\rangle|S^2\rangle \dots |S^{p-1}\rangle|0\rangle|\lambda\rangle$ defined for arbitrary $S \in \widehat{\text{Paths}}_{p-1}$, where $|0\rangle$ is some basis state of the register, corresponding to the p -th level of the dilated basis $\widehat{\text{Paths}}$. Then we can prepare a state $|S\rangle|\tilde{w}_\lambda\rangle|\lambda\rangle$ as follows:

$$I \otimes W |S\rangle|0\rangle|\lambda\rangle = |S\rangle|\tilde{w}_\lambda\rangle|\lambda\rangle, \quad (161)$$

where identity I acts on the register $|S\rangle$.

Now following the outlined prescription we construct the efficient circuit for the pretty good measurement E for the PBT protocol in Fig. 10. The circuit should be understood as acting on the dilated space spanned by $(T^0, T^1, \dots, T^p, \lambda) \in \widehat{\text{Paths}}$, which forms the Gelfand–Tsetlin basis. The ancilla registers used for the dilation should be understood as discarded after the computation. Let us comment on Fig. 10.

Firstly, the Schur transform maps the standard basis into the mixed Schur basis which is labelled usually by $|M, T\rangle$, where M is a Gelfand–Tsetlin pattern and T is a mixed Young tableau. We assume a tensor product structure in the mixed Schur basis for different vertices T^i of the path $T \in \widehat{\text{Paths}}$, where all registers T^2, \dots, T^p are assumed to be dilated, according to the procedure explained in Section 6.1. Since T^0 and T^1 are always constant, we omit those registers from the diagram. The last level T^{p+1} of the path T is labelled by λ and indicates the irreducible representation. The cyclic permutation gate $\pi = (12 \dots p) = \sigma_1 \sigma_2 \dots \sigma_{p-1}$ acts only on $p - 1$ wires of the dilated Gelfand–Tsetlin basis, and each of the transpositions σ_i act only locally in the registers T^{i-1}, T^i, T^{i+1} (σ_1 acts only on T^2 , and σ_2 acts only on T^2, T^3). W prepares the state $|\tilde{w}_\lambda\rangle$ conditioned

on λ , i.e. $W_\lambda|0\rangle = |\tilde{w}_\lambda\rangle$ and are controlled on λ as well. The phase gates ω_{p+1}^{ki} act only on the state $|0\rangle$ in the register T^p , when they are controlled on the condition $T^{p-1} = T^{p+1} = \lambda$. Finally, the measured outcome $k = 0$ corresponds to the failure of the protocol, otherwise $k \in [p]$ indicates the port, where Bob should find the teleported state $|\psi\rangle$ of dimension d .

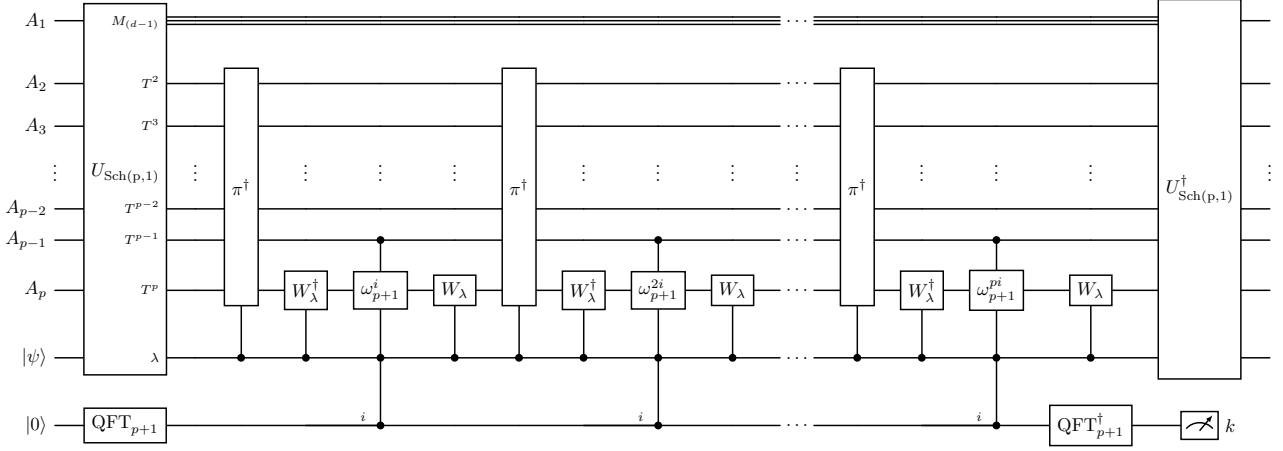


FIGURE 10. The circuit implementation of the pretty good measurement for port-based teleportation. The registers T^2, T^3, \dots, T^p are assumed to be dilated according to Section 6.1. The total qubit and gate cost is upper bounded by $\text{poly}(p, d)$.

Now we argue that the complexity of our circuit is $\text{poly}(p, d)$:

- (1) The complexity of implementing the mixed Schur transform according to Section 4.5 is $O(\text{poly}(p, d))$. The number of ancilla qubits needed to implement the mixed Schur transform isometry and create a Naimark's dilation after the mixed Schur transfer is also polynomial $\text{poly}(d, \log(p))$. This is so because the number of compositions of the integer p into d non-negative parts is $\binom{p+d-1}{p}$, so $\log\left(\binom{p+d-1}{p}\right) = \text{poly}(d, \log(p))$.
- (2) The complexity of implementing $\pi = \sigma_1 \sigma_2 \dots \sigma_{p-1}$ is also $\text{poly}(p, d)$, since each transposition operator σ_i acts locally on the registers T^{i-1}, T^i, T^{i+1} . Namely σ_i is a 2×2 rotation in the register T^i controlled from T^{i-1}, T^{i+1} and λ . So using the standard methods (e.g. Given's rotations) it can be implemented with complexity upper bounded by $\text{poly}(d, \log(p))$.²⁰
- (3) W operator implements λ -controlled $(d+1) \times (d+1)$ operator W_λ on the register T^p . The number of qubits in the register T^p is $\text{poly}(d, \log(p))$. The coefficients of the matrix W_λ are determined from eq. (159) and Lemma B.1 and are easy to compute in classical time $\text{poly}(d, \log(p))$. Therefore, implementing W would have the gate complexity $\text{poly}(d, \log(p))$.
- (4) ω_{p+1}^{ki} denotes a simple-to-implement gate $\omega_{p+1}^{ki}|0\rangle\langle 0| + |0^\perp\rangle\langle 0^\perp|$ in the register T^p conditioned on the registers $T^{p-1} = T^{p+1} = \lambda$. This has complexity $\text{poly}(d, \log(p))$.
- (5) Finally, the complexity of the Quantum Fourier Transform QFT_{p+1} is $\text{poly}(p)$.

6.3. Exponentially improved lower bound for non-local quantum computation. Port-based teleportation has interesting applications in holography and non-local quantum computation [May19; May22], where it was argued that the complexity of the local operation controls the amount of entanglement needed to implement it non-locally, using ideas from AdS/CFT correspondence. In particular, it was derived in [May22, Lemma 9] that port-based teleportation can be used to lower bound the amount of entanglement needed to implement a given channel (from a large class of one-sided quantum channels) non-locally in terms of the so-called *interaction-class circuit complexity* \mathcal{C} [May22, Definition 3] denoted by \mathcal{C} . Port-based teleportation can also be used to find an upper bound [BK11; Spe16; May22]. The bounds read as

$$\Omega(\log \log \mathcal{C}) \leq E_c \leq O(\mathcal{C} \cdot 2^{\mathcal{C}}), \quad (162)$$

where E_c is the entanglement cost needed to implement non-locally a unitary with complexity \mathcal{C} [May22]. The derivation of the lower bound uses a trivial upper bound $\exp(O(p))$ for the complexity of the port-based teleportation in terms of the number of ports p , see [May22, Equation 47]. It is pointed out in [May22, page 28] that a better implementation of the port-based teleportation protocol would lead to a better lower bound.

²⁰Alternatively, one can go back to the standard basis via inverse mixed Schur transform, implement a simple permutation gate corresponding to π and then go back to the Gelfand–Tsetlin basis via mixed Schur transform. That also would also have complexity $\text{poly}(p, d)$

Complexity of our implementation of PBT protocol is $\text{poly}(p)$, therefore this immediately translates, according to [May22, Lemma 9], to a better lower bound:

$$\Omega(\log \mathcal{C}) \leq E_c, \quad (163)$$

thus improving exponentially upon the previous bound.

ACKNOWLEDGEMENTS

DG thanks Tudor Giurgica-Tiron, Quynh Nguyen, Aram Harrow, Hari Krovi, Philip Verduyn Lunel, Rene Allerstorfer and Florian Speelman for useful discussions. DG, AB, and MO were supported by an NWO Vidi grant (Project No VI.Vidi.192.109).

REFERENCES

- [AH21] Sam Armon and Tom Halverson. “Transition Matrices Between Young’s Natural and Seminormal Representations”. In: *The Electronic Journal of Combinatorics* 28.3 (2021), P3.15. DOI: [10.37236/10081](https://doi.org/10.37236/10081). arXiv: [2012.03828](https://arxiv.org/abs/2012.03828) (cit. on p. 3).
- [AISW20] Jayadev Acharya, Ibrahim Issa, Nirmal V. Shende, and Aaron B. Wagner. “Estimating quantum entropy”. In: *IEEE Journal on Selected Areas in Information Theory* 1.2 (2020), pp. 454–468. DOI: [10.1109/JSAIT.2020.3015235](https://doi.org/10.1109/JSAIT.2020.3015235) (cit. on p. 2).
- [All+23] Rene Allerstorfer, Matthias Christandl, Dmitry Grinko, Ion Nechita, Maris Ozols, Denis Rochette, and Philip Verduyn Lunel. “Monogamy of highly symmetric states”. Submitted to QIP 2024. 2023 (cit. on pp. 5, 27).
- [BBFS22] Mario Berta, Francesco Borderi, Omar Fawzi, and Volkher B. Scholz. “Semidefinite programming hierarchies for constrained bilinear optimization”. In: *Mathematical Programming* 194.1 (July 2022), pp. 781–829. DOI: [10.1007/s10107-021-01650-1](https://doi.org/10.1007/s10107-021-01650-1). arXiv: [1810.12197](https://arxiv.org/abs/1810.12197) (cit. on p. 26).
- [BCH06] Dave Bacon, Isaac L. Chuang, and Aram W. Harrow. “Efficient quantum circuits for Schur and Clebsch–Gordan transforms”. In: *Physical Review Letters* 97.17 (Oct. 2006). DOI: [10.1103/physrevlett.97.170502](https://doi.org/10.1103/physrevlett.97.170502). arXiv: [quant-ph/0407082](https://arxiv.org/abs/quant-ph/0407082) (cit. on pp. 2, 5, 17, 19, 20, 22).
- [BCS20] Ivan Bardet, Benoît Collins, and Gunjan Sapra. “Characterization of equivariant maps and application to entanglement detection”. In: *Annales Henri Poincaré* 21.10 (2020), pp. 3385–3406. DOI: [10.1007/s00023-020-00941-1](https://doi.org/10.1007/s00023-020-00941-1). arXiv: [1811.08193](https://arxiv.org/abs/1811.08193) (cit. on p. 3).
- [Ben+93] Charles H Bennett, Gilles Brassard, Claude Crépeau, Richard Jozsa, Asher Peres, and William K Wootters. “Teleporting an unknown quantum state via dual classical and Einstein-Podolsky-Rosen channels”. In: *Physical review letters* 70.13 (1993), p. 1895 (cit. on p. 27).
- [Ben+94] Georgia Benkart, Manish Chakrabarti, Thomas Halverson, Robert Leduc, Chanyoung Y. Lee, and Jeffrey Stroemer. “Tensor product representations of general linear groups and their connections with Brauer algebras”. In: *Journal of Algebra* 166.3 (1994), pp. 529–567. DOI: [10.1006/jabr.1994.1166](https://doi.org/10.1006/jabr.1994.1166). URL: <https://core.ac.uk/download/pdf/82480893.pdf> (cit. on pp. 2, 3, 11, 16).
- [Ben96] Georgia Benkart. “Commuting actions—A tale of two groups”. In: *Lie Algebras and Their Representations*. Vol. 194. Contemporary Mathematics. American Mathematical Society, 1996. DOI: [10.1090/conm/194/02387](https://doi.org/10.1090/conm/194/02387) (cit. on pp. 3, 11).
- [Ber12] Sonya Berg. “A quantum algorithm for the quantum Schur–Weyl transform”. PhD thesis. University of California, Davis, 2012. arXiv: [1205.3928](https://arxiv.org/abs/1205.3928) (cit. on p. 3).
- [BGSV12] Christine Bachoc, Dion C. Gijswijt, Alexander Schrijver, and Frank Vallentin. “Invariant semidefinite programs”. In: *Handbook on Semidefinite, Conic and Polynomial Optimization*. Ed. by Miguel F. Anjos and Jean B. Lasserre. Boston, MA: Springer, 2012, pp. 219–269. DOI: [10.1007/978-1-4614-0769-0_9](https://doi.org/10.1007/978-1-4614-0769-0_9). arXiv: [1007.2905](https://arxiv.org/abs/1007.2905) (cit. on p. 5).
- [BK11] Salman Beigi and Robert König. “Simplified instantaneous non-local quantum computation with applications to position-based cryptography”. In: *New Journal of Physics* 13.9 (2011), p. 093036 (cit. on pp. 27, 31).
- [BL68] Lawrence C. Biedenharn and James D. Louck. “A pattern calculus for tensor operators in the unitary groups”. In: *Communications in Mathematical Physics* 8.2 (1968), pp. 89–131 (cit. on p. 37).
- [BLMMO21] Harry Buhrman, Noah Linden, Laura Mančinska, Ashley Montanaro, and Maris Ozols. “Quantum majority and other Boolean functions with quantum inputs”. Talk at QIP’21. 2021. URL: <https://youtu.be/0149tmUimhk> (cit. on pp. 3, 5).
- [BLMMO22] Harry Buhrman, Noah Linden, Laura Mančinska, Ashley Montanaro, and Maris Ozols. “Quantum majority vote”. In: (2022). arXiv: [2211.11729](https://arxiv.org/abs/2211.11729) (cit. on p. 2).
- [BO20] Daria V. Bulgakova and Oleg Ogievetsky. “Fusion procedure for the walled Brauer algebra”. In: *Journal of Geometry and Physics* 149 (2020), p. 103580. DOI: [10.1016/j.geomphys.2019.103580](https://doi.org/10.1016/j.geomphys.2019.103580). arXiv: [1911.10537](https://arxiv.org/abs/1911.10537) (cit. on p. 13).
- [Bra37] Richard Brauer. “On algebras which are connected with the semisimple continuous groups”. In: *Annals of Mathematics* 38.4 (1937), pp. 857–872. DOI: [10.2307/1968843](https://doi.org/10.2307/1968843) (cit. on pp. 3, 11).
- [Bra72] Ola Bratteli. “Inductive limits of finite dimensional C^* -algebras”. In: *Transactions of the American Mathematical Society* 171 (1972), pp. 195–234. DOI: [10.1090/S0002-9947-1972-0312282-2](https://doi.org/10.1090/S0002-9947-1972-0312282-2) (cit. on p. 7).

- [BS12] Jonathan Brundan and Catharina Stroppel. “Gradings on walled Brauer algebras and Khovanov’s arc algebra”. In: *Advances in Mathematics* 231.2 (2012), pp. 709–773. DOI: [10.1016/j.aim.2012.05.016](https://doi.org/10.1016/j.aim.2012.05.016). arXiv: [1107.0999](https://arxiv.org/abs/1107.0999) (cit. on pp. 11, 12).
- [BSH21] Maria Balanzó-Juandó, Michał Studziński, and Felix Huber. “Positive maps from the walled Brauer algebra”. 2021. arXiv: [2112.12738](https://arxiv.org/abs/2112.12738) (cit. on p. 3).
- [Buh+16] Harry Buhrman, Łukasz Czekaj, Andrzej Grudka, Michał Horodecki, Paweł Horodecki, Marcin Markiewicz, Florian Speelman, and Sergii Strelchuk. “Quantum communication complexity advantage implies violation of a Bell inequality”. In: *Proceedings of the National Academy of Sciences* 113.12 (2016), pp. 3191–3196 (cit. on pp. 26, 27).
- [Bul20] Daria V. Bulgakova. “Some aspects of representation theory of walled Brauer algebras”. PhD thesis. Aix Marseille Université, Jan. 2020. URL: <https://hal.archives-ouvertes.fr/tel-02554375> (cit. on pp. 3, 11).
- [Can11] Constantin Candu. “The continuum limit of $gl(M|N)$ spin chains”. In: *Journal of High Energy Physics* 2011.7 (2011), p. 69. DOI: [10.1007/JHEP07\(2011\)069](https://doi.org/10.1007/JHEP07(2011)069). arXiv: [1012.0050](https://arxiv.org/abs/1012.0050) (cit. on p. 3).
- [CDDM08] Anton Cox, Maud De Visscher, Stephen Doty, and Paul Martin. “On the blocks of the walled Brauer algebra”. In: *Journal of Algebra* 320.1 (2008), pp. 169–212. DOI: [10.1016/j.jalgebra.2008.01.026](https://doi.org/10.1016/j.jalgebra.2008.01.026). arXiv: [0709.0851](https://arxiv.org/abs/0709.0851) (cit. on pp. 4, 12).
- [Chr+21] Matthias Christandl, Felix Leditzky, Christian Majenz, Graeme Smith, Florian Speelman, and Michael Walter. “Asymptotic performance of port-based teleportation”. In: *Communications in Mathematical Physics* 381.1 (2021), pp. 379–451. DOI: [10.1007/s00220-020-03884-0](https://doi.org/10.1007/s00220-020-03884-0). arXiv: [1809.10751](https://arxiv.org/abs/1809.10751) (cit. on pp. 3, 27).
- [CL96] William Y.C. Chen and James D. Louck. “Interpolation for symmetric functions”. In: *Advances in mathematics* 117.1 (1996), pp. 147–156 (cit. on p. 42).
- [Cox12] Anton Cox. *Representation theory of finite dimensional algebras*. 2012. URL: <http://www.staff.city.ac.uk/a.g.cox/LT> (cit. on p. 7).
- [CST10] T. Ceccherini-Silberstein, F. Scarabotti, and F. Tolli. *Representation Theory of the Symmetric Groups: The Okounkov-Vershik Approach, Character Formulas, and Partition Algebras*. Cambridge Studies in Advanced Mathematics. Cambridge University Press, 2010. URL: <https://books.google.com/books?id=3zx1A0uPrKQC> (cit. on p. 3).
- [CTV23] Yeow Meng Chee, Hoang Ta, and Van Khu Vu. “Efficient approximation of quantum channel fidelity exploiting symmetry”. 2023. arXiv: [arXiv:2308.15884](https://arxiv.org/abs/2308.15884) [quant-ph] (cit. on p. 26).
- [DLS18] Stephen Doty, Aaron Lauve, and George H. Seelinger. “Canonical idempotents of multiplicity-free families of algebras”. In: *L’Enseignement Mathématique* 64.1/2 (2018), pp. 23–63. DOI: [10.4171/LEM/64-1/2-2](https://doi.org/10.4171/LEM/64-1/2-2). arXiv: [1606.08900](https://arxiv.org/abs/1606.08900) (cit. on pp. 5, 7, 41).
- [DS22] Piotr Dulian and Adam Sawicki. “Matrix concentration inequalities and efficiency of random universal sets of quantum gates”. 2022. arXiv: [2202.05371](https://arxiv.org/abs/2202.05371) (cit. on p. 3).
- [Ebl+22] Daniel Ebler, Michał Horodecki, Marcin Marciniak, Tomasz Młynik, Marco Túlio Quintino, and Michał Studziński. “Optimal universal quantum circuits for unitary complex conjugation”. 2022. arXiv: [2206.00107](https://arxiv.org/abs/2206.00107) (cit. on p. 5).
- [EG] John Enyang and Frederick M Goodman. *The seminormal representations of the Brauer algebras*. URL: <https://homepage.divms.uiowa.edu/~goodman/PREPRINTS/seminormalformbrauer9.pdf> (cit. on p. 5).
- [Eti+11] Pavel Etingof, Oleg Golberg, Sebastian Hensel, Tiankai Liu, Alex Schwendner, Dmitry Vaintrob, and Elena Yudovina. *Introduction to Representation Theory*. Vol. 59. Student mathematical library. American Mathematical Society, 2011. arXiv: [0901.0827](https://arxiv.org/abs/0901.0827). URL: <https://books.google.com/books?id=RS6IAwAAQBAJ> (cit. on pp. 12, 16).
- [Fan+14] Heng Fan, Yi-Nan Wang, Li Jing, Jie-Dong Yue, Han-Duo Shi, Yong-Liang Zhang, and Liang-Zhu Mu. “Quantum cloning machines and the applications”. In: *Physics Reports* 544.3 (2014), pp. 241–322. DOI: [10.1016/j.physrep.2014.06.004](https://doi.org/10.1016/j.physrep.2014.06.004). arXiv: [1301.2956](https://arxiv.org/abs/1301.2956) (cit. on p. 3).
- [FTH23] Jiani Fei, Sydney Timmerman, and Patrick Hayden. “Efficient Quantum Algorithm for Port-based Teleportation”. To appear simultaneously. 2023 (cit. on p. 5).
- [GBO23] Dmitry Grinko, Adam Burchardt, and Maris Ozols. 2023. URL: <https://github.com/dgrinko/walledbrauer-gtbasis> (cit. on pp. 14, 29).
- [GO22] Dmitry Grinko and Maris Ozols. “Linear programming with unitary-equivariant constraints”. In: (2022). arXiv: [2207.05713](https://arxiv.org/abs/2207.05713) (cit. on pp. 2, 5, 12, 16, 23, 24, 26, 27, 41).
- [Hal96] Thomas Halverson. “Characters of the centralizer algebras of mixed tensor representations of $GL(r, \mathbb{C})$ and the quantum group $U_q(gl(r, \mathbb{C}))$ ”. In: *Pacific Journal of Mathematics* 174.2 (1996), pp. 359–410. DOI: [10.2140/pjm.1996.174.359](https://doi.org/10.2140/pjm.1996.174.359) (cit. on pp. 2, 3).
- [Har05] Aram W. Harrow. “Applications of coherent classical communication and the Schur transform to quantum information theory”. PhD thesis. MIT, 2005. arXiv: [quant-ph/0512255](https://arxiv.org/abs/quant-ph/0512255). URL: <http://hdl.handle.net/1721.1/34973> (cit. on pp. 2, 3, 5, 17–20, 22, 37).
- [HHJWY17] Jeongwan Haah, Aram W. Harrow, Zhengfeng Ji, Xiaodi Wu, and Nengkun Yu. “Sample-optimal tomography of quantum states”. In: *IEEE Transactions on Information Theory* 63.9 (2017), pp. 5628–5641. DOI: [10.1109/tit.2017.2719044](https://doi.org/10.1109/tit.2017.2719044). arXiv: [1508.01797](https://arxiv.org/abs/1508.01797) (cit. on p. 2).
- [HKMV21] Felix Huber, Igor Klep, Victor Magron, and Jurij Volčič. “Dimension-free entanglement detection in multipartite Werner states”. 2021. arXiv: [2108.08720](https://arxiv.org/abs/2108.08720) (cit. on p. 5).

- [HLM21] Austin Hulse, Hanqing Liu, and Iman Marvian. “Qudit circuits with $SU(d)$ symmetry: Locality imposes additional conservation laws”. 2021. arXiv: [2105.12877](#) (cit. on p. 3).
- [How22] R.M. Howe. *An Invitation to Representation Theory: Polynomial Representations of the Symmetric Group*. Springer Undergraduate Mathematics Series. Springer International Publishing, 2022. URL: <https://books.google.com/> (cit. on p. 3).
- [HS18] Vojtěch Havlíček and Sergii Strelchuk. “Quantum schur sampling circuits can be strongly simulated”. In: *Physical review letters* 121.6 (2018), p. 060505 (cit. on p. 5).
- [HST19] Vojtěch Havlíček, Sergii Strelchuk, and Kristan Temme. “Classical algorithm for quantum $SU(2)$ Schur sampling”. In: *Physical Review A* 99.6 (2019), p. 062336 (cit. on p. 5).
- [HSW22] Tharon Holdsworth, Vishal Singh, and Mark M. Wilde. “Quantifying the performance of approximate teleportation and quantum error correction via symmetric two-PPT-extendibility”. 2022. arXiv: [2207.06931](#) (cit. on p. 26).
- [IH08] Satoshi Ishizaka and Tohya Hiroshima. “Asymptotic teleportation scheme as a universal programmable quantum processor”. In: *Phys. Rev. Lett.* 101.24 (Dec. 2008), p. 240501. DOI: [10.1103/PhysRevLett.101.240501](#). arXiv: [0807.4568](#) (cit. on pp. 5, 27).
- [IH09] Satoshi Ishizaka and Tohya Hiroshima. “Quantum teleportation scheme by selecting one of multiple output ports”. In: *Physical Review A* 79.4 (2009), p. 042306 (cit. on pp. 5, 27).
- [JK20] Ji Hye Jung and Myunggho Kim. “Supersymmetric polynomials and the center of the walled Brauer algebra”. In: *Algebras and Representation Theory* 23.5 (2020), pp. 1945–1975. DOI: [10.1007/s10468-019-09922-3](#). arXiv: [1508.06469](#) (cit. on p. 12).
- [Jor09] Stephen P Jordan. “Permutational quantum computing”. In: (2009). arXiv: [0906.2508](#) (cit. on p. 18).
- [Key06] Michael Keyl. “Quantum state estimation and large deviations”. In: *Reviews in Mathematical Physics* 18.01 (2006), pp. 19–60. DOI: [10.1142/S0129055X06002565](#). arXiv: [quant-ph/0412053](#) (cit. on p. 2).
- [KMSH21] Piotr Kopszak, Marek Mozrzyk, Michał Studziński, and Michał Horodecki. “Multiport based teleportation – transmission of a large amount of quantum information”. In: *Quantum* 5 (Nov. 2021), p. 576. DOI: [10.22331/q-2021-11-11-576](#). arXiv: [2008.00856](#) (cit. on pp. 3, 27).
- [Koe08] Steffen Koenig. “A panorama of diagram algebras”. In: *Trends in Representation Theory of Algebras and Related Topics*. Ed. by Andrzej Skowroński. EMS Series of Congress Reports. European Mathematical Society, 2008, pp. 491–540. DOI: [10.4171/062-1/12](#) (cit. on p. 3).
- [Koi89] Kazuhiko Koike. “On the decomposition of tensor products of the representations of the classical groups: by means of the universal characters”. In: *Advances in Mathematics* 74.1 (1989), pp. 57–86. DOI: [10.1016/0001-8708\(89\)90001-1](#) (cit. on pp. 2, 3, 11, 16).
- [Kos03] Masashi Kosuda. “A new proof for some relations among axial distances and hook-lengths”. In: *Tokyo Journal of Mathematics* 26.1 (2003), pp. 199–228 (cit. on p. 41).
- [KR07] Yusuke Kimura and Sanjaye Ramgoolam. “Branes, anti-branes and Brauer algebras in gauge-gravity duality”. In: *Journal of High Energy Physics* 2007.11 (Nov. 2007), pp. 078–078. DOI: [10.1088/1126-6708/2007/11/078](#). arXiv: [0709.2158](#) (cit. on p. 3).
- [Kro19] Hari Krovi. “An efficient high dimensional quantum Schur transform”. In: *Quantum* 3 (Feb. 2019), p. 122. DOI: [10.22331/q-2019-02-14-122](#). arXiv: [1804.00055](#) (cit. on p. 2).
- [KS18] William M. Kirby and Frederick W. Strauch. “A practical quantum algorithm for the Schur transform”. In: *Quantum Information & Computation* 18.9&10 (2018), pp. 721–742. DOI: [10.26421/QIC18.9-10-1](#). arXiv: [1709.07119](#) (cit. on pp. 2, 17).
- [KW01a] Michael Keyl and Reinhard F. Werner. “Estimating the spectrum of a density operator”. In: *Physical Review A* 64.5 (Oct. 2001), p. 052311. DOI: [10.1103/PhysRevA.64.052311](#). arXiv: [quant-ph/0102027](#) (cit. on p. 2).
- [KW01b] Michael Keyl and Reinhard F. Werner. “The rate of optimal purification procedures”. In: *Annales Henri Poincaré* 2.1 (Feb. 2001), pp. 1–26. DOI: [10.1007/PL00001027](#). arXiv: [quant-ph/9910124](#) (cit. on p. 3).
- [LB70] James D. Louck and Lawrence C. Biedenharn. “Canonical unit adjoint tensor operators in $U(n)$ ”. In: *Journal of Mathematical Physics* 11.8 (1970), pp. 2368–2414. DOI: [10.1063/1.1665404](#) (cit. on p. 42).
- [Led20] Felix Leditzky. “Optimality of the pretty good measurement for port-based teleportation”. 2020. arXiv: [2008.11194](#) (cit. on pp. 3, 27).
- [Lou08] James D. Louck. *Unitary Symmetry and Combinatorics*. World Scientific Publishing Company, 2008. URL: <https://books.google.com/books?id=akZkDQAAQBAJ> (cit. on p. 7).
- [May19] Alex May. “Quantum tasks in holography”. In: *Journal of High Energy Physics* 2019.10 (2019), pp. 1–39 (cit. on pp. 27, 31).
- [May22] Alex May. “Complexity and entanglement in non-local computation and holography”. In: *Quantum* 6 (2022), p. 864 (cit. on pp. 27, 31, 32).
- [MHS14] Marek Mozrzyk, Michał Horodecki, and Michał Studziński. “Structure and properties of the algebra of partially transposed permutation operators”. In: *Journal of Mathematical Physics* 55.3 (2014), p. 032202. DOI: [doi.org/10.1063/1.4869027](#). arXiv: [1308.2653](#) (cit. on pp. 3, 5).
- [MRW18a] David Maslen, Daniel N. Rockmore, and Sarah Wolff. “Separation of Variables and the Computation of Fourier Transforms on Finite Groups, II”. In: *Journal of Fourier Analysis and Applications* 24.1 (2018), pp. 226–284. DOI: [10.1007/s00041-016-9516-4](#). arXiv: [1512.02445](#) (cit. on p. 24).
- [MRW18b] David Maslen, Daniel N. Rockmore, and Sarah Wolff. “The efficient computation of Fourier transforms on semisimple algebras”. In: *Journal of Fourier Analysis and Applications* 24 (2018), pp. 1377–1400. arXiv: [1609.02634](#) (cit. on p. 24).

- [MSH18] Marek Mozrzykmas, Michał Studziński, and Michał Horodecki. “A simplified formalism of the algebra of partially transposed permutation operators with applications”. In: *Journal of Physics A: Mathematical and Theoretical* 51.12 (2018), p. 125202. DOI: [10.1088/1751-8121/aaad15](https://doi.org/10.1088/1751-8121/aaad15). arXiv: [1708.02434](https://arxiv.org/abs/1708.02434) (cit. on pp. 3, 5).
- [MSK21] Marek Mozrzykmas, Michał Studziński, and Piotr Kopszak. “Optimal multi-port-based teleportation schemes”. In: *Quantum* 5 (June 2021), p. 477. DOI: [10.22331/q-2021-06-17-477](https://doi.org/10.22331/q-2021-06-17-477). arXiv: [2011.09256](https://arxiv.org/abs/2011.09256) (cit. on pp. 3, 27).
- [MSSH18] Marek Mozrzykmas, Michał Studziński, Sergii Strelchuk, and Michał Horodecki. “Optimal port-based teleportation”. In: *New Journal of Physics* 20.5 (May 2018), p. 053006. DOI: [10.1088/1367-2630/aab8e7](https://doi.org/10.1088/1367-2630/aab8e7). arXiv: [1707.08456](https://arxiv.org/abs/1707.08456) (cit. on pp. 3, 27).
- [Naz96] Maxim Nazarov. “Young’s orthogonal form for Brauer’s centralizer algebra”. In: *Journal of Algebra* 182.3 (1996), pp. 664–693. DOI: [10.1006/jabr.1996.0195](https://doi.org/10.1006/jabr.1996.0195). URL: <https://core.ac.uk/download/pdf/82261192.pdf> (cit. on p. 5).
- [NC97] Michael A. Nielsen and Isaac L. Chuang. “Programmable quantum gate arrays”. In: *Physical Review Letters* 79.2 (July 1997), pp. 321–324. DOI: [10.1103/PhysRevLett.79.321](https://doi.org/10.1103/PhysRevLett.79.321). arXiv: [quant-ph/9703032](https://arxiv.org/abs/quant-ph/9703032) (cit. on p. 27).
- [Ngu23] Quynh T. Nguyen. “The mixed Schur transform: efficient quantum circuit and applications”. To appear simultaneously. 2023 (cit. on p. 5).
- [Nik07] Pavel P. Nikitin. “The centralizer algebra of the diagonal action of the group $GL_n(\mathbb{C})$ in a mixed tensor space”. In: *Journal of Mathematical Sciences* 141.4 (2007), pp. 1479–1493. DOI: [10.1007/s10958-007-0053-1](https://doi.org/10.1007/s10958-007-0053-1) (cit. on pp. 2–5, 11).
- [NPR21] Ion Nechita, Clément Pellegrini, and Denis Rochette. “A geometrical description of the universal $1 \rightarrow 2$ asymmetric quantum cloning region”. 2021. arXiv: [2106.09655](https://arxiv.org/abs/2106.09655) (cit. on pp. 3, 5).
- [NPR23] Ion Nechita, Clément Pellegrini, and Denis Rochette. “The asymmetric quantum cloning region”. In: *Letters in Mathematical Physics* 113.3 (June 2023), p. 74. DOI: [10.1007/s11005-023-01694-8](https://doi.org/10.1007/s11005-023-01694-8). arXiv: [2209.11999](https://arxiv.org/abs/2209.11999) (cit. on p. 5).
- [OV96] Andrei Okounkov and Anatoly Vershik. “A new approach to representation theory of symmetric groups”. In: *Selecta Mathematica, New Series* 2.4 (1996), pp. 581–605. DOI: [10.1007/BF02433451](https://doi.org/10.1007/BF02433451) (cit. on pp. 7, 42).
- [OW16] Ryan O’Donnell and John Wright. “Efficient quantum tomography”. In: *Proceedings of the Forty-Eighth Annual ACM Symposium on Theory of Computing*. STOC’16. New York, NY, USA: Association for Computing Machinery, 2016, pp. 899–912. DOI: [10.1145/2897518.2897544](https://doi.org/10.1145/2897518.2897544). arXiv: [1508.01907](https://arxiv.org/abs/1508.01907) (cit. on p. 2).
- [OW17] Ryan O’Donnell and John Wright. “Efficient quantum tomography II”. In: *Proceedings of the 49th Annual ACM Symposium on Theory of Computing*. STOC’17. New York, NY, USA: Association for Computing Machinery, 2017, pp. 962–974. DOI: [10.1145/3055399.3055454](https://doi.org/10.1145/3055399.3055454). arXiv: [1612.00034](https://arxiv.org/abs/1612.00034) (cit. on p. 2).
- [PBP21] Jason Pereira, Leonardo Banchi, and Stefano Pirandola. “Characterising port-based teleportation as universal simulator of qubit channels”. In: *Journal of Physics A: Mathematical and Theoretical* 54.20 (2021), p. 205301 (cit. on p. 27).
- [PLL19] Stefano Pirandola, Riccardo Laurenza, Cosmo Lupo, and Jason L Pereira. “Fundamental limits to quantum channel discrimination”. In: *npj Quantum Information* 5.1 (2019), p. 50 (cit. on p. 27).
- [QDSSM19a] Marco Túlio Quintino, Qingxiuxiong Dong, Atsushi Shimbo, Akihito Soeda, and Mio Murao. “Probabilistic exact universal quantum circuits for transforming unitary operations”. In: *Physical Review A* 100.6 (2019), p. 062339. DOI: [10.1103/PhysRevA.100.062339](https://doi.org/10.1103/PhysRevA.100.062339). arXiv: [1909.01366](https://arxiv.org/abs/1909.01366) (cit. on pp. 5, 26).
- [QDSSM19b] Marco Túlio Quintino, Qingxiuxiong Dong, Atsushi Shimbo, Akihito Soeda, and Mio Murao. “Reversing unknown quantum transformations: Universal quantum circuit for inverting general unitary operations”. In: *Phys. Rev. Lett.* 123.21 (Nov. 2019), p. 210502. DOI: [10.1103/PhysRevLett.123.210502](https://doi.org/10.1103/PhysRevLett.123.210502). arXiv: [1810.06944](https://arxiv.org/abs/1810.06944) (cit. on pp. 5, 26).
- [QE21] Marco Túlio Quintino and Daniel Ebler. “Deterministic transformations between unitary operations: Exponential advantage with adaptive quantum circuits and the power of indefinite causality”. In: *Quantum* 6 (Mar. 2021), p. 679. DOI: [10.22331/q-2022-03-31-679](https://doi.org/10.22331/q-2022-03-31-679). eprint: [2109.08202](https://arxiv.org/abs/2109.08202) (cit. on pp. 5, 26).
- [RMB21] Denis Rosset, Felipe Montealegre-Mora, and Jean-Daniel Bancal. “RepLAB: A computational / numerical approach to representation theory”. In: *Quantum Theory and Symmetries*. Ed. by M. B. Paranjape, Richard MacKenzie, Zora Thomova, Pavel Winternitz, and William Witczak-Krempa. Springer, 2021, pp. 643–653. DOI: [10.1007/978-3-030-55777-5_60](https://doi.org/10.1007/978-3-030-55777-5_60). arXiv: [1911.09154](https://arxiv.org/abs/1911.09154) (cit. on p. 5).
- [Rut48] Daniel Edwin Rutherford. *Substitutional analysis*. Edinburgh University Press, 1948 (cit. on pp. 3, 39).
- [RW92] Arun Ram and Hans Wenzl. “Matrix units for centralizer algebras”. In: *Journal of Algebra* 145.2 (1992), pp. 378–395 (cit. on p. 25).
- [Sag13] Bruce E. Sagan. *The symmetric group: representations, combinatorial algorithms, and symmetric functions*. Graduate Texts in Mathematics. Springer New York, 2013. URL: <https://books.google.com/books?id=Y6vTBwAAQAAJ> (cit. on pp. 3, 28).
- [SHM13] Michał Studziński, Michał Horodecki, and Marek Mozrzykmas. “Commutant structure of $U^{\otimes(n-1)} \otimes U^*$ transformations”. In: *Journal of Physics A: Mathematical and Theoretical* 46.39 (Sept. 2013), p. 395303. DOI: [10.1088/1751-8113/46/39/395303](https://doi.org/10.1088/1751-8113/46/39/395303). arXiv: [1305.6183](https://arxiv.org/abs/1305.6183) (cit. on pp. 3, 5).

- [SIGA05] Valerio Scarani, Sofyan Iblisdir, Nicolas Gisin, and Antonio Acín. “Quantum cloning”. In: *Rev. Mod. Phys.* 77.4 (Nov. 2005), pp. 1225–1256. DOI: [10.1103/RevModPhys.77.1225](https://doi.org/10.1103/RevModPhys.77.1225). arXiv: [quant-ph/0511088](https://arxiv.org/abs/quant-ph/0511088) (cit. on p. 3).
- [SMK21] Michał Studziński, Marek Mozrzykmas, and Piotr Kopszak. “Degradation of the resource state in port-based teleportation scheme”. 2021. arXiv: [2105.14886](https://arxiv.org/abs/2105.14886) (cit. on p. 3).
- [SMK22] Michał Studziński, Marek Mozrzykmas, and Piotr Kopszak. “Square-root measurements and degradation of the resource state in port-based teleportation scheme”. In: *Journal of Physics A: Mathematical and Theoretical* 55.37 (2022), p. 375302 (cit. on p. 27).
- [SMKH22] Michał Studziński, Marek Mozrzykmas, Piotr Kopszak, and Michał Horodecki. “Efficient multi port-based teleportation schemes”. In: *IEEE Transactions on Information Theory* (2022). DOI: [10.1109/TIT.2022.3187852](https://doi.org/10.1109/TIT.2022.3187852). arXiv: [2008.00984](https://arxiv.org/abs/2008.00984) (cit. on pp. 3, 5, 27).
- [SMZ22] Adam Sawicki, Lorenzo Mattioli, and Zoltán Zimborás. “Universality verification for a set of quantum gates”. In: *Phys. Rev. A* 105.5 (May 2022), p. 052602. DOI: [10.1103/PhysRevA.105.052602](https://doi.org/10.1103/PhysRevA.105.052602). arXiv: [2111.03862](https://arxiv.org/abs/2111.03862) (cit. on p. 3).
- [Spe16] Florian Speelman. “Instantaneous non-local computation of low T -depth quantum circuits”. In: *11th Conference on the Theory of Quantum Computation, Communication and Cryptography (TQC 2016)*. Ed. by Anne Broadbent. Vol. 61. Leibniz International Proceedings in Informatics (LIPIcs). Dagstuhl, Germany: Schloss Dagstuhl–Leibniz-Zentrum fuer Informatik, 2016, 9:1–9:24. DOI: [10.4230/LIPIcs.TQC.2016.9](https://doi.org/10.4230/LIPIcs.TQC.2016.9) (cit. on p. 31).
- [SS15] Antonio Sartori and Catharina Stroppel. “Walled Brauer algebras as idempotent truncations of level 2 cyclotomic quotients”. In: *Journal of Algebra* 440 (2015), pp. 602–638. DOI: [10.1016/j.jalgebra.2015.06.018](https://doi.org/10.1016/j.jalgebra.2015.06.018). arXiv: [1411.2771](https://arxiv.org/abs/1411.2771) (cit. on p. 12).
- [SS22] Oskar Słowik and Adam Sawicki. “Calculable lower bounds on efficiency of universal sets of quantum gates”. 2022. arXiv: [2201.11774](https://arxiv.org/abs/2201.11774) (cit. on p. 3).
- [SS23] Sergii Strelchuk and Michał Studziński. “Minimal port-based teleportation”. In: *New Journal of Physics* (2023) (cit. on p. 27).
- [SSMH17] Michał Studziński, Sergii Strelchuk, Marek Mozrzykmas, and Michał Horodecki. “Port-based teleportation in arbitrary dimension”. In: *Scientific reports* 7.1 (Sept. 2017), p. 10871. DOI: [10.1038/s41598-017-10051-4](https://doi.org/10.1038/s41598-017-10051-4). arXiv: [1612.09260](https://arxiv.org/abs/1612.09260) (cit. on pp. 3, 27).
- [ST17] Alexei M. Semikhatov and Ilya Yu. Tipunin. “Quantum walled Brauer algebra: commuting families, baxterization, and representations”. In: *Journal of Physics A: Mathematical and Theoretical* 50.6 (Jan. 2017), p. 065202. DOI: [10.1088/1751-8121/50/6/065202](https://doi.org/10.1088/1751-8121/50/6/065202). arXiv: [1512.06994](https://arxiv.org/abs/1512.06994) (cit. on pp. 5, 14).
- [ST21] Vikesh Siddhu and Sridhar Tayur. “Five starter pieces: quantum information science via semi-definite programs”. 2021. arXiv: [2112.08276](https://arxiv.org/abs/2112.08276) (cit. on pp. 5, 25).
- [Sta13] Richard P Stanley. “Algebraic combinatorics”. In: *Springer* 20.22 (2013), p. 4 (cit. on p. 28).
- [Ste87] John R Stembridge. “Rational tableaux and the tensor algebra of \mathfrak{gl}_n ”. In: *Journal of Combinatorial Theory, Series A* 46.1 (1987), pp. 79–120 (cit. on pp. 9, 16).
- [Tur89] Vladimir Georgievich Turaev. “Operator invariants of tangles, and R-matrices”. In: *Izvestiya Rossiiskoi Akademii Nauk. Seriya Matematicheskaya* 53.5 (1989), pp. 1073–1107. URL: <http://mi.mathnet.ru/izv1288> (cit. on pp. 3, 11).
- [VK92] Naum Ya. Vilenkin and Anatoli U. Klimyk. “Representations in the Gel’fand-Tsetlin Basis and Special Functions”. In: *Representation of Lie Groups and Special Functions: Volume 3: Classical and Quantum Groups and Special Functions*. Dordrecht: Springer Netherlands, 1992, pp. 361–446. DOI: [10.1007/978-94-017-2881-2_5](https://doi.org/10.1007/978-94-017-2881-2_5). URL: https://doi.org/10.1007/978-94-017-2881-2_5 (cit. on pp. 18, 20, 37).
- [VO05] Anatoly Vershik and Andrei Okounkov. “A new approach to the representation theory of the symmetric groups. II”. In: *Journal of Mathematical Sciences* 131 (2005), pp. 5471–5494. DOI: [10.1007/s10958-005-0421-7](https://doi.org/10.1007/s10958-005-0421-7). arXiv: [math/0503040](https://arxiv.org/abs/math/0503040) (cit. on pp. 7, 42).
- [War79] Edward Waring. “Problems concerning interpolations”. In: *Philosophical transactions of the Royal Society of London* 69 (1779), pp. 59–67. URL: <https://www.jstor.org/stable/106408?seq=6> (cit. on p. 42).
- [Wat18] John Watrous. *The Theory of Quantum Information*. Cambridge University Press, 2018. URL: <https://cs.uwaterloo.ca> (cit. on pp. 5, 23, 25).
- [Wri16] John Wright. “How to learn a quantum state”. PhD thesis. Carnegie Mellon University, 2016. URL: <http://reports-archive.adm.cs.cmu.edu/anon/2016/abstracts/16-108.html> (cit. on p. 2).
- [WSV12] Henry Wolkowicz, Romesh Saigal, and Lieven Vandenbergh. *Handbook of Semidefinite Programming: Theory, Algorithms, and Applications*. International Series in Operations Research & Management Science. Springer, 2012. DOI: [10.1007/978-1-4615-4381-7](https://doi.org/10.1007/978-1-4615-4381-7). URL: <https://books.google.com/books?id=ErLSBwAAQBAJ> (cit. on p. 25).
- [YSM21] Satoshi Yoshida, Akihito Soeda, and Mio Murao. “Universal construction of decoders from encoding black boxes”. 2021. arXiv: [2110.00258](https://arxiv.org/abs/2110.00258) (cit. on pp. 5, 26).
- [YSM22] Satoshi Yoshida, Akihito Soeda, and Mio Murao. “Reversing unknown qubit-unitary operation, deterministically and exactly”. 2022. arXiv: [2209.02907](https://arxiv.org/abs/2209.02907) (cit. on p. 5).
- [ZKW07] Yong Zhang, Louis H Kauffman, and Reinhard F Werner. “Permutation and its partial transpose”. In: *International Journal of Quantum Information* 05.04 (2007), pp. 469–507. DOI: [10.1142/S021974990700302X](https://doi.org/10.1142/S021974990700302X). arXiv: [quant-ph/0606005](https://arxiv.org/abs/quant-ph/0606005) (cit. on p. 3).
- [ZLLSK23] Han Zheng, Zimu Li, Junyu Liu, Sergii Strelchuk, and Risi Kondor. “Speeding up learning quantum states through group equivariant convolutional quantum ansätze”. 2023. arXiv: [2112.07611](https://arxiv.org/abs/2112.07611) (cit. on pp. 3, 5).

APPENDIX A. CLEBSCH–GORDAN COEFFICIENTS

This appendix summarizes formulas from [VK92, Chapter 18] for evaluating the (dual) Clebsch–Gordan²¹ coefficients of U_d . Recall from Section 2.3 that a Gelfand–Tsetlin pattern $M \in \text{GT}(\lambda, d)$ is a column vector

$$M = \begin{bmatrix} \mathbf{m}_d \\ \vdots \\ \mathbf{m}_1 \end{bmatrix}, \quad (164)$$

where $\mathbf{m}_n = (m_{1,n}, \dots, m_{n,n})$ are row vectors of non-decreasing integers subject to interlacing relations (30). For any row \mathbf{m}_n and integer $i \in \{1, \dots, n\}$, we denote by $\mathbf{m}_n^{\pm i}$ the vector \mathbf{m}_n with entry $m_{i,n}$ replaced by $m_{i,n} \pm 1$. Let us fix any symbol $x \in [d]$. We define Gelfand–Tsetlin patterns M^+ and M^- by modifying the top $d - x + 1$ rows of M as follows:

$$M = \begin{bmatrix} \mathbf{m}_d \\ \vdots \\ \mathbf{m}_x \\ \mathbf{m}_{x-1} \\ \vdots \\ \mathbf{m}_1 \end{bmatrix}, \quad M^+ = \begin{bmatrix} \mathbf{m}_d^{+i_d} \\ \vdots \\ \mathbf{m}_x^{+i_x} \\ \mathbf{m}_{x-1} \\ \vdots \\ \mathbf{m}_1 \end{bmatrix}, \quad M^- = \begin{bmatrix} \mathbf{m}_d^{-i_d} \\ \vdots \\ \mathbf{m}_x^{-i_x} \\ \mathbf{m}_{x-1} \\ \vdots \\ \mathbf{m}_1 \end{bmatrix}, \quad (165)$$

for some integers i_x, \dots, i_d where $1 \leq i_j \leq j$. Intuitively, this means that the semistandard tableau M^+ is obtained from M by adding a box containing x in the row i_x , and then consecutively bumping the entries j from row i_j downwards the tableau.

For any $x \in [d]$, the Gelfand–Tsetlin patterns corresponding to x and its dual are defined as follows:

$$X^+ := \begin{bmatrix} 1 & 0 & 0 & \dots & 0 & 0 & 0 \\ 1 & 0 & 0 & \dots & 0 & 0 & 0 \\ \dots & \dots & \dots & \dots & \dots & \dots & \dots \\ 1 & 0 & \dots & 0 & \dots & \dots & \dots \\ 0 & \dots & 0 & \dots & \dots & \dots & \dots \\ \dots & \dots & \dots & \dots & \dots & \dots & \dots \\ 0 & 0 & \dots & \dots & \dots & \dots & \dots \\ 0 & \dots & \dots & \dots & \dots & \dots & \dots \end{bmatrix} \begin{matrix} d \\ d-1 \\ \dots \\ x \\ x-1 \\ \dots \\ 2 \\ 1 \end{matrix}, \quad X^- := \begin{bmatrix} 0 & 0 & 0 & \dots & 0 & 0 & -1 \\ 0 & 0 & 0 & \dots & 0 & -1 & \dots \\ \dots & \dots & \dots & \dots & \dots & \dots & \dots \\ 0 & 0 & \dots & -1 & \dots & \dots & \dots \\ 0 & \dots & 0 & \dots & \dots & \dots & \dots \\ \dots & \dots & \dots & \dots & \dots & \dots & \dots \\ 0 & 0 & \dots & \dots & \dots & \dots & \dots \\ 0 & \dots & \dots & \dots & \dots & \dots & \dots \end{bmatrix} \begin{matrix} d \\ d-1 \\ \dots \\ x \\ x-1 \\ \dots \\ 2 \\ 1 \end{matrix}. \quad (166)$$

Now we can define the Clebsch–Gordan coefficients $c_{M^\pm, M}^{x, \pm}$ uniformly as

$$c_{M^\pm, M}^{x, \pm} := c_{M^\pm, M}^{X^\pm}, \quad (167)$$

where $c_{M^\pm, M}^{X^\pm}$ is the product of *reduced Wigner coefficients*:

$$c_{M^\pm, M}^{X^\pm} = \prod_{n=x+1}^d \left(\begin{array}{cc|c} \mathbf{m}_n & \mathbf{x}_n^\pm & \mathbf{m}_n^{\pm i_n} \\ \mathbf{m}_{n-1} & \mathbf{x}_{n-1}^\pm & \mathbf{m}_{n-1}^{\pm i_{n-1}} \end{array} \right). \quad (168)$$

The *reduced Wigner coefficients* [Har05, p. 152] or *scalar factors* [VK92, p. 385] are defined as follows. We take two consecutive rows \mathbf{m}_n and \mathbf{m}_{n-1} ($1 < n \leq d$) of a Gelfand–Tsetlin pattern M and modify them at positions $1 \leq i \leq n$ and $1 \leq j \leq n-1$. The corresponding reduced Wigner coefficients are

$$\left(\begin{array}{cc|c} \mathbf{m}_n & (1, \mathbf{0}_{n-1}) & \mathbf{m}_n^{+i} \\ \mathbf{m}_{n-1} & (0, \mathbf{0}_{n-2}) & \mathbf{m}_{n-1} \end{array} \right) = \left| \frac{\prod_{j=1}^{n-1} (\ell_{j,n-1} - \ell_{i,n} - 1)}{\prod_{j \neq i} (\ell_{j,n} - \ell_{i,n})} \right|^{1/2}, \quad (169)$$

$$\left(\begin{array}{cc|c} \mathbf{m}_n & (1, \mathbf{0}_{n-1}) & \mathbf{m}_n^{+i} \\ \mathbf{m}_{n-1} & (1, \mathbf{0}_{n-2}) & \mathbf{m}_{n-1}^{+j} \end{array} \right) = S(i, j) \left| \frac{\prod_{k \neq j} (\ell_{k,n-1} - \ell_{i,n} - 1) \prod_{k \neq i} (\ell_{k,n} - \ell_{j,n-1} - 1)}{\prod_{k \neq i} (\ell_{k,n} - \ell_{i,n}) \prod_{k \neq j} (\ell_{k,n-1} - \ell_{j,n-1} - 1)} \right|^{1/2}, \quad (170)$$

$$\left(\begin{array}{cc|c} \mathbf{m}_n & (\mathbf{0}_{n-1}, -1) & \mathbf{m}_n^{-i} \\ \mathbf{m}_{n-1} & (\mathbf{0}_{n-2}, 0) & \mathbf{m}_{n-1} \end{array} \right) = \left| \frac{\prod_{j=1}^{n-1} (\ell_{j,n-1} - \ell_{i,n})}{\prod_{j \neq i} (\ell_{j,n} - \ell_{i,n})} \right|^{1/2}, \quad (171)$$

$$\left(\begin{array}{cc|c} \mathbf{m}_n & (\mathbf{0}_{n-1}, -1) & \mathbf{m}_n^{-i} \\ \mathbf{m}_{n-1} & (\mathbf{0}_{n-2}, -1) & \mathbf{m}_{n-1}^{-j} \end{array} \right) = S(i, j) \left| \frac{\prod_{k \neq j} (\ell_{k,n-1} - \ell_{i,n}) \prod_{k \neq i} (\ell_{k,n} - \ell_{j,n-1} + 1)}{\prod_{k \neq i} (\ell_{k,n} - \ell_{i,n}) \prod_{k \neq j} (\ell_{k,n-1} - \ell_{j,n-1} + 1)} \right|^{1/2}. \quad (172)$$

where $\mathbf{0}_n$ denotes a row vector with n zeros, $\ell_{k,s} := m_{k,s} - k$, $S(i, j) := 1$ if $i \leq j$ and $S(i, j) := -1$ if $i > j$.

²¹Also known as Wigner coefficients [BL68; Har05].

More explicitly, the Clebsch–Gordan coefficient $c_{M^+,M}^{x,+}$ is equal to the product of the reduced Wigner coefficients obtained by cutting the Gelfand–Tsetlin patterns M , x and M^\pm into pairs of consecutive rows:

$$c_{M^+,M}^{x,+} = \left(\begin{array}{cc|c} \mathbf{m}_x & (1, \mathbf{0}) & \mathbf{m}_x^{+i_x} \\ \mathbf{m}_{x-1} & (0, \mathbf{0}) & \mathbf{m}_{x-1} \end{array} \right) \cdot \prod_{n=x+1}^d \left(\begin{array}{cc|c} \mathbf{m}_n & (1, \mathbf{0}) & \mathbf{m}_n^{+i_n} \\ \mathbf{m}_{n-1} & (1, \mathbf{0}) & \mathbf{m}_{n-1}^{+i_{n-1}} \end{array} \right). \quad (173)$$

On the other hand, for arbitrary M^+ which is not of the form (165), Clebsch–Gordan coefficient $c_{M^+,M}^{x,+} = 0$. A dual Clebsch–Gordan coefficient $c_{M^-,M}^{x,-}$ is given by the product of dual reduced Wigner coefficients:

$$c_{M^-,M}^{x,-} = \left(\begin{array}{cc|c} \mathbf{m}_x & (\mathbf{0}, -1) & \mathbf{m}_x^{-i_x} \\ \mathbf{m}_{x-1} & (\mathbf{0}, 0) & \mathbf{m}_{x-1} \end{array} \right) \cdot \prod_{n=x+1}^d \left(\begin{array}{cc|c} \mathbf{m}_n & (\mathbf{0}, -1) & \mathbf{m}_n^{-i_n} \\ \mathbf{m}_{n-1} & (\mathbf{0}, -1) & \mathbf{m}_{n-1}^{-i_{n-1}} \end{array} \right). \quad (174)$$

On the other hand, for arbitrary M^-,M which is not of the form (165), dual Clebsch–Gordan coefficient $c_{M^-,M}^{x,-} = 0$.

We can summarize the above definitions succinctly as follows. We can define Clebsch–Gordan coefficients $c_{N(k),M(k)}^{x,\pm} = 0$ for arbitrary $k \in [d]$, $\lambda \in \widehat{U}_k$, $N(k), M(k) \in \text{GT}(\lambda, k)$, $x \in [k]$ recursively as

$$c_{N(k),M(k)}^{x,\pm} = (z^\pm)^{\mathbf{m}_k, \mathbf{n}_k}_{\mathbf{m}_{k-1}, \mathbf{n}_{k-1}} \cdot c_{N(k-1),M(k-1)}^{x,\pm}, \quad (175)$$

where for every $k \in [d]$ and Gelfand–Tsetlin patterns of length $k-1$ we define

$$c_{N(k-1),M(k-1)}^{k,\pm} := \delta_{N(k-1),M(k-1)}, \quad (176)$$

and the coefficients $(z^\pm)^{\mathbf{m}_k, \mathbf{n}_k}_{\mathbf{m}_{k-1}, \mathbf{n}_{k-1}}$ are defined for $\mathbf{m}_{k-1} \sqsubseteq \mathbf{m}_k$ and $\mathbf{n}_{k-1} \sqsubseteq \mathbf{n}_k$ as

$$(z^+)^{\mathbf{m}_k, \mathbf{n}_k}_{\mathbf{m}_{k-1}, \mathbf{n}_{k-1}} := \begin{cases} \left(\begin{array}{cc|c} \mathbf{m}_k & (1, \mathbf{0}) & \mathbf{m}_k^{+i} \\ \mathbf{m}_{k-1} & (1, \mathbf{0}) & \mathbf{m}_{k-1}^{+j} \end{array} \right) & \mathbf{n}_k = \mathbf{m}_k^{+i}, \mathbf{n}_{k-1} = \mathbf{m}_{k-1}^{+j} \text{ for some } i \in [k], j \in [k-1] \\ \left(\begin{array}{cc|c} \mathbf{m}_k & (1, \mathbf{0}) & \mathbf{m}_k^{+i} \\ \mathbf{m}_{k-1} & (\mathbf{0}, 0) & \mathbf{m}_{k-1}^{+j} \end{array} \right) & \mathbf{n}_k = \mathbf{m}_k^{+i}, \text{ for some } i \in [k], \\ 1 & \mathbf{m}_k = \mathbf{n}_k, \mathbf{m}_{k-1} = \mathbf{n}_{k-1}, \\ 0 & \text{otherwise} \end{cases} \quad (177)$$

and

$$(z^-)^{\mathbf{m}_k, \mathbf{n}_k}_{\mathbf{m}_{k-1}, \mathbf{n}_{k-1}} := \begin{cases} \left(\begin{array}{cc|c} \mathbf{m}_k & (\mathbf{0}, -1) & \mathbf{m}_k^{-i} \\ \mathbf{m}_{k-1} & (\mathbf{0}, -1) & \mathbf{m}_{k-1}^{-j} \end{array} \right) & \mathbf{n}_k = \mathbf{m}_k^{-i}, \mathbf{n}_{k-1} = \mathbf{m}_{k-1}^{-j} \text{ for some } i \in [k], j \in [k-1] \\ \left(\begin{array}{cc|c} \mathbf{m}_k & (\mathbf{0}, -1) & \mathbf{m}_k^{-i} \\ \mathbf{m}_{k-1} & (\mathbf{0}, 0) & \mathbf{m}_{k-1}^{-j} \end{array} \right) & \mathbf{n}_k = \mathbf{m}_k^{-i}, \text{ for some } i \in [k], \\ 1 & \mathbf{m}_k = \mathbf{n}_k, \mathbf{m}_{k-1} = \mathbf{n}_{k-1}, \\ 0 & \text{otherwise.} \end{cases} \quad (178)$$

If either $\mathbf{m}_{k-1} \sqsubseteq \mathbf{m}_k$ or $\mathbf{n}_{k-1} \sqsubseteq \mathbf{n}_k$ is not satisfied then we define $(z^\pm)^{\mathbf{m}_k, \mathbf{n}_k}_{\mathbf{m}_{k-1}, \mathbf{n}_{k-1}} := 0$.

APPENDIX B. PROOF OF THEOREM 3.2

Definition 3.1. Let $p, q \geq 0$ be integers and $d \in \mathbb{C}$. The walled Brauer algebra $\mathcal{B}_{p,q}^d$ is a finite-dimensional associative algebra over \mathbb{C} generated by $\sigma_1, \dots, \sigma_{p+q-1}$ subject to the following relations:

$$(a) \sigma_i^2 = 1 \ (i \neq p), \quad (b) \sigma_i \sigma_{i+1} \sigma_i = \sigma_{i+1} \sigma_i \sigma_{i+1} \ (i \neq p-1, p), \quad (c) \sigma_i \sigma_j = \sigma_j \sigma_i \ (|i-j| > 1), \quad (42)$$

$$(d) \sigma_p^2 = d \sigma_p, \quad (e) \sigma_p \sigma_{p \pm 1} \sigma_p = \sigma_p, \quad (f) \sigma_p \sigma_i = \sigma_i \sigma_p \ (i \neq p \pm 1), \quad (43)$$

$$(g) \sigma_p \sigma_{p+1} \sigma_{p-1} \sigma_p \sigma_{p-1} = \sigma_p \sigma_{p+1} \sigma_{p-1} \sigma_p \sigma_{p+1}, \quad (44)$$

$$(h) \sigma_{p-1} \sigma_p \sigma_{p+1} \sigma_{p-1} \sigma_p = \sigma_{p+1} \sigma_p \sigma_{p+1} \sigma_{p-1} \sigma_p. \quad (45)$$

Theorem 3.2 (Gelfand–Tsetlin basis for $\mathcal{A}_{p,q}^d$). For any $\lambda \in \widehat{\mathcal{A}}_{p,q}^d$, the following map $\psi_\lambda: \mathcal{A}_{p,q}^d \rightarrow \text{End}(\mathbb{C}^{\text{Paths}(\lambda)})$ is an irreducible representation of $\mathcal{A}_{p,q}^d$. Given a generator σ_i of $\mathcal{A}_{p,q}^d$, $i = 1, \dots, p+q-1$, the matrix $\psi_\lambda(\sigma_i)$ acts on the Gelfand–Tsetlin basis vectors $|T\rangle$ with $T \in \text{Paths}(\lambda)$ as follows:

$$\psi_\lambda(\sigma_i) |T\rangle = \frac{1}{r_i(T)} |T\rangle + \sqrt{1 - \frac{1}{r_i(T)^2}} |\sigma_i T\rangle, \quad \text{for } i \neq p, \quad (59)$$

$$\psi_\lambda(\sigma_p) |T\rangle = c(T) |v_T\rangle, \quad |v_T\rangle := \sum_{T' \in \mathcal{M}(T)} c(T') |T'\rangle, \quad \text{for } i = p, \quad (60)$$

where $r_i(T)$ is the walled axial distance defined in eq. (56), $\sigma_i T$ denotes the mixed standard Young tableau T with cell fillings permuted according to σ_i (see Section 2.4), and the coefficient $c(T) \in \mathbb{R}$ is given by

$$c(T) := \sqrt{(d + \text{cont}(a_T)) \frac{\prod_{c \in \text{RC}(T^{p-1})} (\text{cont}(a_T) - \text{cont}(c))}{\prod_{a \in \text{AC}(T^{p-1}) \setminus a_T} (\text{cont}(a_T) - \text{cont}(a))}} \quad (61)$$

where a_T is the mobile element of T , and RC/AC are the sets of removable/addable cells.

Proof. We will prove the theorem in three steps. First, we check that such action defines a representation of $\mathcal{A}_{p,q}^d$ by checking the relations in eq. (42) for transpositions. The relations for transpositions in eq. (59) are defined in the same way as the Young–Yamanouchi basis of the symmetric group [Rut48]. It is essentially folklore knowledge today, however, we still provide the proof for completeness. Next, we check the relations in eqs. (43) to (45) for the contraction σ_p . Finally, we prove that such representation is irreducible. For simplicity, we will write σ_i instead of $\psi_\lambda(\sigma_i)$.

(a) To verify $\sigma_i^2 = 1$, consider the action of σ_i on the invariant subspaces V_T spanned by $\{|T\rangle, |\sigma_i T\rangle\}$ for each $T \in \text{Paths}(\lambda)$. It is clear from eq. (59) that the matrix $\sigma_i|_{V_T}$ of this action is

$$\sigma_i|_{V_T} = \begin{pmatrix} \frac{1}{r_i(T)} & \sqrt{1 - \frac{1}{r_i(T)^2}} \\ \sqrt{1 - \frac{1}{r_i(T)^2}} & -\frac{1}{r_i(T)} \end{pmatrix},$$

meaning that trivially $(\sigma_i|_{V_T})^2 = 1$. Since that holds for every $T \in \text{Paths}(\lambda)$, then $\sigma_i^2 = 1$ holds.

(b) To verify $(\sigma_i \sigma_{i+1})^3 = 1$, consider for every $T \in \text{Paths}(\lambda)$ the action of $\sigma_i \sigma_{i+1}$ (according to eq. (59)) on the invariant vector space $V_T := \text{span}\{|T\rangle, |\sigma_i T\rangle, |\sigma_{i+1} \sigma_i T\rangle, |\sigma_i \sigma_{i+1} \sigma_i T\rangle, |(\sigma_{i+1} \sigma_i)^2 T\rangle, |\sigma_i (\sigma_{i+1} \sigma_i)^2 T\rangle\}$. Now if we define $a := r_i(T)$, $b := r_i(\sigma_{i+1} \sigma_i T)$, $c := r_i((\sigma_{i+1} \sigma_i)^2 T)$, then the action of σ_i and σ_{i+1} on the V_T in the above basis is given by the following matrices:

$$\sigma_i|_{V_T} = \begin{pmatrix} \frac{1}{a} & \sqrt{1 - \frac{1}{a^2}} & 0 & 0 & 0 & 0 \\ \sqrt{1 - \frac{1}{a^2}} & -\frac{1}{a} & 0 & 0 & 0 & 0 \\ 0 & 0 & \frac{1}{b} & \sqrt{1 - \frac{1}{b^2}} & 0 & 0 \\ 0 & 0 & \sqrt{1 - \frac{1}{b^2}} & -\frac{1}{b} & 0 & 0 \\ 0 & 0 & 0 & 0 & \frac{1}{c} & \sqrt{1 - \frac{1}{c^2}} \\ 0 & 0 & 0 & 0 & \sqrt{1 - \frac{1}{c^2}} & -\frac{1}{c} \end{pmatrix}, \sigma_{i+1}|_{V_T} = \begin{pmatrix} \frac{1}{c} & 0 & \sqrt{1 - \frac{1}{c^2}} & 0 & 0 & 0 \\ 0 & \frac{1}{b} & 0 & 0 & \sqrt{1 - \frac{1}{b^2}} & 0 \\ \sqrt{1 - \frac{1}{c^2}} & 0 & -\frac{1}{c} & 0 & 0 & 0 \\ 0 & 0 & 0 & \frac{1}{a} & 0 & \sqrt{1 - \frac{1}{a^2}} \\ 0 & \sqrt{1 - \frac{1}{b^2}} & 0 & 0 & -\frac{1}{b} & 0 \\ 0 & 0 & 0 & \sqrt{1 - \frac{1}{a^2}} & 0 & -\frac{1}{a} \end{pmatrix}$$

Taking into account the fact $b = a + c$, it is easy to verify that $(\sigma_i|_{V_T} \sigma_{i+1}|_{V_T})^3 = 1$. Since this holds for any $T \in \text{Paths}(\lambda)$, it must be $(\sigma_i \sigma_{i+1})^3 = 1$.

(c) Finally, to verify the relation $\sigma_i \sigma_j = \sigma_j \sigma_i$ for $(|i - j| > 1)$ just note, that $\sigma_i \sigma_j T = \sigma_j \sigma_i T$ and $a := r_i(\sigma_j T) = r_i(T)$, $b := r_j(\sigma_i T) = r_j(T)$. It means that on $W_T := \text{span}\{|T\rangle, |\sigma_i T\rangle, |\sigma_j T\rangle, |\sigma_j \sigma_i T\rangle\}$ we have a tensor product structure:

$$\sigma_i|_{W_T} = \begin{pmatrix} \frac{1}{a} & \sqrt{1 - \frac{1}{a^2}} & 0 & 0 \\ \sqrt{1 - \frac{1}{a^2}} & -\frac{1}{a} & 0 & 0 \\ 0 & 0 & \frac{1}{a} & \sqrt{1 - \frac{1}{a^2}} \\ 0 & 0 & \sqrt{1 - \frac{1}{a^2}} & -\frac{1}{a} \end{pmatrix} = I_2 \otimes \begin{pmatrix} \frac{1}{a} & \sqrt{1 - \frac{1}{a^2}} \\ \sqrt{1 - \frac{1}{a^2}} & -\frac{1}{a} \end{pmatrix},$$

$$\sigma_j|_{W_T} = \begin{pmatrix} \frac{1}{b} & 0 & \sqrt{1 - \frac{1}{b^2}} & 0 \\ 0 & \frac{1}{b} & 0 & \sqrt{1 - \frac{1}{b^2}} \\ \sqrt{1 - \frac{1}{b^2}} & 0 & -\frac{1}{b} & 0 \\ 0 & \sqrt{1 - \frac{1}{b^2}} & 0 & -\frac{1}{b} \end{pmatrix} = \begin{pmatrix} \frac{1}{b} & \sqrt{1 - \frac{1}{b^2}} \\ \sqrt{1 - \frac{1}{b^2}} & -\frac{1}{b} \end{pmatrix} \otimes I_2,$$

and consecutively $\sigma_i|_{V_T} \sigma_j|_{V_T} = \sigma_j|_{V_T} \sigma_i|_{V_T}$. Therefore, $\sigma_i \sigma_j = \sigma_j \sigma_i$ when $|i - j| > 1$.

(d) For each $T \in \text{Paths}(\lambda)$ there is an invariant subspace $V_T := \text{span}\{|T'\rangle \mid T' \in \mathcal{M}(T)\}$. If $\mathcal{M}(T) = \emptyset$, then we assume $V_T := \text{span}\{|T\rangle\}$. Note that $\|v_T\|_2^2 = d$, according to Corollary B.3. Moreover, it is easy to see from the definition that $\sigma_p|_{V_T} = |v_T\rangle\langle v_T|$. From this it is obvious $(\sigma_p|_{V_T})^2 = d \cdot \sigma_p|_{V_T}$, and that implies $\sigma_p^2 = d \cdot \sigma_p$.

(f) To check $\sigma_p \sigma_i = \sigma_i \sigma_p$ ($i \neq p \pm 1$), we define $W_T := \text{span}\{|T'\rangle \mid T' \in \mathcal{M}(T) \cup \mathcal{M}(\sigma_i T)\} \simeq V_T \otimes \text{span}\{|1\rangle, |\sigma_i\rangle\}$, where $V_T := \text{span}\{|T'\rangle \mid T' \in \mathcal{M}(T)\}$. Here we have a similar tensor product structure as in the case of transpositions making these generators commute. Namely, since $r_i(T) = r_i(T')$ for every $T' \in \mathcal{M}(T)$, we have

$$\sigma_p|_{W_T} = d(|v_T\rangle\langle v_T|_{V_T}) \otimes I_2, \sigma_i|_{W_T} = I_{|\mathcal{M}(T)|} \otimes \begin{pmatrix} \frac{1}{r_i(T)} & \sqrt{1 - \frac{1}{r_i(T)^2}} \\ \sqrt{1 - \frac{1}{r_i(T)^2}} & -\frac{1}{r_i(T)} \end{pmatrix}.$$

Therefore $\sigma_p \sigma_i = \sigma_i \sigma_p$ ($i \neq p \pm 1$) holds.

(e) Now let's first check the relation $\sigma_p \sigma_{p-1} \sigma_p = \sigma_p$. Note that we can conveniently write generators σ_p and σ_{p-1} in terms of the path algebra matrix units, specifically highlighting only the relevant ones:

$$\sigma_p = \sum_{\mu \in B(\lambda)} \sum_{\nu \in C(\lambda, \mu)} \sum_{\substack{S_1 \in \text{Paths}(\nu) \\ S_2 \in \text{Paths}(\mu, \lambda) \\ m, m' \in \mathcal{M}(\lambda, \mu, \nu)}} c(\mu, m) c(\mu, m') |S_1 \circ (\nu, \mu, m, \mu) \circ S_2\rangle \langle S_1 \circ (\nu, \mu, m', \mu) \circ S_2| \quad (179)$$

$$\sigma_{p-1} = \sum_{\mu \in B(\lambda)} \sum_{\nu \in C(\lambda, \mu)} \sum_{\substack{S_1 \in \text{Paths}(\nu) \\ S_2 \in \text{Paths}(\mu, \lambda) \\ m \in \mathcal{M}(\lambda, \mu, \nu)}} f(\nu, \mu, m) |S_1 \circ (\nu, \mu, m, \mu) \circ S_2\rangle \langle S_1 \circ (\nu, \mu, m, \mu) \circ S_2| + \dots, \quad (180)$$

where we use the following notation:

$$\begin{aligned} B(\lambda) &:= \{\mu \in \hat{\mathcal{A}}_{p-1,0}^d \mid \exists T \in \text{Paths}(\lambda) : T^{p-1} = T^{p+1} = \mu\}, \\ C(\lambda, \mu) &:= \{\nu \in \hat{\mathcal{A}}_{p-2,0}^d \mid \exists T \in \text{Paths}(\lambda) : T^{p-1} = T^{p+1} = \mu, T^{p-2} = \nu\}, \\ \mathcal{M}(\lambda, \mu, \nu) &:= \{m \in \hat{\mathcal{A}}_{p,0}^d \mid \exists T \in \text{Paths}(\lambda) : T^{p-1} = T^{p+1} = \mu, T^{p-2} = \nu, T^p = m\}, \\ c(\mu, m) &:= c(T) \text{ for arbitrary } T \in \text{Paths}(\lambda) : T^{p-1} = T^{p+1} = \mu, T^p = m, \\ f(\nu, \mu, m) &:= \frac{1}{r_{p-1}(T)} \text{ for arbitrary } T \in \text{Paths}(\lambda) : T^{p-2} = \nu, T^{p-1} = \mu, T^p = m. \end{aligned}$$

In eq. (180) we do not write terms with the matrix units which multiply to zero with the matrix units from the sum of eq. (179). We also abuse the notation by forgetting that ν, μ, m are actually pairs of Young diagrams: we only refer to the left diagrams by dropping the subscript l . Using eqs. (179) and (180) we can deduce by direct multiplication, that $\sigma_p \sigma_{p-1} \sigma_p = \sigma_p$ is equivalent to

$$\sum_{m \in \mathcal{M}(\lambda, \mu, \nu)} f(\nu, \mu, m) \cdot c(\mu, m)^2 = 1 \quad (181)$$

for every $\mu \in B(\lambda)$, $\nu \in C(\lambda, \mu)$, $S_1 \in \text{Paths}(\nu)$, $S_2 \in \text{Paths}(\mu, \lambda)$. Let $c := \mu \setminus \nu$ be the cell containing $p-1$, it is a corner cell of μ , i.e. $c \in RC(\mu)$. Then eq. (181) is equivalent to

$$\sum_{m \in AC(\mu)} \frac{d + \text{cont}(m)}{\text{cont}(m) - \text{cont}(c)} \frac{\prod_{v \in RC(\mu)} (\text{cont}(m) - \text{cont}(v))}{\prod_{v \in AC(\mu) \setminus m} (\text{cont}(m) - \text{cont}(v))} = 1 \quad (182)$$

for every $\mu \in B(\lambda)$ and $c \in RC(\mu)$. By rewriting the previous formula as

$$d \cdot \sum_{m \in AC(\mu)} \frac{\prod_{w \in RC(\mu) \setminus c} (\text{cont}(m) - \text{cont}(w))}{\prod_{v \in AC(\mu) \setminus m} (\text{cont}(m) - \text{cont}(v))} + \sum_{m \in AC(\mu)} \text{cont}(m) \frac{\prod_{w \in RC(\mu) \setminus c} (\text{cont}(m) - \text{cont}(w))}{\prod_{v \in AC(\mu) \setminus m} (\text{cont}(m) - \text{cont}(v))} = 1,$$

and using Corollary B.5 we conclude that eq. (181) holds, finishing the proof of $\sigma_p \sigma_{p-1} \sigma_p = \sigma_p$. Similar proof also works for the relation (f) $\sigma_p \sigma_{p+1} \sigma_p = \sigma_p$ which we do not repeat here.

(g) Finally, checking the relations in eq. (44) is the same in spirit as for (e), but more cumbersome. Let's first write the generators in terms of matrix units, specifically highlighting only the relevant ones:

$$\sigma_p = \sum_{\substack{\mu \in B(\lambda) \\ (\nu_1, \nu_2) \in C(\lambda, \mu)}} \sum_{\substack{S_1 \in \text{Paths}_{p-2}(\nu_1) \\ S_2 \in \text{Paths}_{p+2}(\nu_2, \lambda) \\ m, m' \in \mathcal{M}(\lambda, \nu_2, \mu, \nu_1)}} c(\mu, m) c(\mu, m') |S_1 \circ (\nu_1, \mu, m, \mu, \nu_2) \circ S_2\rangle \langle S_1 \circ (\nu_1, \mu, m', \mu, \nu_2) \circ S_2| \quad (183)$$

$$\begin{aligned} \sigma_{p-1} = & \sum_{\substack{\mu \in B(\lambda) \\ (\nu_1, \nu_2) \in C(\lambda, \mu)}} \sum_{\substack{S_1 \in \text{Paths}_{p-2}(\nu_1) \\ S_2 \in \text{Paths}_{p+2}(\nu_2, \lambda) \\ m \in \mathcal{M}(\lambda, \nu_2, \mu, \nu_1)}} \left(f_{p-1}(\nu_1, \mu, m) |S_1 \circ (\nu_1, \mu, m, \mu, \nu_2) \circ S_2\rangle \langle S_1 \circ (\nu_1, \mu, m, \mu, \nu_2) \circ S_2| + \right. \\ & \left. + \sqrt{1 - f_{p-1}^2(\nu_1, \mu, m)} |S_1 \circ (\nu_1, \sigma_{p-1} \mu, m, \mu, \nu_2) \circ S_2\rangle \langle S_1 \circ (\nu_1, \mu, m, \mu, \nu_2) \circ S_2| \right) + \dots \end{aligned} \quad (184)$$

$$\begin{aligned} \sigma_{p+1} = & \sum_{\substack{\mu \in B(\lambda) \\ (\nu_1, \nu_2) \in C(\lambda, \mu)}} \sum_{\substack{S_1 \in \text{Paths}_{p-2}(\nu_1) \\ S_2 \in \text{Paths}_{p+2}(\nu_2, \lambda) \\ m \in \mathcal{M}(\lambda, \nu_2, \mu, \nu_1)}} \left(f_{p+1}(m, \mu, \nu_2) |S_1 \circ (\nu_1, \mu, m, \mu, \nu_2) \circ S_2\rangle \langle S_1 \circ (\nu_1, \mu, m, \mu, \nu_2) \circ S_2| + \right. \\ & \left. + \sqrt{1 - f_{p+1}^2(m, \mu, \nu_2)} |S_1 \circ (\nu_1, \mu, m, \sigma_{p+1} \mu, \nu_2) \circ S_2\rangle \langle S_1 \circ (\nu_1, \mu, m, \mu, \nu_2) \circ S_2| \right) + \dots \end{aligned} \quad (185)$$

where we use the following notation, similar to (e):

$$\begin{aligned}
B(\lambda) &:= \{\mu \in \widehat{\mathcal{A}}_{p-1,0}^d \mid \exists T \in \text{Paths}(\lambda) : T^{p-1} = T^{p+1} = \mu\}, \\
C(\lambda, \mu) &:= \{(\nu_1, \nu_2) \in \widehat{\mathcal{A}}_{p-2,0}^d \times \widehat{\mathcal{A}}_{p,2}^d \mid \exists T \in \text{Paths}(\lambda) : T^{p-2} = \nu_1, T^{p-1} = T^{p+1} = \mu, T^{p+2} = \nu_2\} \\
\mathcal{M}(\lambda, \nu_2, \mu, \nu_1) &:= \{m \in \widehat{\mathcal{A}}_{p,0}^d \mid \exists T \in \text{Paths}(\lambda) : T^{p-2} = \nu_1, T^{p-1} = T^{p+1} = \mu, T^{p+2} = \nu_2, T^p = m\}, \\
c(\mu, m) &:= c(T) \text{ for arbitrary } T \in \text{Paths}(\lambda) \text{ s.t. } T^{p-1} = T^{p+1} = \mu, T^p = m, \\
f_{p-1}(\nu_1, \mu, m) &:= \frac{1}{r_{p-1}(T)} \text{ for arbitrary } T \in \text{Paths}(\lambda) : T^{p-2} = \nu_1, T^{p-1} = \mu, T^p = m, \\
f_{p+1}(\mu, m, \nu_2) &:= \frac{1}{r_{p+1}(T)} \text{ for arbitrary } T \in \text{Paths}(\lambda) : T^p = m, T^{p+1} = \mu, T^{p+2} = \nu_2.
\end{aligned}$$

With this notation we deduce by direct multiplication that the condition (g) is equivalent to the following statement. Namely, for every $\mu \in B(\lambda)$, $(\nu_1, \nu_2) \in C(\lambda, \mu)$, $S_1 \in \text{Paths}(\nu_1)$, $S_2 \in \text{Paths}(\nu_2)$, $m_1, m_2 \in \mathcal{M}(\lambda, \nu_2, \mu, \nu_1)$:

$$c(\mu, m_1)c(\mu, m_2)(f_{p-1}(\nu_1, \mu, m_2) - f_{p+1}(m_2, \mu, \nu_2)) \left(\sum_{m \in \mathcal{M}(\lambda, \nu_2, \mu, \nu_1)} c^2(\mu, m) f_{p-1}(\nu_1, \mu, m) f_{p+1}(m, \mu, \nu_2) \right) = 0, \quad (186)$$

$$\begin{aligned}
&\delta_{\mu', \sigma_{p-1}\mu} \delta_{\mu', \sigma_{p+1}\mu} \delta_{\nu_1, \nu_2} c(\mu, m_1) c(\mu, m_2) (f_{p-1}(\nu_1, \mu', m_2) - f_{p+1}(m_2, \mu', \nu_2)) \cdot \\
&\cdot \left(\sum_{m \in \mathcal{M}(\lambda, \nu_2, \mu, \nu_1)} c(\mu, m) c(\mu', m) \sqrt{1 - f_{p-1}^2(\nu_1, \mu, m)} \sqrt{1 - f_{p+1}^2(m, \mu, \nu_2)} \right) = 0, \quad (187)
\end{aligned}$$

$$\begin{aligned}
&\delta_{\mu', \sigma_{p-1}\mu} \delta_{\mu', \sigma_{p+1}\mu} \delta_{\nu_1, \nu_2} c(\mu, m_1) c(\mu, m_2) \left(\sqrt{1 - f_{p-1}^2(\nu_1, \mu', m_2)} - \sqrt{1 - f_{p+1}^2(m_2, \mu', \nu_2)} \right) \cdot \\
&\cdot \left(\sum_{m \in \mathcal{M}(\lambda, \nu_2, \mu, \nu_1)} c(\mu, m) c(\mu', m) \sqrt{1 - f_{p-1}^2(\nu_1, \mu, m)} \sqrt{1 - f_{p+1}^2(m, \mu, \nu_2)} \right) = 0. \quad (188)
\end{aligned}$$

eqs. (187) and (188) hold because when $\nu_1 = \nu_2$ then $f_{p-1}(\nu_1, \mu', m_2) = f_{p+1}(m_2, \mu', \nu_2)$. Moreover, when $\nu_1 = \nu_2$ then $f_{p-1}^2(\nu_1, \mu, m_2) = f_{p+1}^2(m_2, \mu, \nu_2)$ and eq. (186) trivially holds. Finally, in the case $\nu_1 \neq \nu_2$ eq. (186) also holds because:

$$\sum_{m \in \mathcal{M}(\lambda, \nu_2, \mu, \nu_1)} c^2(\mu, m) f_{p-1}(\nu_1, \mu, m) f_{p+1}(m, \mu, \nu_2) = 0, \quad (189)$$

which follows from Lemma B.4 by a similar technique which was used to show eq. (181) in Corollary B.5. Similar proof also works for the relation (h) which we do not repeat here.

Finally, we need to show the irreducibility of our representation. Due to Lemma B.7 the spectrum of Jucys–Murphy elements in our basis coincides with the canonical definition of the action of Jucys–Murphy elements in the Gelfand–Tsetlin basis [DLS18; GO22]. Since Jucys–Murphy elements generate a maximal commutative subalgebra of $\mathcal{A}_{p,q}^d$ their action uniquely determines the basis. Therefore our basis coincides with the Gelfand–Tsetlin basis from [DLS18; GO22], which is originally defined for irreducible representations.²² \square

Lemma B.1. *For every $\mu \vdash p$ and $\lambda \vdash p-1$, such that $\lambda \rightarrow \mu$ there holds*

$$d + \text{cont}(\mu \setminus \lambda) = p \cdot \frac{d_\lambda}{d_\mu} \cdot \frac{m_\mu}{m_\lambda} \quad (190)$$

where d_λ and m_λ are dimensions of the symmetric and unitary groups irreducible representation λ .

Proof. Use the hook length formula (14) for d_λ and the hook-content formula (20) for m_λ :

$$p \cdot \frac{d_\lambda}{d_\mu} \cdot \frac{m_{\mu,d}}{m_\lambda} = p \cdot \frac{\frac{(p-1)!}{\prod_{u \in \lambda} h(u)}}{\frac{p!}{\prod_{u \in \mu} h(u)}} \cdot \frac{\prod_{u \in \mu} (d + \text{cont}(u))}{\prod_{u \in \lambda} h(u)} = d + \text{cont}(\mu \setminus \lambda). \quad (191)$$

\square

Lemma B.2 ([Kos03]). *For every $\mu \vdash p$ and $\lambda \vdash p-1$, such that $\lambda \rightarrow \mu$, we denote the added cell by $x := \mu \setminus \lambda$. Then there holds*

$$\frac{\prod_{a \in AC(\lambda) \setminus x} (\text{cont}(x) - \text{cont}(a))}{\prod_{c \in RC(\lambda)} (\text{cont}(x) - \text{cont}(c))} = p \cdot \frac{d_\lambda}{d_\mu} \quad (192)$$

where d_λ is the dimension of the symmetric group irrep λ .

²²Alternatively, one can use Proposition B.6 together with Lemma B.7 and the results from [DLS18; GO22].

Corollary B.3. For every T such that $\mathcal{M}(T) \neq \emptyset$ there holds $\|v_T\|_2^2 = d$.

Proof. Denote $\lambda := T_l^{p-1}$ and use Lemmas B.1 and B.2:

$$\|v_T\|_2^2 = \sum_{S \in \mathcal{M}(T)} c(S)^2 = \sum_{\substack{\mu \in \mathcal{A}_{p,0}^d \\ \mu: \lambda \rightarrow \mu}} \frac{m_\mu}{m_\lambda} = d, \quad (193)$$

where the last equality is due to Pieri's rule for the irreducible representations of the unitary group. \square

Lemma B.4 ([War79; LB70; CL96]). For each integer $k \geq 0$, we have

$$\sum_{i=1}^n \frac{x_i^k}{\prod_{i \neq j} (x_i - x_j)} = h_{k-n+1}(x_1, \dots, x_n), \quad (194)$$

where h_r is complete r -homogeneous symmetric polynomial, which is defined as $h_r = 0$ for $r < 0$ and $h_0 = 1$.

Corollary B.5. For every Young diagram λ and arbitrary $c \in RC(\lambda)$ the following holds:

$$\sum_{m \in AC(\lambda)} \frac{\prod_{w \in RC(\lambda) \setminus c} (\text{cont}(m) - \text{cont}(w))}{\prod_{v \in AC(\lambda) \setminus m} (\text{cont}(m) - \text{cont}(v))} = 0, \quad \sum_{m \in AC(\lambda)} \text{cont}(m) \frac{\prod_{w \in RC(\lambda) \setminus c} (\text{cont}(m) - \text{cont}(w))}{\prod_{v \in AC(\lambda) \setminus m} (\text{cont}(m) - \text{cont}(v))} = 1$$

Proof. Note that the degree of the numerator as polynomial in $\text{cont}(m)$ is $|AC(\mu)| - 2$ in the first case and $|AC(\mu)| - 1$ in the second case. Now just apply Lemma B.4 with $n = |AC(\mu)|$ and variables being $\{\text{cont}(m) \mid m \in AC(\mu)\}$. \square

Proposition B.6. If there is a basis B for the representation ρ of the finite-dimensional associative semisimple algebra \mathcal{A} such that:

- (1) $\forall |S\rangle, |T\rangle \in B \exists b \in \mathcal{A} : \rho(b)|T\rangle = |S\rangle + |v\rangle$, where $|v\rangle \in \text{span}\{B \setminus |S\rangle\}$,
- (2) $\forall |S\rangle, |T\rangle \in B \exists a_S, a_T \in \mathcal{A}$ such that $\rho(a_S) = |S\rangle\langle S|$, $\rho(a_T) = |T\rangle\langle T| \in \text{End}(V)$,

then $\rho(a_S b a_T) = |S\rangle\langle T|$ and, consecutively, this representation is irreducible.

Proof. The conclusion $\rho(a_S b a_T) = |S\rangle\langle T|$ is trivial, since for every $|T'\rangle \in B$:

$$\rho(a_S b a_T)|T'\rangle = \rho(a_S)\rho(b)\rho(a_T)|T'\rangle = |S\rangle\langle S|\rho(b)|T\rangle\langle T|T'\rangle = \delta_{T,T'}|S\rangle\langle S|(|S\rangle + |v\rangle) = \delta_{T,T'}|S\rangle. \quad (195)$$

Then the representation must be irreducible because there are no invariant subspaces. This result is also known as Burnside's theorem on matrix algebras. \square

Lemma B.7. The action of Jucys–Murphy elements is diagonal in the Gelfand–Tsetlin basis and the spectrum is given by the walled content $\text{wcont}_k(T)$:

$$J_k|T\rangle = \text{wcont}_k(T)|T\rangle \quad (196)$$

Proof. For $k \leq p$ this is just a statement of the same result for the symmetric group, e.g. see [OV96; VO05]. The proof for that case can be done by induction by exploiting the relation $J_{k+1} = \sigma_k J_k \sigma_k + \sigma_k$. The base of the induction is trivial. Now using the induction step we can immediately see that

$$\begin{aligned} J_{k+1}|T\rangle &= (\sigma_k J_k \sigma_k + \sigma_k)|T\rangle = (\sigma_k J_k + 1)\sigma_k|T\rangle = (\sigma_k J_k + 1)\left(\frac{1}{r_k(T)}|T\rangle + \sqrt{1 - \frac{1}{r_k(T)^2}}|\sigma_k T\rangle\right) \\ &= \frac{1}{r_k(T)}|T\rangle + \sqrt{1 - \frac{1}{r_k(T)^2}}|\sigma_k T\rangle + \sigma_k\left(\frac{\text{wcont}_k(T)}{r_k(T)}|T\rangle + \text{wcont}_k(\sigma_k T)\sqrt{1 - \frac{1}{r_k(T)^2}}|\sigma_k T\rangle\right) \\ &= \left(\frac{\text{wcont}_k(T)}{r_k(T)} + 1\right)\left(\frac{|T\rangle}{r_k(T)} + \sqrt{1 - \frac{1}{r_k(T)^2}}|\sigma_k T\rangle\right) + \text{wcont}_k(\sigma_k T)\sqrt{1 - \frac{1}{r_k(T)^2}}\left(-\frac{|\sigma_k T\rangle}{r_k(T)} + \sqrt{1 - \frac{1}{r_k(T)^2}}|T\rangle\right) \\ &= \left(\frac{1}{r_k(T)} + \frac{\text{wcont}_k(T) - \text{wcont}_{k+1}(T)}{r_k(T)^2} + \text{wcont}_{k+1}\right)|T\rangle + \sqrt{1 - \frac{1}{r_k(T)^2}}\left(1 + \frac{\text{wcont}_k(T) - \text{wcont}_{k+1}(T)}{r_k(T)}\right)|\sigma_k T\rangle \\ &= \text{wcont}_k(T)|T\rangle, \end{aligned} \quad (197)$$

where we used that $\text{wcont}_k(\sigma_k T) = \text{wcont}_{k+1}(T)$, $r_k(\sigma_k T) = -r_k(T)$ and $r_k(T) = \text{wcont}_{k+1}(T) - \text{wcont}_k(T)$.

Similarly, for $k \geq p+1$ we have a similar relation $J_{k+1} = \sigma_k J_k \sigma_k + \sigma_k$ and the same argument holds, assuming that $J_{p+1}|T\rangle = \text{wcont}_{p+1}(T)|T\rangle$. However, for $k = p+1$ we need to prove the claim separately.

To show the claim for $k = p+1$, recall that $J_{p+1} = d - \rho$, where $\rho := \sum_{i=1}^p (i, p)\sigma_p(i, p)$ and (i, p) is a transposition between sites i and p with the convention $(p, p) := 1$. Without loss of generality assume that $q = 1$. Note that since J_{p+1} commutes with $\mathcal{A}_{p,0}^d$, J_{p+1} must be diagonal in the Gelfand–Tsetlin basis and it has the same eigenvalues for every path T which goes through a given vertex μ at the level p in the Bratteli diagram. Therefore, we now assume $T \in \text{Paths}(\lambda)$ has the property $T^p = \mu$. There are two cases:

- (1) If $\lambda_r = (1)$, then there is no mobile cell in T and the action of σ_p is zero, meaning that $J_{p+1}|T\rangle = d|T\rangle$ which is consistent with $J_{p+1}|T\rangle = \text{wcont}_{p+1}(T)|T\rangle$ for that case.

(2) If $\lambda_r = \emptyset$, then for every $T \in \text{Paths}(\lambda)$ with $T^p = \mu$ we can write:

$$\begin{aligned}
\langle T | \rho | T \rangle &= \frac{1}{d_\mu} \sum_{\substack{T \in \text{Paths}(\lambda) \\ T^p = \mu}} \langle T | \rho | T \rangle = \frac{1}{d_\mu} \sum_{\substack{T \in \text{Paths}(\lambda) \\ T^p = \mu}} \sum_{i=1}^p \langle T | (i, p) \sigma_p(i, p) | T \rangle \\
&= \frac{1}{d_\mu} \sum_{i=1}^p \sum_{\substack{T \in \text{Paths}(\lambda) \\ T^p = \mu}} \langle T | (i, p) \left(\sum_{\substack{S \in \text{Paths}(\lambda) \\ S^p = \mu \\ S^{p-1} = \lambda}} |v_S\rangle \langle v_S| \right) (i, p) | T \rangle = \frac{1}{d_\mu} \sum_{i=1}^p \sum_{\substack{T, S \in \text{Paths}(\lambda) \\ T^p = S^p = \mu \\ S^{p-1} = \lambda}} |\langle v_S | (i, p) | T \rangle|^2 \\
&= \frac{1}{d_\mu} \sum_{i=1}^p \sum_{\substack{T, S \in \text{Paths}(\lambda) \\ T^p = S^p = \mu \\ S^{p-1} = \lambda}} c(S)^2 \cdot |\langle S | (i, p) | T \rangle|^2 = \frac{c(\lambda, \mu)^2}{d_\mu} \sum_{i=1}^p \sum_{\substack{T, S \in \text{Paths}(\lambda) \\ T^p = S^p = \mu \\ S^{p-1} = \lambda}} |\langle S | (i, p) | T \rangle|^2 \\
&= \frac{c(\lambda, \mu)^2}{d_\mu} \sum_{i=1}^p \sum_{\substack{S \in \text{Paths}(\lambda) \\ S^p = \mu \\ S^{p-1} = \lambda}} \langle S | (i, p) \left(\sum_{\substack{T \in \text{Paths}(\lambda) \\ T^p = \mu}} |T\rangle \langle T| \right) (i, p) | S \rangle \\
&= \frac{c(\lambda, \mu)^2}{d_\mu} \sum_{i=1}^p \sum_{\substack{S \in \text{Paths}(\lambda) \\ S^p = \mu \\ S^{p-1} = \lambda}} \langle S | \left(\sum_{\substack{T \in \text{Paths}(\lambda) \\ T^p = \mu}} |T\rangle \langle T| \right) (i, p)^2 | S \rangle = \frac{c(\lambda, \mu)^2}{d_\mu} \sum_{i=1}^p \sum_{\substack{T, S \in \text{Paths}(\lambda) \\ T^p = S^p = \mu \\ S^{p-1} = \lambda}} |\langle S | T \rangle|^2 \\
&= \frac{c(\lambda, \mu)^2}{d_\mu} \cdot p \cdot d_\lambda = p \cdot \frac{d_\lambda}{d_\mu} \cdot \frac{m_\mu}{m_\lambda} = d + \text{cont}(\mu \setminus \lambda), \tag{198}
\end{aligned}$$

where we used Lemmas B.1 and B.2. Therefore

$$\langle T | J_{p+1} | T \rangle = d - \langle T | \rho | T \rangle = -\text{cont}(\mu \setminus \lambda) = -\text{cont}(T^p \setminus T^{p+1}) = \text{wcont}_{p+1}(T). \tag{199}$$

□